The Journal of Antibiotics (2009) 62, 177–180

www.nature.com/ja

ORIGINAL ARTICLE

JBIR-12, a novel antioxidative agent from *Penicillium* sp. NBRC 103941

Miho Izumikawa[1], Aya Nagai[1], Takayuki Doi[2], Motoki Takagi[1] and Kazuo Shin-ya[3]

In the course of our screening program for active compounds from fungal metabolites, we isolated JBIR-12 (1) as a free radical scavenger from the culture broth of *Penicillium* sp. NBRC 103941. Structure elucidation of 1 was carried out using methylated and/or acetylated derivatives of 1. As a consequence, the structure of 1 was determined to be a novel highly oxygenated tetrahydronaphthalene species attached to an acyl chain moiety on the basis of NMR and other spectroscopic data. It was interesting that 1 was spontaneously methylated when left in methanol. Furthermore, isomerization or rearrangements could occur during the derivatization of 1. Compound 1 exhibited potent radical scavenging activity against 1,1-diphenyl-2-picrylhydrazyl radical with an IC_{50} value of 75 μM.
The Journal of Antibiotics (2009) **62,** 177–180; doi:10.1038/ja.2009.13; published online 27 February 2009

Keywords: antioxidative agent; JBIR-12; *Penicillium* sp.; radical scavenging

INTRODUCTION

Free radicals play a causative role in many disease states including atherosclerosis, inflammation, ischemia-reperfusion injury, rheumatism and central nervous diseases.[1] In addition, senility and cancer initiation as well as progression are also believed to involve active oxygen species.[2] In fields of such diseases, an effective antioxidant could be a useful lead compound for the development of a clinically useful drug. Historically, *Penicillium* species have been shown to be producers, with more than 900 bioactive compounds documented.[3] Furthermore, the important pharmaceutical agents, penicillin (antibiotic) and compactin (lipid-lowering agent), were isolated from *Penicillium* spp. Therefore, we carried out the screening for antioxidants from culture broths of *Penicillium* species.

In the course of our screening program from metabolites of *Penicillium* spp., we isolated a novel antioxidative agent, designated as JBIR-12 (**1**), from the culture broth of *Penicillium* sp. NBRC 103941. The structure of **1** contains highly oxygenated tetrahydronaphthalene moiety possessing an acyl chain, and shows unique chemical features. This paper describes the fermentation, isolation, physico-chemical properties, structure elucidation and biological activity of **1** as well as a hypothetical reaction mechanism of the addition of methanol to **1**.

RESULTS AND DISCUSSION

Isolation

The culture (100-ml Erlenmeyer flask ×20) was extracted with 80% Me_2CO (400 ml). The extract was evaporated *in vacuo*, and the residual aqueous concentrate was extracted with EtOAc (100 ml ×3). After drying over Na_2SO_4, the organic layer was evaporated to dryness. The dried residue (1.87 g) was chromatographed on normal-phase medium-pressure liquid chromatography (Purif-Pack SI-60; Moritex, Tokyo, Japan) with an *n*-hexane-EtOAc linear gradient system (0–100% EtOAc), and fractions including major metabolites were collected by LC-MS monitoring. The eluate (70–100% EtOAc, 720 mg) was further separated by a reversed-phase flash column (Purif-Pack ODS-100; Moritex) with an H_2O-MeOH linear gradient system (50–100% MeOH) to yield a major fraction (80–100% MeOH, 276 mg). This eluate was subjected to preparative reversed-phase HPLC developed with 60% aqueous MeCN containing 0.2% formic acid (flow rate: 10 ml min^{-1}) to yield **1** (Rt 9.8 min, 26.1 mg).

Structure elucidation

The physico-chemical properties of **1** are summarized in Table 1. Compound **1** was isolated as a red powder and had the molecular formula $C_{24}H_{28}O_8$ revealed by HR-ESI-MS data (*m/z* 443.1694 $(M-H)^-$, Δ −1.2 mmu). The structure of **1** was established mainly

[1]Biomedicinal Information Research Center (BIRC), Japan Biological Informatics Consortium (JBIC), Koto-ku, Tokyo, Japan; [2]Graduate School of Pharmaceutical Sciences, Tohoku University, Aoba-ku, Sendai, Japan and [3]Biomedicinal Information Research Center (BIRC), National Institute of Advanced Industrial Science and Technology (AIST), Koto-ku, Tokyo, Japan
Correspondence: Dr K Shin-ya, Biomedicinal Information Research Center (BIRC), National Institute of Advanced Industrial Science and Technology (AIST), 2-42 Aomi, Koto-ku, Tokyo 135-0064, Japan.
E-mail: k-shinya@aist.go.jp or Dr M Takagi, Biomedicinal Information Research Center (BIRC), Japan Biological Informatics Consortium (JBIC), 2-42 Aomi, Koto-ku, Tokyo 135-0064, Japan.
E-mail: motoki-takagi@aist.go.jp
Received 4 November 2008; revised 31 January 2009; accepted 2 February 2009; published online 27 February 2009

by NMR analyses of **1** and its chemically modified derivative **3** as follows:

The direct connectivity between protons and carbons was established by the HSQC (heteronuclear single-quantum coherence) spectrum, and the tabulated ^{13}C and ^{1}H NMR spectral data for **1** are shown in Table 2. The ^{1}H-^{1}H DQF (double-quantum filtered)-COSY and HMBC (heteronuclear multiple bond correlation) spectra established two partial structures (Figure 1). The combination of proton coupling constants and ^{1}H-^{1}H correlations in the ^{1}H-^{1}H DQF-COSY constructed an acyl chain substructure as shown in Figure 1. The sequence from 2′-H (δ_H 5.99) to 10′-H (δ_H 0.88) through 3′-H (δ_H 7.36), 4′-H (δ_H 6.37), 5′-H (δ_H 6.67), 6′-H (δ_H 6.20), 7′-H (δ_H 5.88), 8′-H (δ_H 2.14) and 9′-H (δ_H 1.37), in addition to a spin coupling between 8′-H and 11′-H (δ_H 1.03), established the branched alkyl chain moiety. The proton spin coupling constants between 2′-H and 3′-H (J=15.3 Hz), 4′-H and 5′-H (J=14.8 Hz), and 6′-H and 7′-H (J=15.2 Hz), together with the ^{1}H-^{13}C long-range correlations from 2′-H and 3′-H to C-1′ (δ_C 166.8), revealed a (2*E*,4*E*,6*E*)-8-methyldeca-2,4,6-trienoate moiety as shown in Figure 1a.

Oxygenated methylene protons 13-H (δ_H 5.08, 4.68), were ^{1}H-^{13}C long-range coupled to C-5 (δ_C 121.6), C-6 (δ_C 128.2) and C-7 (δ_C 146.3). An aromatic proton, 9-H (δ_H 7.22), was *m*-coupled to C-5 and C-7 in the HMBC spectrum of **1**. Thus, the hydroxymethyl group was deduced to be substituted at the position of C-6. Long-range couplings from 9-H to C-8 (δ_C 153.1) and C-10 (δ_C 140.4), together with the ^{13}C chemical shifts at C-7 and C-8, established the assignments of a benzene ring moiety. A methyl proton, 11-H (δ_H 1.60), was long-range coupled to C-1 (δ_C 76.2), C-2 (δ_C 206.7) and C-10. In the same manner, a methyl proton, 12-H (δ_H 1.54), was long-range coupled to C-2, C-3 (δ_C 85.5) and C-4 (δ_C 194.1). In addition, a long-range coupling was observed between the aromatic proton 9-H and C-1, which indicated that C-1 was located at the *peri* position of 9-H. Thus, highly oxygenated tetrahydronaphthalene moiety was determined as shown in Figure 1b.

Table 1 Physico-chemical properties of 1

Appearance	*Red powder*
Melting point	47–49 °C
$[\alpha]_D^{23}$ (MeOH)	−278.4° (*c* 0.32)
Molecular formula	$C_{24}H_{28}O_8$
HRESIMS (*m/z*)	
	Found: 443.1694 $[M-H]^-$
	Calcd: 443.1706
UV λ_{max} (MeOH) nm (ε)	310 (45 330), 244 (14 330)
IR ν_{max} (KBr) cm^{-1}	1684, 1612, 1302, 1134, 1086, 1005

To establish the substituted position of the acyl chain moiety of **1**, chemical modification was carried out as follows: Treatment of **1** with methyl iodide and potassium carbonate in DMF afforded a (7,8,13)-*O*-trimethyl-JBIR-12 (**2**) as a main derivative. Each ^{1}H-^{13}C long-range correlation from methoxyl groups 7-OMe, 8-OMe and 13-OMe to C-7, C-8 and C-13, respectively, deduced substituted position of their methoxyl groups. Only one hydroxyl group at C-1 could not be methylated, and then **2** was acetylated by acetic anhydride in pyridine to give a (7,8,13)-*O*-trimethyl-1-*O*-acetyl-JBIR-12 (**3**). NOEs between 9-H and 11-H, and 9-H and methyl proton at acetyl residue revealed

Table 2 ^{13}C (125 MHz) and ^{1}H (500 MHz) NMR data for 1 in CD_3OD and ^{13}C (150 MHz) and ^{1}H (600 MHz) NMR data for 3 in $CDCl_3$

	1		*3*	
No.	δ_C	δ_H *(multiplicity, J=Hz)*	δ_C	δ_H *(multiplicity, J=Hz)*
1	76.2		81.3	
2	206.7		200.4	
3	85.5		84.9	
4	194.1		191.7	
5	121.6		122.7	
6	128.2		133.2	
7	146.3		148.4	
8	153.1		157.0	
9	112.6	7.22 (s)	105.6	6.81 (s)
10	140.4		140.3	
11	33.6	1.60 (s)	31.8	1.85 (s)
12	24.0	1.54 (s)	24.6	1.75 (s)
13	57.7	5.08 (d, 12.5)	64.3	4.99 (d, 9.7)
		4.68 (d, 12.5)		4.56 (d, 9.7)
1′	166.8		165.1	
2′	119.0	5.99 (d, 15.3)	119.0	5.98 (d, 15.3)
3′	148.3	7.36 (dd, 15.3, 11.3)	143.0	7.36 (dd, 15.3, 11.5)
4′	129.0	6.37 (dd, 14.8, 11.3)	127.8	6.26 (dd, 14.8, 11.5)
5′	144.0	6.67 (dd, 14.8, 10.8)	142.3	6.53 (dd, 14.8, 10.7)
6′	129.8	6.20 (dd, 15.2, 10.8)	128.2	6.12 (dd, 15.2, 10.7)
7′	147.9	5.88 (dd, 15.2, 8.1)	146.8	5.81 (dd, 15.2, 7.9)
8′	40.2	2.14 (m)	38.8	2.14 (m)
9′	30.6	1.37 (dq, 7.4, 1.2)	29.5	1.35 (dq, 7.3, 1.2)
10′	12.2	0.88 (t, 7.4)	11.7	0.87 (t, 7.3)
11′	20.3	1.03 (d, 6.9)	19.7	1.02 (d, 6.7)
1-OAc, Me			20.8	2.19 (s)
C=O			169.1	
7-OMe			61.8	3.85 (s)
8-OMe			55.9	3.93 (s)
13-OMe			58.6	3.34 (s)

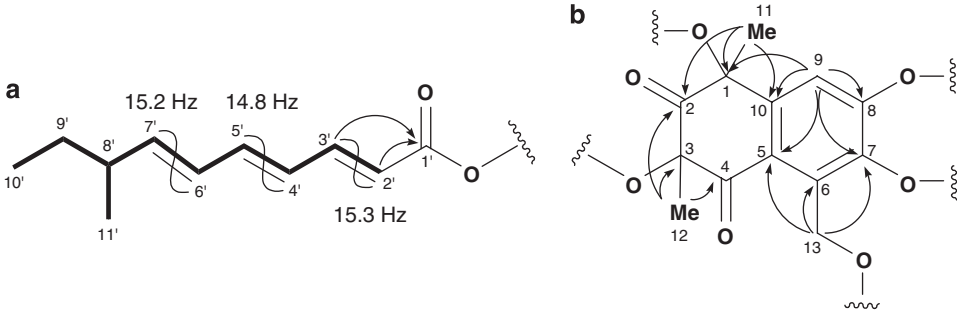

Figure 1 ^{1}H-^{1}H (bold line) and main ^{1}H-^{13}C (arrows) correlations in 2D NMR of **1**.

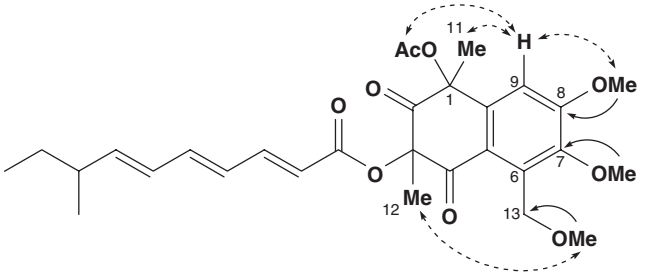

Figure 2 Key ^{1}H-^{13}C (arrows) and NOESY (dashed arrows) correlations in 2D NMR of **3**.

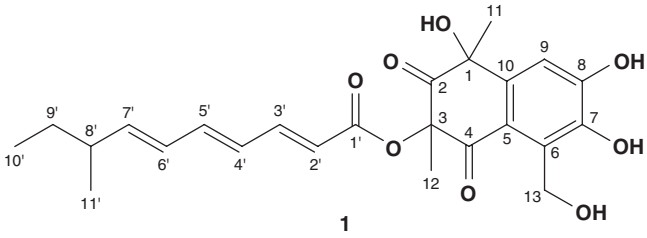

Figure 3 Structure of JBIR-12 (**1**).

that the acyl chain moiety is substituted at the position of C-3 by an ester bond (Figure 2). Thus, the total structure of **1** was elucidated as shown in Figure 3.

During NMR experiments of **1** in methanol-d_4, we observed the appearance of some extra signals corresponding to deuteride methoxyl groups. The LC-MS analyses of this sample indicated that **1** was changed to deuterium labeled mono- or di-*O*-methyl compounds. Hence, we speculated that this reaction occurred by a subsequent process. The hydroxyl group at C-13 in **1** was first displaced with a methoxyl group in MeOH. Further displacement of the hydroxyl group at C-7 with a methoxyl group gradually occurred. Considering into these results, dehydration at C-13 could be accompanied by 1,4-addition of MeOH or 1,2- and 1,4-addition of MeOH through a hypothetical scheme as shown in Figure 4. Furthermore, **1** might be isomerized or rearranged during a derivatization to **2**, as acylation of **2** afforded several minor congeners, of which some methoxyl signals were recognized in its ^{1}H NMR spectrum. Therefore, we could not determine the relative stereochemistry at C-1 and C-3, although an NOE between the methyl proton of the acetyl group and the methyl proton 12-H was observed. This compound seems to keep its structure intact on subtle electron translocation balance. Therefore, **1** is quite an interesting target for total synthesis, which is desired to establish its stereochemistry.

Biosynthetically, **1** is hypothetically produced through the combination of two different pathways. We speculated that (2*E*,4*E*,6*E*)-8-

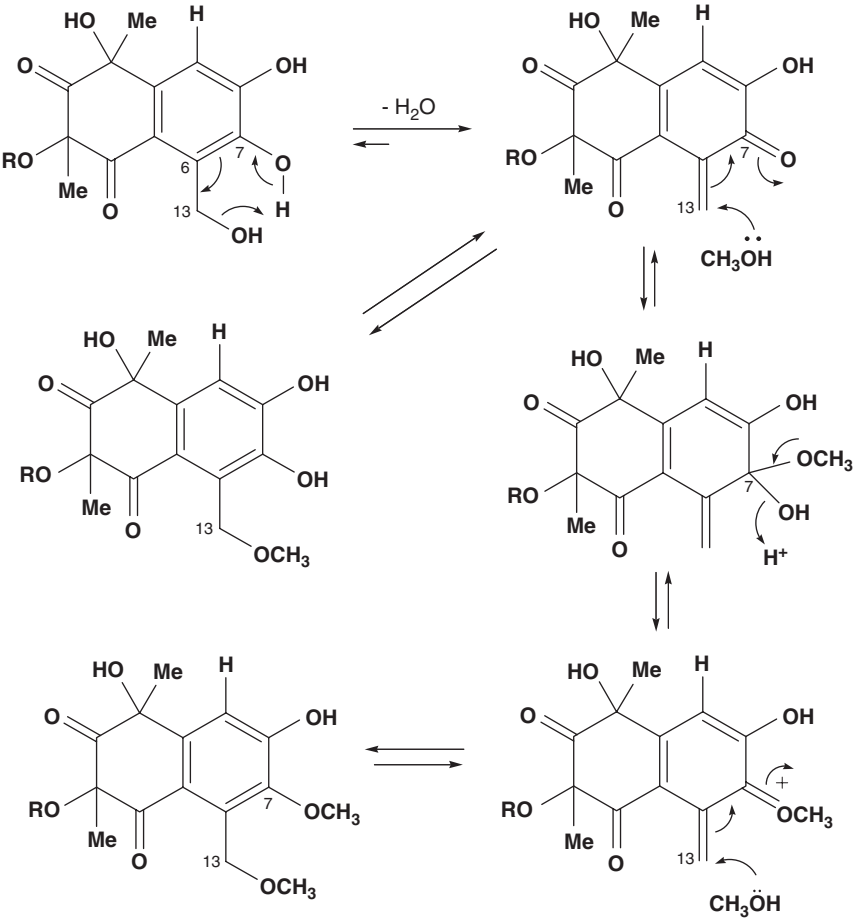

Figure 4 Methylation mechanism at 13-OH and 7-OH.

methyldeca-2,4,6-trienoate moiety is biosynthesized by type-I polyketide synthase, and an oxygenated tetrahydronaphthalene moiety comes from a fungal 1,8-dihydronaphthalene (DHN)-melanin pathway.[4,5] The highly oxygenated and methylated tetrahydronaphthalene moiety and (2*E*,4*E*,6*E*)-8-methyldeca-2,4,6-trienoate moiety are connected through an ester bond. Studies on detailed biosynthetic pathway require further labeling and genetic experiments.

Biological activity

We evaluated 1,1-diphenyl-2-picrylhydrazyl (DPPH) radical scavenging activity by **1**. Compound **1** exhibited DPPH radical scavenging activity with an IC_{50} value of 75 μM, which was almost the same activity as that of α-tocopherol (IC_{50}=50 μM). The structure of **1** involves phenolic hydroxyl groups, which are considered to play a significant role in expressing radical scavenging activity. Actually, the derivatives **2** and **3** did not show any radical scavenging activity at the concentration of 200 μM. Studies on detailed biological activities are now underway.

METHODS

General experimental procedures

Melting point was determined with a Yanagimoto micro melting point apparatus (Yanagimoto, Kyoto, Japan). Optical rotations were operated on a SEPA-300 polarimeter (Horiba, Kyoto, Japan). HR-ESI (electrospray ionization)-MS data were recorded on an LCT-Premier XE mass spectrometer (Waters, Milford, MA, USA). UV and IR spectra were measured on a U-3200 spectrophotometer (Hitachi, Tokyo, Japan) and an FT-720 spectrophotometer (Horiba), respectively. NMR spectra were recorded on an NMR System 600 or 500 NB CL (Varian, Palo Alto, CA, USA). Chemical shifts are reported in p.p.m. relative to chloroform (7.26 p.p.m. for ^{1}H) or chloroform-*d* (77.0 p.p.m. for ^{13}C), and methanol (3.30 p.p.m. for ^{1}H) or methanol-d_4 (49.0 p.p.m. for ^{13}C). Normal- and reversed-phase medium-pressure liquid chromatography was performed on a Purif-Pack SI-60 (Moritex) and a Purif-Pack ODS-100 (Moritex), respectively. Preparative reversed-phase HPLC was carried out on a Senshu Pak PEGASIL ODS (20 i.d. ×150 mm; Senshu Scientific, Tokyo, Japan) with detection by a 2996 photodiode array detector (Waters) and a 3100 mass detector (Waters). Reagents and solvents were of the highest grade available.

Microorganism

Penicillium sp. NBRC 103941 was purchased from the National Institute of Technology and Evaluation (NITE; Tokyo, Japan).

Medium and fermentation

The seed medium, potato dextrose, was composed of 2.4 g l^{-1} Potato Dextrose Broth (BD Biosciences, San Jose, CA, USA). The production medium consisted of 3 g of brown rice (Hitomebore, Miyagi, Japan), 6 mg of Bacto-Yeast extract (BD Biosciences), 3 mg of sodium tartrate, 3 mg KH_2PO_4 and 9 ml of H_2O in a 100-ml Erlenmeyer flask.

Penicillium sp. NBRC 103941 was cultivated in 50-ml test tubes containing 15 ml of a seed medium. The test tubes were shaken on a reciprocal shaker (355 r.p.m.) at 27 °C for 3 days. Aliquots (5 ml) of the culture were transferred to 100-ml Erlenmeyer flasks containing the production medium and incubated in static culture at 27 °C for 14 days.

Methylation and acetylation

Compound **1** (1.1 mg) was dissolved in 250 μl of DMF, mixed with 0.2 mg of K_2CO_3 and 25 μl of methyl iodide and stirred at room temperature overnight. The mixture was diluted with MeOH, evaporated *in vacuo* and applied to preparative reversed-phase HPLC using a PEGASIL-ODS (Senshu Pak, 20 i.d. ×150 mm) developed with 80% aqueous MeOH containing 0.1% formic acid (flow rate: 10 ml min^{-1}) to give (7,8,13)-*O*-trimethyl JBIR-12 (**2**, Rt 13.0 min, 0.5 mg). The structure of **2** was confirmed by LC-MS and NMR analyses.

Compound **2** (0.5 mg) was dissolved in 200 μl of pyridine, mixed with 20 μl of acetic anhydride and stirred at room temperature overnight. The mixture was diluted with H_2O, extracted with EtOAc and the organic extract was evaporated *in vacuo*. This extract was applied to preparative reversed-phase HPLC (Senshu Pak PEGASIL-ODS, 20 i.d. ×150 mm) developed with 85% aqueous MeOH containing 0.075% formic acid (flow rate: 10 ml min^{-1}) to yield (7,8,13)-*O*-trimethyl-1-*O*-acetyl-JBIR-12 (**3**, Rt 11.5 min, 0.4 mg, $C_{29}H_{36}O_9$, *m/z* 529.2438 $(M+H)^+$, Δ 0 mmu). The structure of **3** was established by NMR analyses (Table 2).

DPPH radical scavenging activity

A 96-well multiplate was used for the DPPH radical scavenging assay.[6] Compound **1** and α-tocopherol as a positive control were dissolved in MeOH to prepare samples of 1 mM, before being diluted with MeOH to prepare samples of a linear concentration system of 0.01–0.5 mM. A volume of 90 μl of 200 μM DPPH dissolved in MeOH and 10 μl of sample were mixed in the microplate. After 1 h incubation at room temperature, the absorbance was measured at 540 nm.

ACKNOWLEDGEMENTS

This work was supported by a grant from the New Energy and Industrial Technology Department Organization (NEDO) of Japan.

1 Hammond, B., Kontos, A. & Hess, M. L. Oxygen radicals in the adult respiratory distress syndrome, in myocardial ischemia and reperfusion injury, and in cerebral vascular damage. *Can. J. Physiol. Pharmacol.* **63,** 173–187 (1985).
2 Finkel, T. Radical medicine: treating ageing to cure disease. *Nat. Rev. Mol. Cell Biol.* **6,** 971–976 (2005).
3 Bérdy, J. Bioactive microbial metabolites. *J. Antibiot.* **58,** 1–26 (2005).
4 Wheeler, M. H. & Bell, A. A. Melanins and their importance in pathogenic fungi. In *Current Topics in Medical Mycology* Vol. 2. (ed. McGinnis, M.R.) 338–387 (Springer-Verlag, New York, NY, 1988).
5 Tsai, H. F., Wheeler, M. H., Chang, Y. C. & Kwon-Chung, K. J. A developmentally regulated gene cluster involved in conidial pigment biosynthesis in *Aspergillus fumigatus*. *J. Bacteriol.* **181,** 6469–6477 (1999).
6 Wang, G. J., Lin, S. Y., Wu, W. C. & Hou, W. C. DPPH radical scavenging and semicarbazide-sensitive amine oxidase inhibitory and cytotoxic activities of *Taiwanofungus camphoratus* (Chang-chih). *Biosci. Biotechnol. Biochem.* **71,** 1873–1878 (2007).

The Journal of Antibiotics (2009) 62, 181–190

www.nature.com/ja

ORIGINAL ARTICLE

Microbial degradation of cyclic peptides produced by bacteria

Hajime Kato[1], Kiyomi Tsuji[2] and Ken-ichi Harada[1]

Bacterial strain, B-9, isolated from Lake Tsukui, Japan, and characterized as genus *Sphingosinicella* sp., possesses hydrolytic enzymes capable of degrading various toxic and non-toxic cyanobacterial cyclic peptides, such as microcystins, nodularin, microviridin, microcyclamide and aeruginopeptin. In this study, the degradation activities of the cell extract of B-9 against bacterial cyclic peptides, bacitracin, colistin, polymyxin, mikamycin, thiopeptin and WAP-8294A2, were investigated and the degradation products were analyzed using HPLC and liquid chromatography/ion trap tandem mass spectrometry (LC/ITMS). As a result of extensive experiments, it was confirmed that B-9 could also degrade these bacterial cyclic peptides by hydrolysis of their peptide or ester bonds, except for WAP-8294A2. These results indicated that the functions of the bacterium with its enzymes were further extended and offered the possibility of degrading other types of compounds.
The Journal of Antibiotics (2009) **62,** 181–190; doi:10.1038/ja.2009.8; published online 13 February 2009

Keywords: B-9 strain; biodegradation; cyclic peptide antibiotics; microcystin

INTRODUCTION

In the environment, there are many bacteria with degradation activities against hazardous and harmful compounds. Microcystins (MCs) are such typical compounds produced by cyanobacteria, such as *Microcystis*, *Anabaena* and *Planktothrix*, because they are cyclic heptapeptides showing a potent hepatotoxicity and tumor promoting activity.[1] The strain, B-9, was isolated from Lake Tsukui, Japan as an MC-degrading bacterium in 1997.[2] This strain showed a promising potential for the degradation of MC-related compounds and nodularin.[3] Such an MC-degrading bacterium was first isolated in Australia and was identified as one of the *Sphingomonas* strains (ACM-3962) in 1994.[4] Phenotypically, similar bacteria capable of degrading MC have been reported subsequently all over the world.[5–10] B-9 is 99% similar to the *Sphingosinicella microcystinivorans* strain, Y2, one of these MC-degrading bacteria, based on the 16S rDNA sequence (GenBank accession no. AB084247).[2,11] In a pilot-scale study, the ACM-3962 effectively degraded the microcystin-LR (MCLR) during slow sand-filtration,[12] and a feasible bioreactor, using a B-9 strain immobilized in polyester resin, rapidly removed MC from the lake water.[2]

In an earlier study, we applied B-9 to various cyclic peptides, such as aeruginopeptin, nostophycin, microcyclamide and microviridin, derived from cyanobacteria.[13] As a result of the investigation, it was confirmed that the enzymes included in B-9 could also hydrolyze peptide bonds of several cyanobacterial cyclic peptides that were structurally different from the MCs and nodularin. In addition, the use of the cell extract suggested that all MC-degrading bacteria, including B-9, inherently possessed these capabilities. Although the role of these enzymes for bacteria has not been verified completely, the abilities of these enzymes from microorganisms existing in the natural environment may contribute to environmental self-purification.

A molecular study of the *Sphingomonas* strain, ACM-3962, revealed the presence of three hydrolytic enzymes involved in the degradation. Microcystinase (MlrA) catalyzes the initial ring opening of MCLR at a unique β-amino acid, (2*S*,3*S*,8*S*,9*S*)-3-amino-9-methoxy-2,4,6-trimethyl-10-phenyldeca-4(*E*),6(*E*)-dienoic acid (Adda)-Arg peptide bond to give the linearized MCLR, which is further degraded to a tetrapeptide by MlrB. The third enzyme, MlrC, hydrolyzes the tetrapeptide into smaller peptides and amino acids. The putative protein, MlrD, provided the transport of MCLR and its degradation products across the bacterial cell wall.[14,15] The effective use of an appropriate protease inhibitor could accumulate the following degradation intermediates: the use of EDTA (ethylenediaminetetraacetic acid) accumulated the linearized MCLR (Adda-Glu-Mdha-Ala-Leu-MeAsp-Arg) and tetrapeptide (Adda-Glu-Mdha-Ala), which allowed the MlrA and MlrC to be classified as two metalloproteases, whereas the use of 1,10-phenanthroline characterized MlrB as a possible serine protease.[14,15] Furthermore, the intact Adda was first isolated from MCLR by degradation using a B-9 strain as one of the final products.[16]

As mentioned above, cyanobacteria produce a wealth of bioactive peptide derivatives with a broad range of biological activities and pharmacological properties.[17] Many of these are synthesized on non-ribosomal peptide synthetases (NRPSs).[18–21] Bacteria and fungi also produce structurally characteristic peptides by the NRPS pathway, in which they have various bioactivities, such as anti-microbial and

[1]Graduate School of Environmental and Human Science and Faculty of Pharmacy, Meijo University, Tempaku, Nagoya, Japan and [2]Kanagawa Prefectural Institute of Public Health, Shimomachiya, Chigasaki, Kanagawa, Japan
Correspondence: Professor K-i Harada, Graduate School of Environmental and Human Science and Faculty of Pharmacy, Meijo University, Tempaku, Nagoya 468-8503, Japan.
E-mail: kiharada@ccmfs.meijo-u.ac.jp
Received 9 October 2008; accepted 21 January 2009; published online 13 February 2009

immunosuppressive activities.[21–23] The cyclic peptide is one of the typical products by way of the NRPS pathway and is usually stable against various hydrolytic enzymes, such as trypsin, because of its cyclic structure and unusual constituent amino acids.[4,24] Therefore, it is laborious to reproducibly obtain partially hydrolyzed products in the usual manner. This study focused on the further hydrolytic activity and universality of B-9, therefore; it was applied to representative bacterial cyclic peptides.

MATERIALS AND METHODS

Reagents

The Tris-Cl buffer (pH 7.6), dithiothreitol, HPLC grade methanol and formic acid for column chromatography were purchased from Nacarai Tesque (Kyoto, Japan). The distilled water used for the HPLC and LC/MS mobile phases was purchased from Wako Pure Chemicals (Osaka, Japan).

Bacterial cyclic peptides

Bacitracin, mikamycin, thiopeptin and polymyxin were kindly provided by Dr Ikai (Aichi Prefectural Institute of Public Health, Japan). Colistin was purchased from Wako Pure Chemicals (Osaka, Japan). WAP-8294A2 was provided by Wakamoto Pharmaceutical Co., Ltd. (Tokyo, Japan).

Cell extract of MC-degrading bacterium

The bacterial strain, *Sphingocinisella* B-9, isolated from the surface water of Lake Tsukui, Kanagawa, Japan,[2] was inoculated in a flask containing 100 ml of Sakurai medium composed of 0.2% peptone, 0.1% yeast extract and 0.05% glucose[2] and was incubated at 27 °C and 200 r.p.m. for 3 days. After centrifuging at 3000×*g* for 30 min at 20 °C, the cells were harvested as a pellet and then re-suspended in 20 ml of 50 mM Tris-Cl buffer (pH 7.6) containing 0.5 mM dithiothreitol. The suspension was next extracted using a French pressure press at 10 000 psi and harvested as the cell extract. The absence of resting cells in the cell extract was determined using a microscope.

Degradation of cyclic peptides

Fifty micrograms of the cyclic peptides, bacitracin-A, mikamycin, thiopeptin, colistin, polymyxin and WAP-8294A2 was dissolved in water at a concentration of 1.0 mg ml^{-1}, added to 500 µl of the cell extracts of B-9 and incubated at 27 °C for 24, 48 and 96 h. In addition, the bacitracin, polymyxin and colistin were monitored at 2, 6 and 12 h. MCLR was used as a positive control to confirm the activity of B-9. After incubation, 50 µl of these mixtures was added to 50 µl of methanol containing 0.2% formic acid and centrifuged at 15 000×*g* for 10 min at 20 °C to stop the degradation and to eliminate the proteins. Next, each supernatant was analyzed using HPLC and liquid chromatography/ion trap tandem mass spectrometry (LC/ITMS).

HPLC

The cyclic peptides were analyzed using a high-performance liquid chromatograph equipped with a photodiode array detector. The system consisted of two liquid chromotography (LC) 10A VP pumps, a DGU 12A degasser, a CTO 6A column oven, an SPD 10A VP photodiode array detector and an SCL 10A VP system controller (Shimadzu, Kyoto, Japan). Five microliters of the sample was filtered using an Ultrafree-MC membrane centrifuge filtration unit (hydrophilic PTFE, 0.20 mm, Millipore, Bedford, MA, USA) and loaded onto a TSK-gel ODS-80Ts column (5 µm, 2.0×150 mm, TOSOH, Tokyo, Japan) at 40 °C. The mobile phase was water containing 0.1% formic acid (A) and methanol containing 0.1% formic acid (B). The flow rate was 200 µl min^{-1} and the gradient conditions were initially 40–90% B at 20 min.

LC/ITMS

The cyclic peptides were analyzed using LC/ITMS. The LC separation was carried out using an Agilent 1100 HPLC system (Agilent Technologies, Palo Alto, CA, USA). The sample preparation, column, mobile phase and gradient conditions were the same as those in the HPLC analysis. The entire eluent was directed into the mass spectrometer, in which it was diverted to waste at 2.5 min after injection to avoid any introduction of salts into the ion source. The MS analysis was accomplished using a Finnigan LCQ Deca XP plus ITMS (Thermo Fisher Scientific, San Jose, CA, USA) equipped with an electrospray ionization (ESI) interface. The ESI conditions in the positive ion mode were as follows: capillary temperature, 300 °C; sheath gas flow rate, 35 (arbitrary unit); ESI source voltage, 5000 V; capillary voltage, 43 V; and tube lens offset, 15 V·MS^n (n=1–4). Various scan ranges were used according to the molecular weights of the analytes. The MS^3 and MS^4 spectra were acquired, if possible and if necessary, for the structural analysis study of the degradation products.

RESULTS

Cyclic peptides selected

The bacterial cyclic peptides used in this study are classified structurally into the following two groups: cyclic oligopeptides and cyclic depsipeptides. The former includes bacitracin, colistin and polymyxin, whereas mikamycin, thiopeptin and WAP-8294A2 are included in the latter group, as shown in Figure 1. Bacitracin-A (**1**) is the main component of a mixture of the cyclic peptides containing a dihydrothiazole ring and was used after purification by high-speed countercurrent chromatography .[25] Colistins A (**2A**) and B (**2B**) and polymyxins B1 (**3B1**) and B2 (**3B2**) were used as mixtures.[26–29] A sample containing mikamycins A (**4A**) and B (**4B**), which possess characteristic structures with a different skeleton, also has other related components.[30] Thoipeptin B (**5**) is the main component among the related compounds and is characterized structurally as having several thiazole rings.[31] WAP-8294A2 (**6**) was isolated as an anti-methicillin-resistant *Staphylococcus aureus* agent and is being developed clinically.[32,33]

Degradation behavior

Degradation of these peptides was monitored using HPLC and LC/MS. Figure 2a shows the degradation manner of the cyclic peptides observed using HPLC in the presence of the B-9 cell extract. Three cyclic peptides, bacitracin-A (**1**), colistins A (**2A**) and B (**2B**) and polymyxin B1 (**3B1**), showed similar degradation behavior such that they decomposed smoothly within 12 h as shown in Figure 2a. Polymyxin B2 (**3B2**) is not shown in Figure 2a because it was difficult to observe using HPLC. Figure 3 shows the mass chromatograms monitored at calculated *m/z* of the degradation products of bacitracin-A (**1**) for 48 h. The antibiotic was observed as the doubly charged protonated molecule (*1*) at *m/z* 712.3 in the mass chromatograms, which disappeared completely within 6 h, and the degradation products were detected sequentially. The degraded ions, (*1a*) and (*1b*), were found initially at *m/z* 721 and 647, respectively. The detected intensity of *1a* reached a maximum at 1 h and disappeared by 12 h, and *1b* was observed maximally at 6 h and had disappeared by 12 h. Furthermore, the peaks at *m/z* 521 (*1c*) and 464 (*1d*) were observed at almost the same retention time and were found intensely as the doubly charged ion from 6 h. The ion (*1e*) formed from *1d* was detected at 12 h, and the intensity continued to increase by 48 h.

Colistins A (**2A**) and B (**2B**), whose doubly charged protonated molecules were observed at *m/z* 585.5 and 578.5, respectively, in the spectrum, were degraded quickly and the hydrolyzed products (*m/z* 594 and 587, respectively) were formed within 2 h (data not shown). However, no further degraded products were detected. Polymyxins B1 (**3B1**) and B2 (**3B2**) also provided the doubly charged protonated molecules at *m/z* 602.4 and 595.3, respectively, in the mass spectrum (data not shown). Although the hydrolyzed product of B1 was detected clearly at *m/z* 611.4, the corresponding ion was not detected in the case of B2 (data not shown).

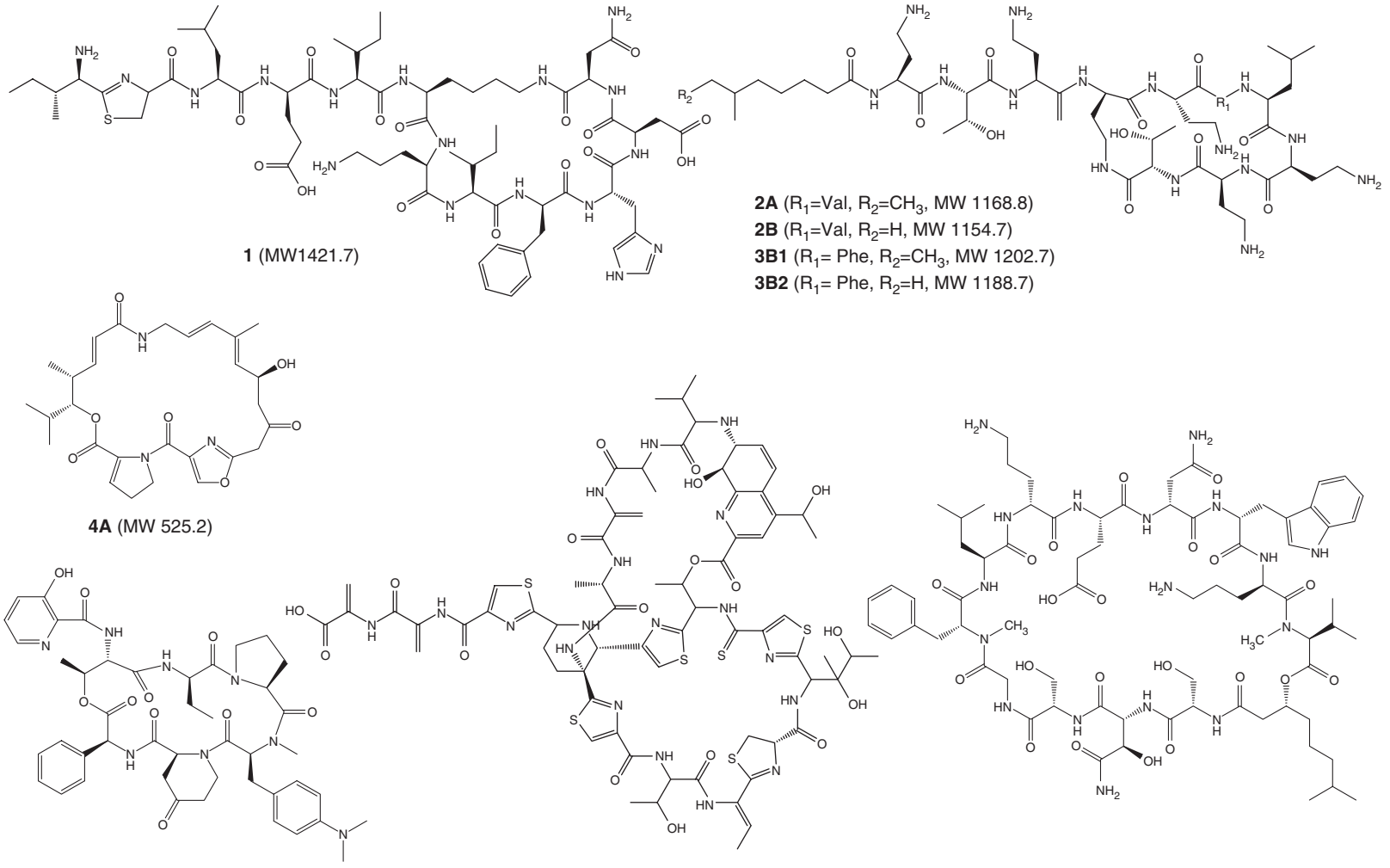

Figure 1 Structures of tested bacterial cyclic peptides.

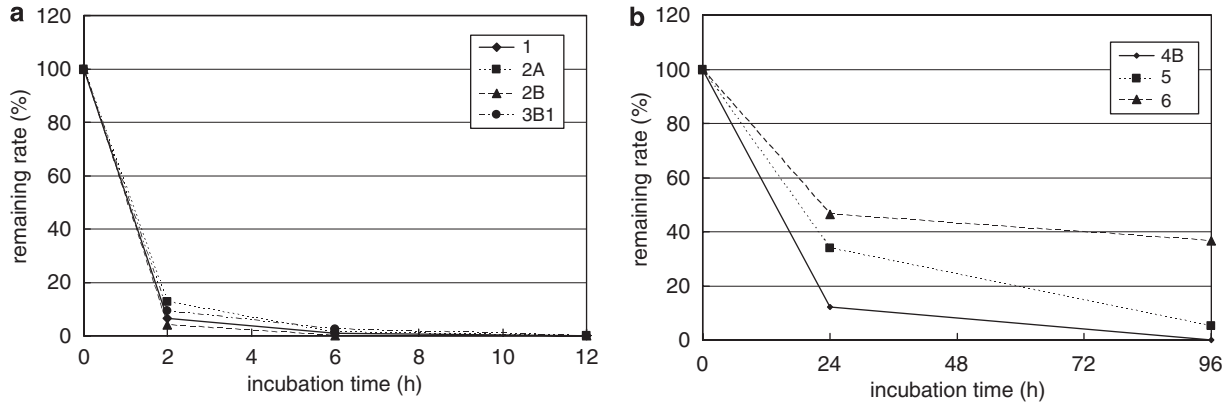

Figure 2 Degradation process of the cyclic peptides observed using HPLC in the presence of the cell extract of B-9. (**a**) Cyclic oligopeptides and (**b**) cyclic depsipeptides.

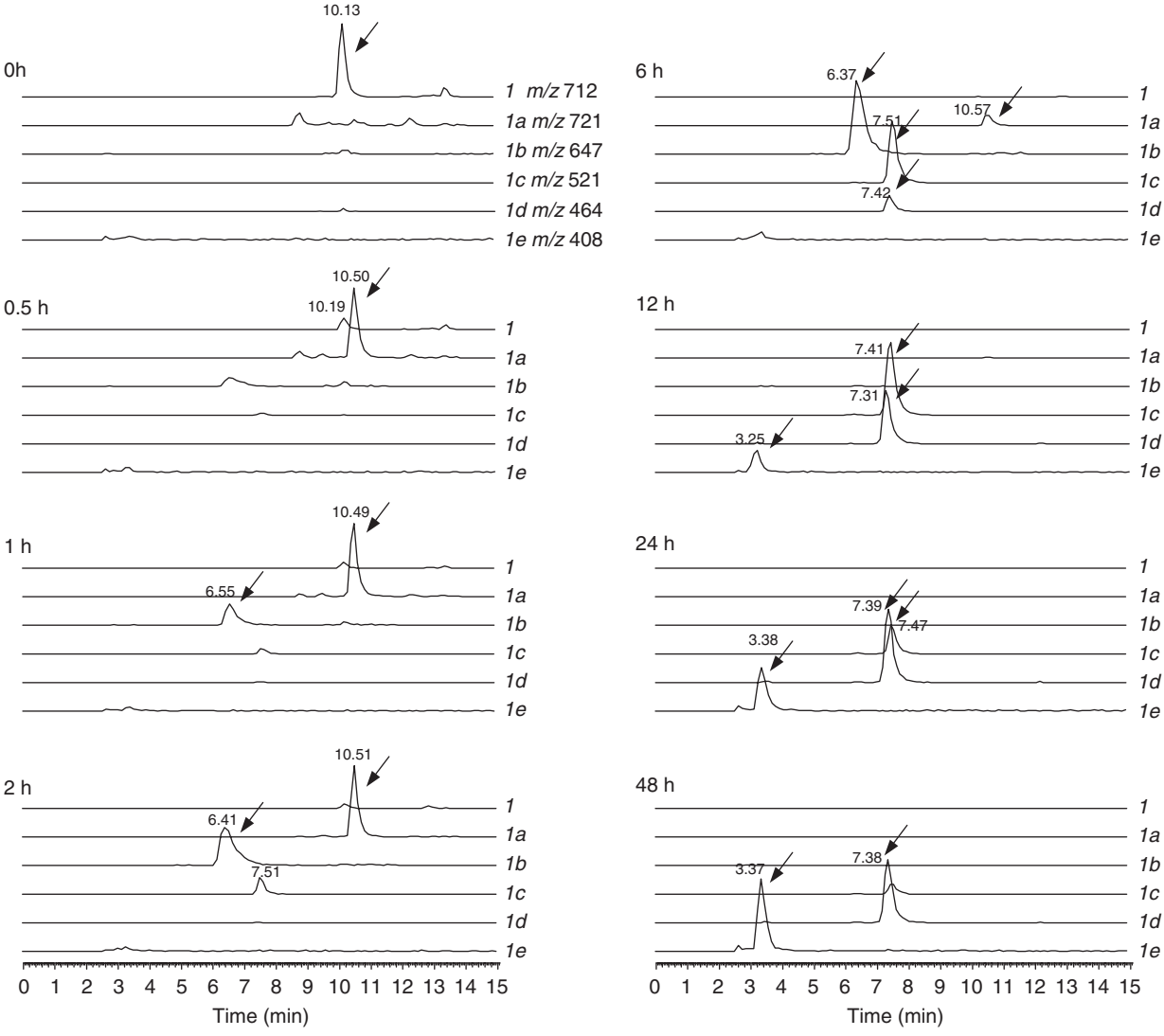

Figure 3 Mass chromatograms of 1 and its expected degradation products (theoretical *m/z* ± 1.5 Da) at 0, 0.5, 1, 2, 6, 12, 24 and 48 h after the beginning of degradation.

For the depsipeptides, mikamycins, thiopeptin and WAP-8294A2, a different degradation behavior was observed as shown in Figure 2b. Although the protonated molecule at *m/z* 526 from mikamycin A (**4A**) was almost degraded within 24 h, no definite degradation products was detected (data not shown). The hydrolyzed ion $(M+H+H_2O)^+$ (*4Ba*) at *m/z* 885.3 from mikamycin B (**4B**) increased with the

Figure 4 Proposed degradation products of the tested cyclic peptides and their monoisotopic molecular weights. (**a**) Cyclic oligopeptides and (**b**) cyclic depsipeptides.

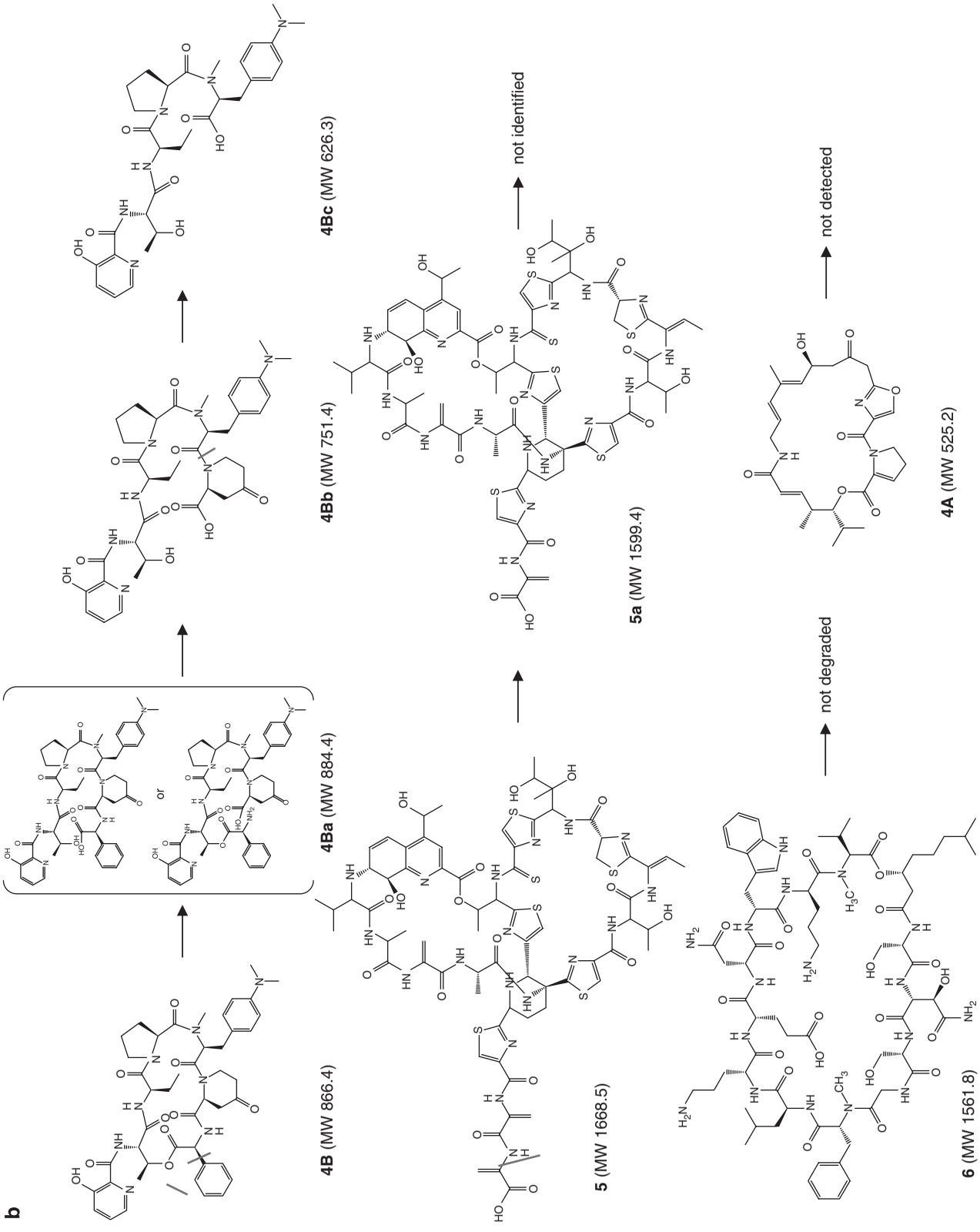

Figure 4 Continued.

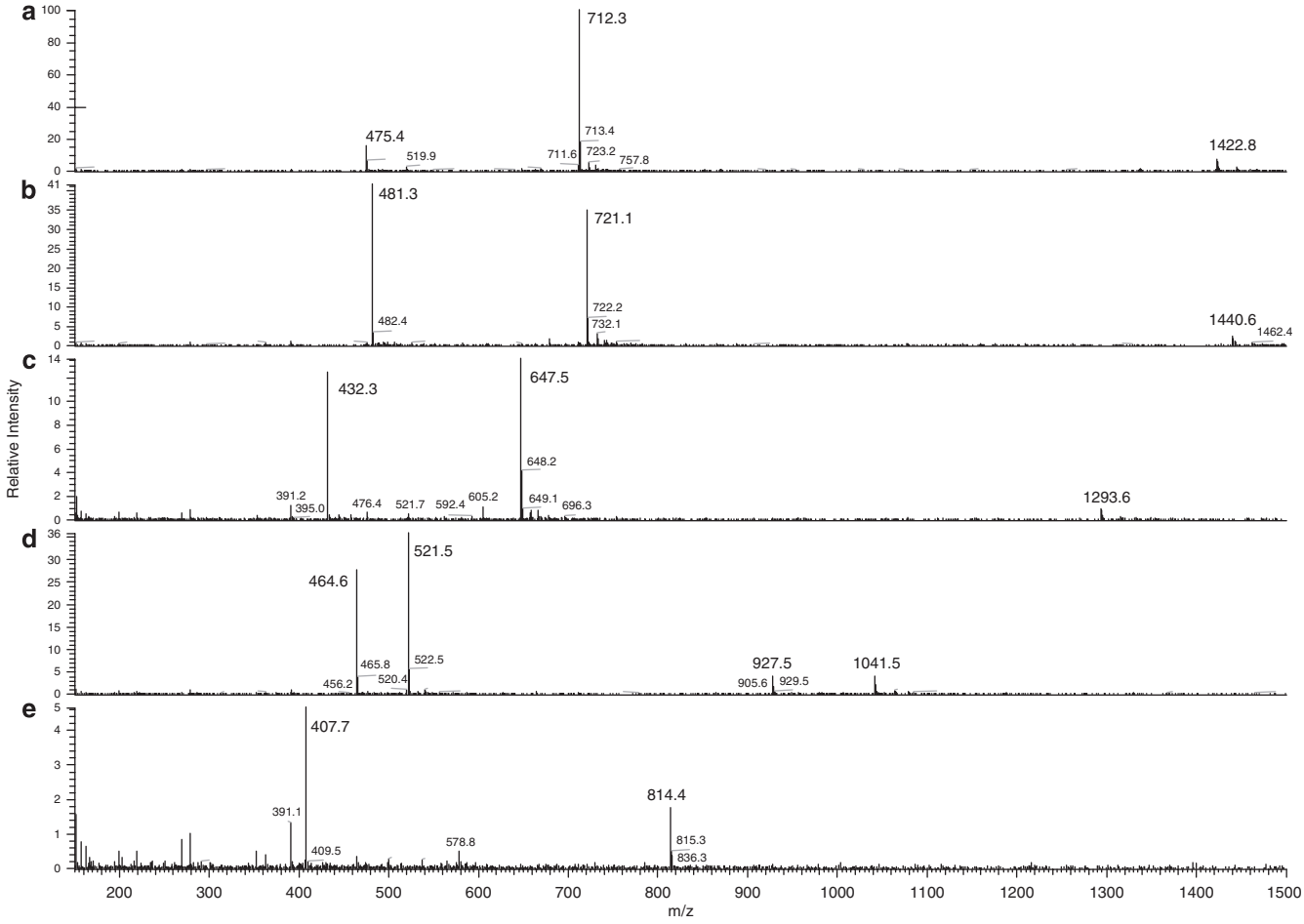

Figure 5 MS spectra of 1 (**a**) and its degradation products (**b**: 1*a*, **c**: 1*b*, **d**: 1*c* and 1*d*, **e**: 1*e*.).

decrease in the protonated molecule at *m/z* 867.4 within 12 h (data not shown). After 6 h, a characteristic ion (*4Bb*) appeared at *m/z* 752.3 and another ion (*4Bc*) was also found at *m/z* 627.5 by 96 h (data not shown). Thiopeptin B (**5**) was relatively resistant to this bacterium, and the protonated molecule (5) at *m/z* 1669.7 was observed even after 24 h (data not shown). However, the ion (5*a*) at *m/z* 1600.2 began to appear after 24 h and continued even at 96 h (data not shown). WAP-8294A2 (**6**) was very stable toward this strain and no degradation occurred during the experimental period.

Structural analysis of degradation products by LC/ITMS

The degradation products were detected using total ion current chromatography. When a degradation product was found, the structure was determined using the mass spectrum, mass chromatogram and MS^n technique. The proposed degradation products of the tested cyclic peptides are summarized in Figure 4. Figure 5 shows the mass spectra of the degradation products of bacitracin-A (**1**). The doubly charged ion (*1a*) at *m/z* 721.1 was formed by hydrolysis of the Phe–His peptide bond of **1**. The formation of the ion *1b* at *m/z* 647.5 was because of the cleavage at the Ile–Phe peptide bond of **1a**. The characteristic doubly charged ion (*1c*) at *m/z* 521.5 was formed by hydrolysis of the His–Asp peptide bond of **1b**. The subsequent degradation product at *m/z* 464.6, as the doubly charged ion that has almost the same retention time as *1d*, was decomposed to several product ions, *m/z* 796.5, 682.4, 554.4 and 441.1, under MS^2 conditions, indicating that a degradation product with the monoisotopic molecular weight of 926.6 was **1d** (Figure 6). The doubly charged ion at *m/z* 407.7 (*1e*) was formed by hydrolysis of the Ile–Orn peptide bond of **1d** (Figure 5). Although colistins A (**2A**) and B (**2B**) were firmly hydrolyzed, no definite degradation products was detected. Polymyxins B1 (**3B1**) and B2 (**3B2**) also showed a behavior similar to that of colistins (**2A** and **2B**) and no degradation product was found, except for the formation of (**3B1**+H_2O) (Figure 4a).

As mentioned above, mikamycin A (**4A**) was almost degraded within 24 h, and no definite degradation products was detected. Mikamycin B (**4B**) provided two degradation products, **4Ba** and **4Bb**. The MS^2 experiments of *4Bb* at *m/z* 752.4, MS^3 at *m/z* 609.2 and MS^4 at *m/z* 405.1 indicated that **4Bb** was the degradation product shown in Figure 7. The compound **4Bc** is a further degraded compound with the monoisotopic molecular weight of 626.3, as shown in Figure 4b. Thiopeptin B (**5**) was relatively stable, and a degradation product was detected as **5a** that corresponds to the loss of the dehydroalanine moiety from the parent compound. WAP-8294A2 (**6**) did not provide any degradation product (Figure 4b).

DISCUSSION

To extend the hydrolytic capability of the MC-degrading enzymes of B-9, we investigated the degradation behavior of the bacterial cyclic peptides in the presence of the B-9 cell extract. The examined peptides were divided structurally into two groups, that is, cyclic oligopeptide

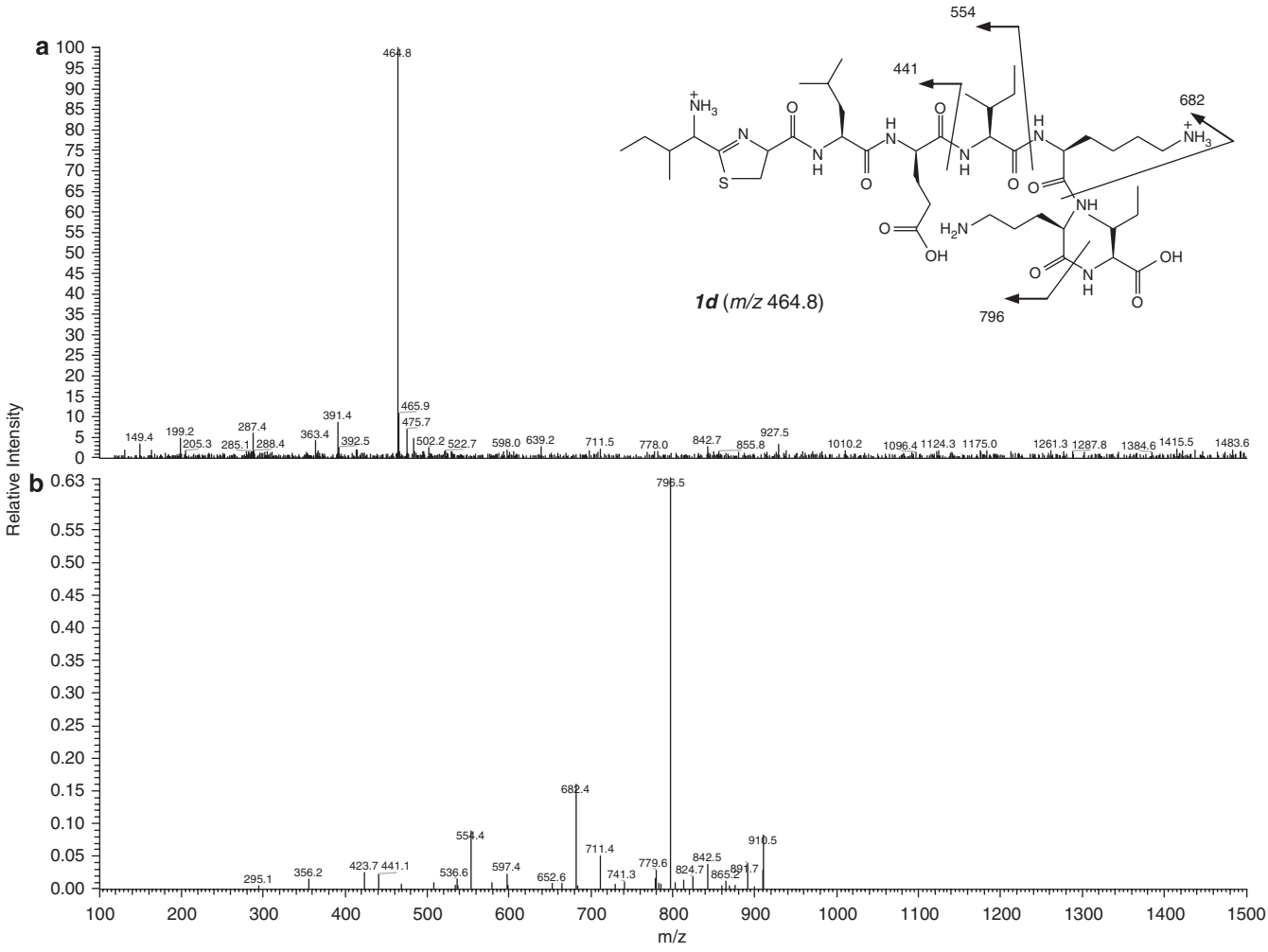

Figure 6 (**a**) LC/MS spectrum of 1*d* and (**b**) MS^2 spectrum of *m/z* 464.8 $(M+2H)^{++}$.

and depsipeptide, which showed individual characteristic features in the degradation behavior. The former, including bacitracin-A (**1**), colistin (**2**) and polymyxin B (**3**), showed a common degradation behavior in which these peptides are first hydrolyzed in the ring moiety to give linearized peptides, followed by hydrolysis of the peptide bonds. In this study, the linearized product (**1a**) and the subsequent hydrolyzed products (**1b**, **1c**, **1d**, and **1e**) of bacitracin-A (**1**) were identified. On the other hand, mikamycin (**4**), thiopeptin B (**5**) and WAP-8294A2 (**6**) in the latter group are depsipeptides with an ester bond but showed different degradation behavior. Usually, the B-9 strain first attacks the ester bond, and the resulting linearized peptide is then subjected to further hydrolysis. The case of mikamycin-B (**4B**) was a typical example, and two degradation products, **4Bb** and **4Bc**, were identified. However, the B-9 strain did not hydrolyze the ester bond, rather it hydrolyzed a peptide bond at the dehydroalanine-dehydroalanine in the C-terminus of thiopeptin B (**5**). This result may be caused by the steric exclusion of the enzymes and WAP-8294A2 (**6**) was strongly subjected to this effect but did not provide any degradation product.

B-9 is a bacterial strain isolated from a eutrophicated lake and belongs to *Sphingosinicella* sp., which can hydrolyze MCs and nodularin using its intracellular enzymes.[3] An earlier study was carried out to investigate further the hydrolytic capabilities of the MC-degrading enzymes of B-9.[13] As a result of this investigation, it was confirmed that the enzymes can also hydrolyze the peptide bonds of several cyanobacterial cyclic peptides that were structurally different from the MCs and nodularin.[13] In this study, the B-9 strain was also applied to the bacterial cyclic peptides, including cyclic oligopeptides and depsipeptides, and interesting results were obtained. On the basis of these results, the hydrolytic behavior using this strain is summarized as follows: (1) The reaction basically occurs at a peptide bond in a cyclic peptide moiety to give a linearized peptide. (2) B-9 initially hydrolyzes an ester bond in a depsipeptide and the resulting peptide is further hydrolyzed. (3) A peptide possessing a bulky ring is hydrolyzed at the acyclic part and no other reaction occurs. (4) The resulting linearized peptide is more quickly hydrolyzed compared with the original one. In some cases, it is difficult to detect the degraded peptides or amino acids.

As mentioned above, B-9 possesses at least three hydrolytic enzymes, namely, MlrA, MlrB and MlrC.[15] Very recently, it was found that another MC-degrading bacterium has additional enzymes that can also hydrolyze peptide bonds (personal communication). It is considered that the degradation capabilities of B-9 are not induced by the degradation substrates but are inherent, because we always used a

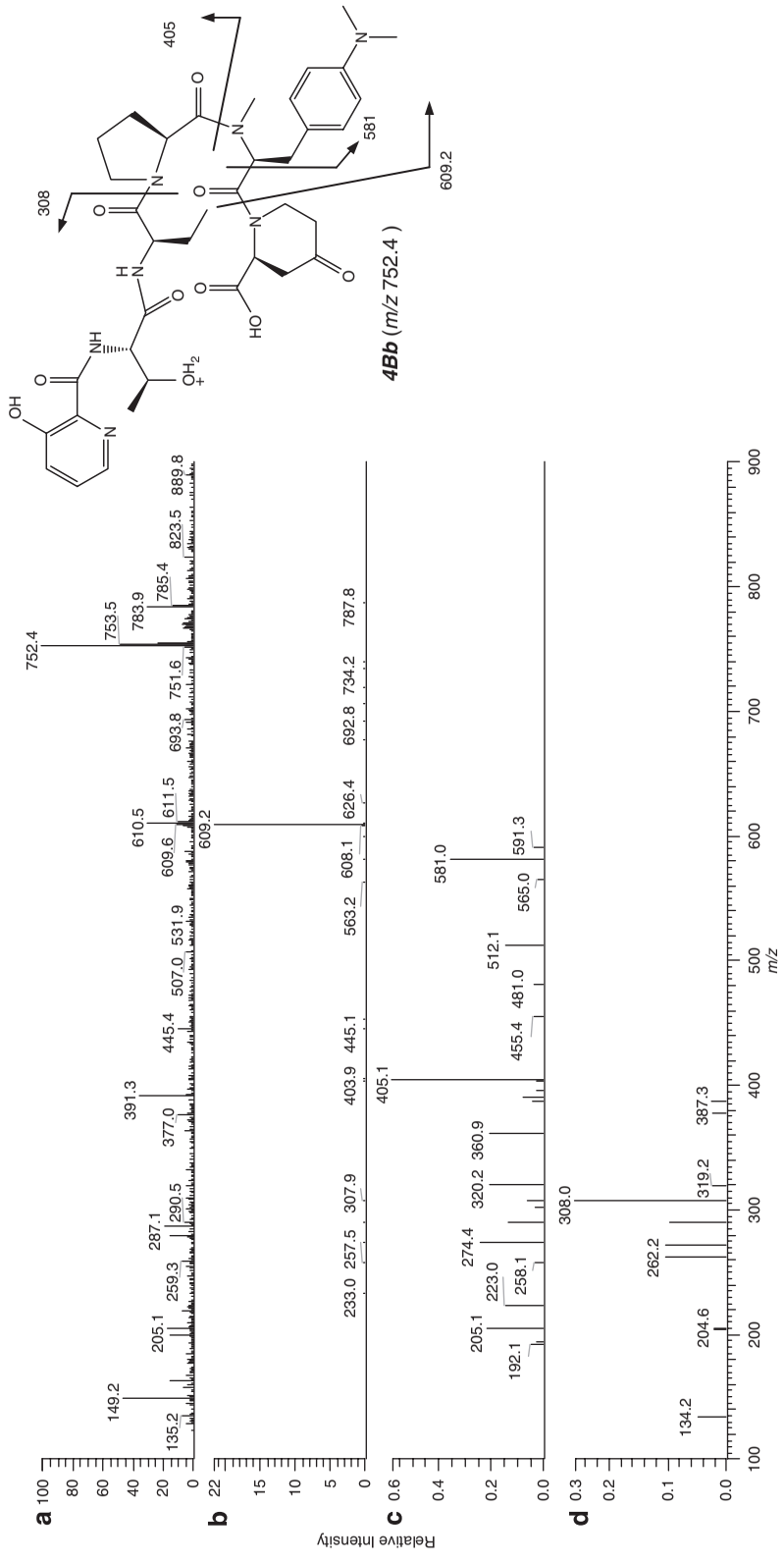

Figure 7 (**a**) LC/MS spectrum of 4Bb, (**b**) MS^2 spectrum of *m/z* 752.4, (**c**) MS^3 spectrum of *m/z* 609.2 and (**d**) MS^4 spectrum of *m/z* 405.1.

bacterial cell extract instead of growing bacteria, and the degradation began without any lag time. These results suggested that the substrate specificity of the hydrolytic enzymes of B-9 is relatively wide and that B-9 can be applied successfully to other cyclic peptides as shown in this study. How many hydrolytic enzymes does B-9 possess and how does B-9 use the inherent enzymes against substrates? It is likely that B-9 has further potential to hydrolyze other types of compounds.

It is laborious to obtain the partially hydrolyzed product of cyclic peptides produced using the NRPS pathway.[18–21] It is known that nagarse and colistinase hydrolyze some cyclic peptides, which are produced by bacteria and belong to the subtilisin family.[27] Subtilisin is a serine protease and cleaves a peptide bond at the C-terminus side of hydrophobic amino acids.[27] To the best of our knowledge, no detailed result has been reported regarding the degradation behavior of cyclic peptides by subtilisin. It is considered that the hydrolytic enzymes from B-9 possess wider substrate specificities similar to that of subtilisin. Therefore, the B-9 strain can be one of the most effective tools for the partial hydrolysis of a cyclic peptide. Indeed, we have succeeded in preparing an immobilized B-9 with a polyester resin,[2] which would be an appropriate and effective way to degrade cyclic peptides.

Conclusions

This study was carried out to further investigate the hydrolytic capabilities of the MC-degrading enzymes of B-9. As a result of this investigation, it was confirmed that the enzymes can also hydrolyze the peptide bonds of several bacterial cyclic peptides. In addition, the use of the cell extract suggested that these unique activities were present inherently in all MC-degrading bacteria, including B-9. Although the role of these enzymes in bacteria is not clarified fully, the abilities of these enzymes in microorganisms existing in the natural environment may contribute to environmental self-purification. On the other hand, this study also indicates the possibility that a technique using B-9 would be a practical method for natural product chemistry.

ACKNOWLEDGEMENTS

The authors thank Dr Yoshitomo Ikai and Mr Azusa Kato for providing several cyclic peptides and WAP-8294A2, respectively.

1 Kuiper-Goodman, T., Falconer, I. & Fitzgerald, J. Human Health Aspects. In *Toxic Cyanobacteria in Water* (eds Chorus, I., Bartram, J.) 113–153 (E & FN Spon, London, 1999).
2 Tsuji, K., Asakawa, M., Anzai, Y., Sumino, T. & Harada, K.-I. Degradation of microcystins using immobilized microorganism isolated in an eutrophic lake. *Chemosphere* **65,** 117–124 (2006).
3 Imanishi, S., Kato, H., Mizuno, M., Tsuji, K. & Harada, K.-I. Bacterial degradation of microcystins and nodularin. *Chem. Res. Toxicol.* **18,** 591–598 (2005).
4 Jones, G. J., Bourne, D. G., Blakeley, R. L. & Doelle, H. Degradation of the cyanobacterial hepatotoxin microcystin by aquatic bacteria. *Nat. Toxins.* **2,** 228–235 (1994).
5 Takenaka, S. & Watanabe, M. F. Microcystin LR degradation by *Pseudomonas aeruginosa* alkaline protease. *Chemosphere* **34,** 749–775 (1997).
6 Park, H. D. *et al.* Degradation of the cyanobacterial hepatotoxin microcystin by a new bacterium isolated from a hypertrophic lake. *Environ. Toxicol.* **16,** 337–343 (2001).
7 Saitou, T., Sugiura, N., Itayama, T., Inamori, Y. & Matsumura, M. Degradation characteristics of microcystins by isolated bacteria from Lake Kasumigaura. *J. Wat. Supply Res. Technol—Aqua.* **52,** 13–18 (2003).
8 Ishii, H., Nishijima, M. & Abe, T. Characterization of degradation process of cyanobacterial hepatotoxins by a gram-negative aerobic bacterium. *Water Res.* **38,** 2667–2676 (2004).
9 Rapala, J. *et al. Paucibacter toxinivorans* gen. nov., sp. nov., a bacterium that degrades cyclic cyanobacterial hepatotoxins microcystins and nodularin. *Int. J. Syst. Evol. Microbiol.* **55,** 1563–1568 (2005).
10 Valeria, A. M., Ricardo, E. J., Stephan, P. & Alberto, W. D. Degradation of Microcystin-RR by *Sphingomonas* sp. CBA4 isolated from San Roque reservoir (Cordoba-Argentina). *Biodegradation* **17,** 447–455 (2006).
11 Maruyama, T. *et al. Sphingosinicellamicrocystinivorans* gen. nov., sp. nov., a microcystin-degrading bacterium. *Int. J. Syst. Evol. Microbiol.* **56,** 85–89 (2006).
12 Bourne, D. G., Blakeley, R. L., Riddles, P. & Jones, G. J. Biodegradation of the cyanobacterial toxin microcystin LR in natural water and biologically active slow sand filters. *Water Res.* **40,** 1294–1302 (2006).
13 Kato, H., Imanishi, S. Y., Tsuji, K. & Harada, K.-I. Microbial degradation of cyanobacterial cyclic peptides. *Water Res.* **41,** 1754–1762 (2007).
14 Bourne, D. G. *et al.* Enzymatic pathway for the bacterial degradation of the c yanobacterial cyclic peptide toxin microcystin LR. *Appl. Environ. Microbiol.* **62,** 4086–4094 (1996).
15 Bourne, D. G., Riddles, P., Jones, G. J., Smith, W. & Blakeley, R. L. Characterisation of a gene cluster involved in bacterial degradation of the cyanobacterial toxin microcystin LR. *Environ. Toxicol.* **16,** 523–534 (2001).
16 Harada, K.-I. *et al.* Isolation of Adda from microcystin-LR by microbial degradation. *Toxicon* **44,** 107–109 (2004).
17 Harada, K.-I. Production of secondary metabolites by freshwater cyanobacteria. *Chem. Pharm. Bull (Tokyo)* **52,** 889–899 (2004).
18 Dittmann, E., Neilan, B. A., Erhard, M., von Dohren, H. & Borner, T. Insertional mutagenesis of a peptide synthetase gene that is responsible for hepatotoxin production in the cyanobacterium Microcystis aeruginosa PCC 7806. *Mol. Microbiol.* **26,** 779–787 (1997).
19 Nishizawa, T., Asayama, M., Fujii, K., Harada, K.-I. & Shirai, M. Genetic analysis of the peptide synthetase genes for a cyclic heptapeptide microcystin in Microcystis spp. *J. Biochem.* **126,** 520–529 (1999).
20 Nishizawa, T. *et al.* Polyketide synthase gene coupled to the peptide synthetase module involved in the biosynthesis of the cyclic heptapeptide microcystin. *J. Biochem.* **127,** 779–789 (2000).
21 Demain, A. L. Pharmaceutically active secondary metabolites of microorganisms. *Appl. Microbiol. Biotechnol.* **52,** 455–463 (1999).
22 Butler, M. S. The role of natural product chemistry in drug discovery. *J. Nat. Prod.* **67,** 2141–2153 (2004).
23 Newman, D. J. & Cragg, G. M. Natural products as sources of new drugs over the last 25 years. *J. Nat. Prod.* **70,** 461–477 (2007).
24 Tsuji, K. *et al.* Stability of microcystins from cyanobacteria: effect of light on decomposition and isomerization. *Environ. Sci. Technol.* **28,** 173–177 (1994).
25 Harada, K.-I. *et al.* Isolation of bacitracins A and F by high-speed countercurrent chromatography. *J. Chromatogr.* **538,** 203–212 (1991).
26 Ikai, Y. *et al.* Total structures of colistin minor components. *J. Antibiot.* **51,** 492–498 (1998).
27 Suzuki, T., Hayashi, K. & Fujikawa, K. Studies on the chemical structures of colistin. III Enzymic hydrolysis of colistin A. *J. Biochem.* **54,** 412–418 (1964).
28 Suzuki, T., Hayashi, K., Fujikawa, K. & Tukamoto, K. Studies on the chemical structures of colistin. IV. Chemical structure of colistin B. *J. Biochem.* **56,** 182–189 (1964).
29 Thomas, A. H., Thomas, J. M. & Holloway, I. Microbiological and chemical analysis of polymyxin B and polymyxin E (colistin) sulphates. *Analyst* **105,** 1068–1075 (1980).
30 Watanabe, K. Studies on mikamycin IV. The isolation and properties of mikamycin B. *J. Antibiot.* **13,** 57–61 (1960).
31 Miyairi, N. *et al.* Thiopeptin, a new feed additive antibiotic: microbiological and chemical studies. *Antimicrob. Agents Chemother.* **1,** 192–196 (1971).
32 Kato, A. *et al.* A novel anti-MRSA antibiotic produced by *Lysobacter* sp. *J. Am. Chem. Soc.* **119,** 6680–6681 (1997).
33 Kato, A. *et al.* A new anti-MRSA antibiotic complex, WAP-8294A I. Taxonomy, isolation and biological activities. *J. Antibiot.* **51,** 929–935 (1998).

The Journal of Antibiotics (2009) 62, 191–194

www.nature.com/ja

ORIGINAL ARTICLE

Albucidin: a novel bleaching herbicide from *Streptomyces albus* subsp. *chlorinus* NRRL B-24108

Donald R Hahn, Paul R Graupner, Eleanor Chapin, John Gray, D Heim, Jeffrey R Gilbert and B Clifford Gerwick

A novel nucleoside phytotoxin, albucidin (1), was isolated from the culture broth of *Streptomyces albus* subsp. *chlorinus* NRRL B-24108 using bioassay directed fractionation. The structure of the new natural product, albucidin, was determined by NMR and MS; however, the compound has been reported earlier in the literature following synthetic modification of oxetanocin. This is the first report of herbicidal activity for compounds of this structural type. Albucidin shows high levels of broad spectrum activity following post-emergence applications as well as moderate levels of pre-emergence activity. Accordingly, albucidin could be an important new lead for herbicide discovery.
The Journal of Antibiotics (2009) **62,** 191–194; doi:10.1038/ja.2009.11; published online 27 February 2009

Keywords: albucidin; oxetanocin; phytotoxic; phytotoxin; herbicidal; *Streptomyces albus*

INTRODUCTION

Natural products have served as leads or starting points for the development and commercialization of numerous agricultural chemicals. In most cases, synthetic optimization has been necessary to address limitations in potency or field translation, although there are exceptions. For example, the commercial insecticide, spinosyn, is derived directly from the fermentation of *Saccharopolyspora spinosa*.[1] However, both the strobilurin fungicides and the pyrethroid insecticides are the products of synthetic optimization of natural products with poor photostability.[2,3] Particularly significant among herbicides derived from natural products are glufosinate, a phosphorylated amino acid present in the microbial tripeptides, phosalacine and bialaphos, and the triketone herbicides that were derived from the synthetic optimization of leptospermone.[4] In both cases, these herbicides introduced new modes-of-action for commercial weed control, an important success factor for new products. In the course of screening for new natural product herbicides, we identified a novel phytotoxic metabolite, albucidin (**1**), from the culture broth of an actinomycete (Figure 1). This metabolite showed herbicidal activity against a broad spectrum of weeds. The isolation and biological activity of the metabolite as well as physiochemical properties and structural elucidation are provided in this report.

RESULTS

Fermentation and isolation

Streptomyces albus subsp. *chlorinus* NRRL B-24108 was fermented in shake flasks. The production of **1** began at 6 days and increased to a maximum at 12–13 days. Greater than 90% of the phytotoxic activity in shake flask cultures was localized in the broth and could be partitioned from the aqueous broth into butanol. Isolation was achieved by semi-preparative chromatography under isocratic conditions in which the activity eluted at 6.9 min. A strong absorbance was recorded at this retention time with absorbance maxima of 200 and 257 nm. The total recovered yield was approximately 2 mg l^{-1} fermentation. Interestingly, the activity eluted later under neutral pH conditions than under acidic conditions, which gave an early indication of the presence of an amine. The compound was not stable under acidic conditions ($<$50% recovery at pH 2, 24 h; $\sim$100% recovery at pH 6.5, 24 h).

Structural assignment

The ESI LC/MS analysis of **1** indicated a molecular weight of 221, with accurate mass CI giving the molecular ion $[M+H]^+$=222.0988, $C_9H_{12}N_5O_2$ requiring 222.0991. With initial NMR analysis suggesting a nucleoside, ESI LC/MS/MS was then used to probe the nature of the nucleoside base. Non-selective fragmentation of the molecule yielded an ion at *m/z* 136, the MS/MS spectrum of this fragment ion was acquired, and compared with that from standard samples of adenosine and 2-aminopurine riboside. The spectra for **1** and adenosine were nearly identical, whereas those from **1** and 2-aminopurine riboside gave peak intensities that were significantly different. This indicated that the position of the amino group for **1** was located at C-6′.

The NMR analysis of **1** in D_2O exhibited broad signals, but revealed a nucleoside with fewer aliphatic signals than expected for adenosine. An adenine base was suggested by the two downfield signals (between 8.5 and 8.0 p.p.m.), and confirmed as described by MS. The aliphatic protons resonated as broad signals, not allowing the measurement of any coupling constants (Table 1). Analysis of an HMQC experiment

Discovery Research, Dow AgroSciences, LLC, Indianapolis, IN, USA
Correspondence: Dr DR Hahn, Discovery Research, Dow AgroSciences, LLC, 9330 Zionsville Rd, Indianapolis, IN 48268-1054, USA.
E-mail: drhahn@dow.com
Received 10 December 2008; revised 23 January 2009; accepted 25 January 2009; published online 27 February 2009

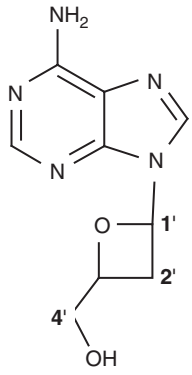

Figure 1 Structure of albucidin (**1**).

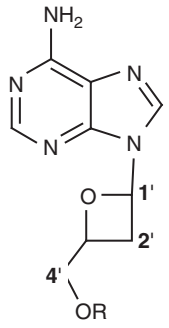

1 R=H
2 R=Acetyl

Figure 3 Structure of acetylated albucidin (**2**).

Table 1 1H NMR data for 1 and acetylated product 2

Assignment	***1*** *(D_2O)*	***2*** *(CD_3OD)*	*J (for 2)* *(Hz)*
Adenine-H	8.5	8.6	—
Adenine-H	8.2	8.2	—
1	6.6	6.7	6.9, 6.9
2	3.4	3.5	12.4, 6.9, 6.9
	3.3	3.3	12.4, 6.9, 6.9
3	4.9	5.0	m
4	3.9	4.5	12.8, 5.1
	3.7	4.4	12.8, 2.9
Acetyl Me	—	2.2	—

Table 2 Pre-emergence activity of 1[a]

Rate	*AVEFA*	*ECHCG*	*HELAN*	*IPOHE*
g per ha	*Visual injury (%)*			
2000	80	95	95	85
1000	50	90	90	80
500	45	60	80	80
250	20	20	75	75
125	0	0	75	75
62.5	0	0	65	50

[a]See text for species abbreviations.

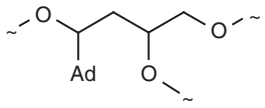

Figure 2 Identified spin system from 2D NMR spectroscopy, Ad=adenine.

indicated the presence of two methylene and two methine groups, only one methylene of which was not substituted with an oxygen atom. The molecular formula of $C_9H_{11}N_5O_2$ allowed for seven unsaturations, six of which were accounted for by the adenosine base, indicating one unsaturation for this portion of the molecule, suggesting the presence of one ring, and thus one hydroxy group. Analysis of the 2D COSY spectrum indicated that the upfield methylene was indeed located between the two methines giving the spin system shown in Figure 2. With only two oxygen atoms accounted for by the molecular formula, the final ring may be assembled through ether linkages to give three possible structures for the molecule—a 3-, 4- or 5-member ring—two of which were described in the literature. Comparison with this literature data suggested that the compound contained an oxetane ring,[5] rather than a furan ring [6] or an epoxide.

Confirmation of this assignment came from the acetylated derivative (**2**), which was readily prepared from **1** with acetic anhydride in pyridine (Figure 3). Comparison of the ^1H NMR spectrum of **2** in $CDCl_3$ indicated a large downfield shift for the terminal methylene protons confirming the site of the hydroxy group in albucidin, and thus the oxetane ring.

Biological activity

Plants emerging from albucidin-treated soil (pre-emergence test) were severely stunted. Broadleaf weeds were more sensitive than grasses and most did not develop beyond the cotyledonary stage. At lower rates, the plants did develop some new growth that was bleached. The pre-emergence activity listed in Table 2 suggests that the mode of action is a metabolic perturbation not limited to bleaching, as most plants did not develop beyond the cotyledonary stage.

The post-emergence activity of albucidin is shown in Table 3. The onset of symptoms after post-emergence application was extremely slow, as only the new growth developed subsequent to the application initially appeared bleached. Most plants continued to grow following treatment. Pre-existing growth on the plants at the time of treatment did not show symptoms until many weeks after treatment. Symptoms progressed in severity with time, and chlorotic new growth ultimately became necrotic. Most plants treated at higher rates (>100 g per ha) died 28–35 days after application.

DISCUSSION

This is the first report of the natural product, albucidin (MW 221.0913; $C_9H_{11}N_5O_2$), isolated from a novel strain of *S. albus* subsp. *chlorinus* (NRRL B-24108). The structure was discovered earlier as a semisynthetic derivative of the natural anti-viral oxetanocin from *Bacillus megaterium*.[5,7] The IC_{50} of 2′-desmethoxy oxetanocin A (**1**) against HIV was approximately 10-fold better than that of oxetanocin A. However, subsequent synthetic efforts indicated that carbocylic analogs of oxetanocin were more potent anti-viral agents than analogs with an oxetanosyl *N*-glycoside;[8–10] therefore, **1** was not investigated further. It is not known whether the anti-viral activity reported for

Table 3 Post-emergent activity of 1, 21-day grading[a]

Conc. (p.p.m.)	220	110	55	27	14
	Visual injury (%)				
GOSHI	70	45	40	25	25
BRSNN	85	80	65	65	45
GLXMA	80	60	60	60	45
BEAVA	85	70	70	70	65
STEME	90	75	70	50	45
XANST	98	90	85	80	80
CHEAL	75	55	65	50	40
IPOHE	85	75	70	70	45
AMARE	90	75	70	50	60
ABUTH	85	80	75	65	55
VIOAR	75	50	50	30	20
POLCO	90	85	75	70	65
ZEAMX	95	75	65	20	0
ORYSA	65	55	40	60	35
TRZAX	88	85	45	20	10
ALOMY	98	75	60	20	0
ECHCG	85	80	70	65	30
DIGSA	90	75	65	65	60
SORVU	95	90	80	60	10
AVEFA	98	90	75	40	35
CYPES	75	65	0	0	0

[a]See text for species abbreviations.

oxetanocin and related compounds is linked to the herbicidal activity discovered for **1**.

Albucidin is a very potent herbicide (lethality at rates less than 100 g per ha in some species) that induces chlorosis and bleaching in many grass and broadleaf weeds. Although potent, the onset of symptoms after post-emergence application is very slow and effects are seen principally in new growth. The mode of action has not been pursued, but the speed of action and progression of symptoms are relatively unique and suggest that the mode of action may be new. It seems possible that the slow onset of symptoms from **1** reflects a requirement for *in planta* activation. Hydantocidin, a nucleoside-type phytotoxin, is phosphorylated *in planta* to the active inhibitor of adenylosuccinate synthase.[11] Whether phosphorylation resulting in bioactivation of albucidin may similarly occur is unknown and under investigation.

EXPERIMENTAL SECTION

Taxonomy of the producing organism

The albucidin producing organism, strain LW030448, was isolated from soil at Lilly Research Laboratories in Indianapolis, IN, USA. Strain LW030448 produced well-branched vegetative mycelia and aerial hyphae, which were flexous or loose spirals. The spores were round with a smooth surface (Figure 4). Substrate mycelium was yellow to brown and aerial mycelial color was gray to green-yellow. The strain could use adonitol, inositol, mannitol and xylose for growth and could not grow at temperatures below 25 °C. The partial 16S rDNA sequence (accession number DQ069278) as well as morphological and growth characteristics of strain LW030448 were highly similar to *S. albus* ATCC 3004. Therefore, strain LW030448 was identified as a unique subspecies, *S. albus* subsp. *chlorinus*, distinguishable by a characteristic brilliant green-yellow pigment produced in the aerial mycelium on Oatmeal Agar (ISP-3). Strain LW030448 has been deposited in the Agricultural Research Service Culture Collection at the National Center for Agricultural Utilization Research, Peoria, Illinois, USA under the accession number NRRL B-24108.

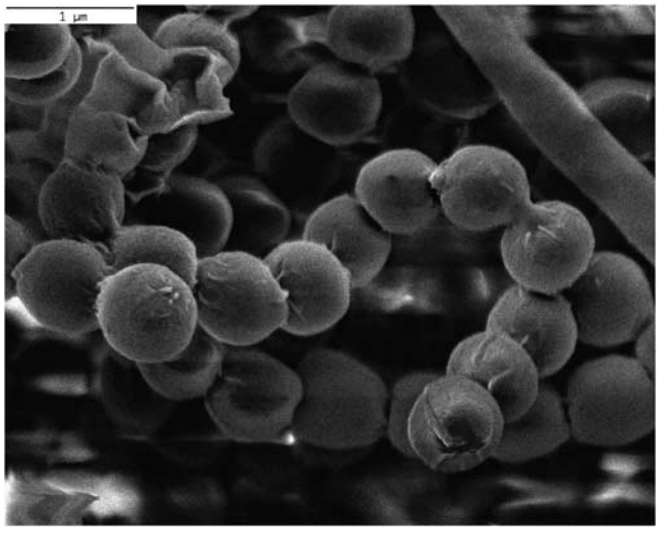

Figure 4 Scanning electron micrograph of *Streptomyces albus* subsp. *chlorinus* LW030448.

Fermentation and isolation

Strain LW030448 was fermented in Medium G (500 ml per 2.8 l-baffled Fernbach flask (Bellco, Vineland, NJ, USA)). Medium G contained soybean flour Nutrisoy (ADM, Decatur, IL, USA) 5 g, dextrose 10 g, glycerin 10 g, starch solubles 5 g, potato dextrin 20 g, corn steep solids 5 g, $CaCO_3$ 3 g, phytic acid 1 g, cane molasses 10 g, $FeCl_2 \bullet 4\ H_2O$ 0.1 g, $ZnCl_2$ 0.1 g, $MnCl_2 \bullet 4\ H_2O$ 0.1 g and $MgSO_4 \bullet 7\ H_2O$ 0.5 g in 1 l of deionized water; pH 7.0. The flasks were inoculated with plugs from freshly sporulated agar culture and incubated at 29 °C, 150 r.p.m. for 13 days. Fermentation broth (50 l) was separated from the mycelium by centrifugation and the phytotoxic activity partitioned from the aqueous broth into butanol (150 l).

Isolation was achieved by re-dissolving the dried butanol extract in 25% aqueous acetonitrile and fractionating by semi-preparative chromatography on reversed-phase C-18 (column 10 mm×25 cm, 5 µm particle size, flow rate 5 ml min^{-1}) under isocratic conditions of 6% acetonitrile in water at pH 6.5. The active metabolite eluted at a retention time of 6.9 min based on bioassay against *Echinochloa crus-galli* and *Helianthus annuus* using procedures described earlier.[12]

NMR sectroscopy

The NMR spectra were acquired on a Bruker 400 MHz spectrometer (Bruker BioSpin, Billerica, MA, USA), operating at 400.13 MHz. The sample was dissolved in 0.25 ml of D_2O, and placed in a 5 mm Shigemi micro-tube (Shigemi Inc, Allison Park, PA, USA). For the 1H/1H COSY, 256 experiments consisting of 1 K data points were collected with 96 transients collected per experiment. ^{13}C data were acquired using a 2D inverse-detected HMQC experiment. For this data set, 256 experiments were acquired over 2 K data points, with 160 transients per experiment.

Mass spectrometry

The LC/MS analysis was carried out using a Finnigan TSQ-700 triple quadrupole mass spectrometer (Finnigan-MAT, San Jose, CA, USA) equipped with both electrospray (ESI) and atmospheric pressure chemical oxidation (APCI) interfaces. Gradient high-performance liquid chromatography separations were accomplished on a Kromacil C-18 4.5×250 mm column (Eka Chemicals Separation Products, Bohus, Sweden), with simultaneous UV (254 nm) and mass spectral detection (positive ESI and APCI in both MS and MS/MS modes).

Accurate mass analyses were carried out using a Finnigan MAT-95q magnetic sector mass spectrometer (Finnigan-MAT) using both electron ionization, and methane chemical ionization. Samples were introduced through the direct exposure probe, and perfluorokerosene was used as an internal standard.

Acetylation of albucidin

A very small sample (<1 mg) of **1** was dissolved in pyridine (0.25 ml) and acetic anhydride (0.1 ml). The solution was stirred overnight and the excess solvents were removed by evaporation. Purification by high-performance liquid chromatography yielded the monoacetate of albucidin (**2**); MS (+ve ESI); 264 (100%, M+), 136 (40%): NMR, see Table 1.

Biological activity

Pre-emergence and post-emergent herbicide tests were conducted in a manner similar to that described earlier.[13] Whole plant activity was assessed on the following species using one or both of the above means of application: *Gossypium hirsutum* (GOSHI), *Brassica napus* (BRSNN), *Glycine max* (GLXMA), *Beta vulgaris* (BEAVA), *Stellaria media* (STEME), *Xanthium strumarium* (XANST), *Chenopodium album* (CHEAL), *Ipomoea hederacea* (IPOHE), *Amaranthum retroflexus* (AMARE), *Abutilon theophrasti* (ABUTH), *Viola arvensis* (VIOAR), *Polygonum convolvulus* (POLCO), *Zea mays* (ZEAMX), *Orysa sativa* (ORYSA), *Triticum aestivum* (TRZAX), *Alopecurus myosuroides* (ALOMY), *E. crus-galli* (ECHCG), *Digitaria sanguinalis* (DIGSA), *Sorghum vulgare* (SORVU), *Avena fatua* (AVEFA), *Cyperus esculentus* (CYPES) and *H. annuus* (HELAN). Plants were seeded in sandy loam soil (pre-emergence testing) or a commercial potting mix containing 30% organic matter (post-emergence testing). For post-emergence applications, each pot was thinned to 2–25 plants per pot, depending on species. Plants were grown to a height of 3–10 cm before application. Albucidin was dissolved in methanol and diluted with 25% aqueous acetone containing 0.05% non-ionic surfactant. Serial dilutions were carried out in a solvent mixture containing 25% acetone and 0.05% non-ionic surfactant to achieve the desired p.p.m. concentrations. Each spray concentration was applied with an atomizer driven by compressed air at a pressure of 22 kPa, and approximately 1.5 ml of total solution was applied to each pot. The plants were returned to a greenhouse (16-h photoperiod, 27 °C day, 24 °C night) for the duration of the study and watered by sub-irrigation. After 21 days, the treated plants were compared with untreated controls and graded on a scale of 0–100, where 0 represented no effect and 100 indicated complete plant death.

For pre-emergence tests, albucidin was dissolved and diluted as described above and applied to the surface of pots seeded with the desired test species. Applications were made with a hand-held syringe equipped with a hollow cone nozzle to distribute the spray solution (2.5 ml per pot) as a course mist. The pots were watered manually to move the chemical into the soil and initiate seed germination. The pots were returned to the greenhouse (16-h photoperiod, 27 °C day, 24 °C night) for the duration of the study and top-watered daily. After 21 days, the emergence and height of plants from treated pots were compared with those of untreated controls on a scale of 0–100 as described above.

ACKNOWLEDGEMENTS

We thank researchers at Eli Lilly & Co. for the original isolation of *S. albus* subsp. *chlorinus* LW030448 from soil, Bill Heeschen of Dow, Midland, MI for the SEM micrograph and Midi Laboratories, Newark, DE for DNA sequencing.

1 Sparks, T. C., Thompson, G., Kirst, H. A., Hertlein, M. B. & Larson, L. L. Biological activity of the spinosyns, new fermentation derived insect control agents, on tobacco budworm (Lepidoptera: *Noctuidae*) larvae. *J. Econ. Entomol.* **91,** 1277–1283 (1998).
2 Sauter, H., Ammermann, E. & Roehl, F. Stobilurins – From natural products to a new class of fungicides. in *Crop Protection Agents from Nature* (ed Copping, L. G.) 50–81 (The Royal Society of Chemistry, Cambridge, 1996).
3 Elliot, M. Synthetic insecticides related to the natural pyrethrins. in *Crop Protection Agents from Nature* (ed. Copping, L. G.) 254–300 (The Royal Society of Chemistry, Cambridge, 1996).
4 Lee, D. L. *et al.* The discovery and structural requirements of inhibitors of p-hydroxylphenylpyruvate dioxygenase. *Weed Sci.* **45,** 601–609 (1997).
5 Kitagawa, M., Hasegawa, S., Saito, S., Shimada, N. & Takita, T. Synthesis and antiviral activity of oxetanocin derivatives. *Tetrahedron Lett.* **32,** 3531–3534 (1991).
6 Yang, T. *et al.* Synthesis of [4-(hydroxyl)tetrahydrofuran-2-yl]nucleosides as a novel class of uridine phosphorylase inhibitors. *Tetrahedron Lett.* **36,** 983–986 (1995).
7 Shimada, N. *et al.* Oxetanocin, a novel nucleoside from bacteria. *J. Antibiot.* **39,** 1623–1625 (1986).
8 Katagiri, N., Morishita, Y., Oosawa, I. & Yamaguchi, M. Artificial oligonucleotides consisting of an analog of nucleoside antibiotics, carbocyclic oxetanocins. *Tetrahedron Lett.* **40,** 6835–6840 (1999).
9 Yamaguchi, T. *et al.* Synthetic nucleosides and nucleotides. 43. Inhibition of vertebrate telomerases by carboxylic oxetanocin G (C.OXT-G) triphosphate analogues and influence of C.OXT-G treatment on telomere length in human HL60 cells. *Nucleosides Nucleotides Nucleic Acids* **25,** 539–551 (2006).
10 Maruyama, T. *et al.* Synthesis and antiviral activity of carbocyclic oxetanocin analogues (C-OXT-A, C-OXT-G) and related compounds. II. *Chem. Pharm. Bull.* **41,** 516–521 (1993).
11 Cseke, C. B. *et al.* 2a-Phosphohydantocidin: The *in vivo* adenylosuccinate synthase inhibitor responsible for hydantocidin phytotoxicity. *Pest. Biochem. Physiol.* **53,** 210–217 (1996).
12 Graupner, P. R. *et al.* The macrocidins: novel cyclic tetramic acids with herbicidal activity produced by *Phoma macrostoma*. *J. Nat. Prod.* **66,** 1558–1561 (2003).
13 Irvine, N. M. *et al.* Synthesis and characterization of synthetic analogs of cinacidin, a novel phytotoxin from *Nectria* sp. *Pest. Manag. Sci.* **64,** 891–899 (2008).

The Journal of Antibiotics (2009) 62, 195–200

www.nature.com/ja

ORIGINAL ARTICLE

Pentacecilides, new inhibitors of lipid droplet formation in mouse macrophages, produced by *Penicillium cecidicola* FKI-3765-1: I. Taxonomy, fermentation, isolation and biological properties

Hiroyuki Yamazaki[1], Kakeru Kobayashi[1], Daisuke Matsuda[1], Kenichi Nonaka[2], Rokuro Masuma[2], Satoshi Ōmura[2] and Hiroshi Tomoda[1]

New compounds designated pentacecilides A to C were isolated from the fermentation broth of *Penicillium cecidicola* FKI-3765-1 by solvent extraction, silica gel column chromatography and preparative HPLC. Pentacecilides A and B dose-dependently inhibited lipid droplet formation in mouse macrophages. Furthermore, pentacecilides A and B were found to inhibit the synthesis of cholesteryl ester in mouse macrophages with respective IC_{50} values of 3.65 and 4.76 μM without any cytotoxic effect, but pentacecilide C showed almost no activity. The study of the mechanism of action strongly suggested that pentacecilides A and B inhibit acyl-CoA: cholesterol acyltransferase activity in macrophages.
The Journal of Antibiotics (2009) **62,** 195–200; doi:10.1038/ja.2009.18; published online 20 March 2009

Keywords: acyl-CoA:cholesterol acyltransferase; fungal metabolite; inhibitor; lipid droplet formation; *Penicillium cecidicola*; pentacecilide; thailandolide

INTRODUCTION

In the early stage of atherosclerogenesis, macrophages penetrate the intima, efficiently take up modified low-density lipoprotein, store cholesterol and fatty acid as a respective form of cholesteryl ester (CE) and triacylglycerol (TG) in cytosolic lipid droplets, and are converted into foam cells, leading to the development of atherosclerosis in the arterial wall. Therefore, inhibition of lipid droplet accumulation in macrophages would be expected to retard the progression of atherosclerosis.[1–4]

In the course of our screening program for microbial inhibitors of lipid droplet formation in mouse macrophages,[5–10] three new compounds designated pentacecilides A to C (Figure 1), structurally related to known thailandolides A and B,[11] were isolated from the culture broth of a soil-isolated fungus, FKI-3765-1. Thailandolides were originally isolated as fungal metabolites from *Talaromyces thailandiasis*,[11] and were not isolated from the culture broth of strain FKI-3765-1. Pentacecilides A and B were found to inhibit lipid droplet formation in mouse macrophages, although the biological activity of thailandolides has not been reported. The structure elucidation of pentacecilides will be described in an accompanying study.[12] In this study, the taxonomy of the producing strain, fermentation, isolation and biological properties of pentacecilides A to C are described.

RESULTS

Taxonomy of strain FKI-3765-1

Colonies on Czapek yeast agar (CYA) after 7 days at 25 °C (Figure 2a) were 44–45 mm in diameter, dense, colliculose, floccose to funiculose, with a smooth margin and white (a). The center of the colony was dark olive (1 pn) in conidial color, exuding clear drops. The reverse side was dark brown (5 pn). Colonies on malt extract agar (Figure 2b) were 49–51 mm in diameter, dense, colliculose, floccose, with a smooth margin, and white (a), without exudate drops. The reverse side was amber (3 lc). Colonies on G25N (Figure 2c) were 5.0–7.0 mm in diameter, pulvinate, floccose, with a smooth margin, and bamboo (2 gc) in color, without exudate drops. The reverse side was bamboo (2 gc). Colonies on CYA after 7 days at 37 °C were dense, colliculose, floccose to funiculose, with a smooth margin, and sand (2 ec) in color. The reverse was cork tan (4 ic). The colony on CYA at 5.0 °C showed no growth.

Conidiophores on CYA were from basal hyphae, rarely branching, 17.5–65 × 2.5–3.5 μm, with a smooth wall. Penicilli from condiophores were biverticillate (consisting of metulae and phialides) and symmetrical (Figure 2d). Metulae were 3–7 branches, which were usually rather appressed or sometimes slightly divergent of larger size, 10–12.5 × 2.5–2.7 μm. Phialides were acerose, 10–15 × 2.5–3.0 μm,

[1]Graduate School of Pharmaceutical Sciences, Kitasato University, Shirokane, Minato-ku, Tokyo, Japan and [2]Kitasato Institute for Life Sciences, Kitasato University, Shirokane, Minato-ku, Tokyo, Japan
Correspondence: Professor H Tomoda, Graduate School of Pharmaceutical Sciences, Kitasato University, 5-9-1 Shirokane, Minato-ku, Tokyo 108-8641, Japan.
E-mail: tomodah@pharm.kitasato-u.ac.jp
Received 15 January 2009; revised 6 February 2009; accepted 10 February 2009; published online 20 March 2009

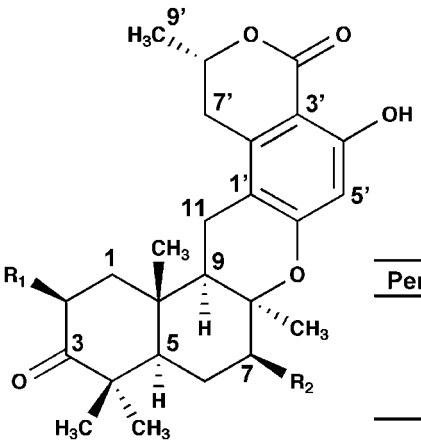

Pentacecilide	R_1	R_2
A	-H	-H
B	-OAc	-H
C	-OAc	-OH

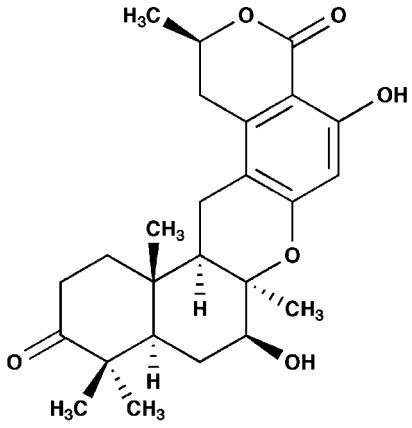

Thailandolide A

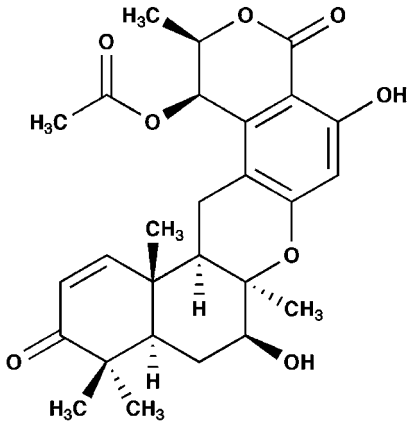

Thailandolide B

Figure 1 Structures of pentacecilides A to C and thailandolides A and B.

with smooth walls. Conidia were subglobose to globose, smooth-walled, 2.7–3.5 (5.0)×2.3–3.0 μm in size, and with divergent long chains (Figure 2e).

From the above morphological characteristics, strain FKI-3765-1 was considered to belong to genus *Penicillium* in the subgenus *Biverticillium* Section *Simplicia*.[13] Furthermore, from the characteristics of the mycelial colors on CYA, the rapid growth at 37 °C on CYA and the length of conidiophores, the strain was considered to be *Penicillium cecidicola*. In addition, the ITS rDNA sequence (550 nucleotides) of strain FKI-3765-1 showed 99.4% similarity to that of *Penicillium cecidicola* (strain name) (accession no. AY787844). As a result, the producing strain FKI-3765-1 was identified as *P. cecidicola*.

Isolation

The 15-day-old whole broth (250 g) was extracted with 0.50 l of acetone. After the acetone extracts were filtered and concentrated to remove acetone, the aqueous solution was extracted with ethyl acetate. The extracts were dried over Na_2SO_4 and concentrated *in vacuo* to dryness to yield a red brown material (438 mg). The material was dissolved in hexane-ethyl acetate (2 : 1, v/v), applied to a silica gel column (10 g), and eluted stepwise with 2 : 1 (v/v) of hexane-ethyl acetate and 100 : 0, 10 : 1, 5 : 1, 1 : 1 and 0 : 100 (v/v) of $CHCl_3$-CH_3OH (100 ml for each solvent). Active fractions from a 5 : 1 solvent containing pentacecilides were concentrated *in vacuo* to dryness to give a red brown oily material (171 mg). The material was finally purified by preparative HPLC (column; PEGASIL ODS (Senshu Scientific Co. Ltd, Tokyo, Japan), 20×250 mm; solvent, 70% CH_3CN; detection, UV at 210 nm; flow rate, 8.0 ml min^{-1}). Under these conditions, pentacecilides A to C were eluted as a peak with a retention time of 30.5, 27.3 and 12.7 min, respectively (Figure 3). The fractions were concentrated *in vacuo* to dryness to give pure pentacecilides A (4.47 mg), B (6.58 mg) and C (24.2 mg) as a white crystal.

Biological properties

Inhibition of lipid droplet formation in macrophages. In the control assay (no drug), mouse peritoneal macrophages accumulated a massive number of lipid droplets in the cytosol. In the presence of pentacecilides A and B at 0.21–24.3 μM, the size and number of lipid droplets in macrophages fell in a dose-dependent manner (data not shown). No morphological changes or cytotoxic effects were observed on macrophages even at the highest dose (21.3–24.3 μM), indicating that pentacecilides A and B specifically inhibit lipid droplet formation in mouse macrophages. Pentacecilide C showed almost no effect on lipid droplet formation in macrophages.

Inhibition of CE synthesis in macrophages. In the control assay (no drug), approximately 40% of exogenously added [^{14}C]oleic acid was

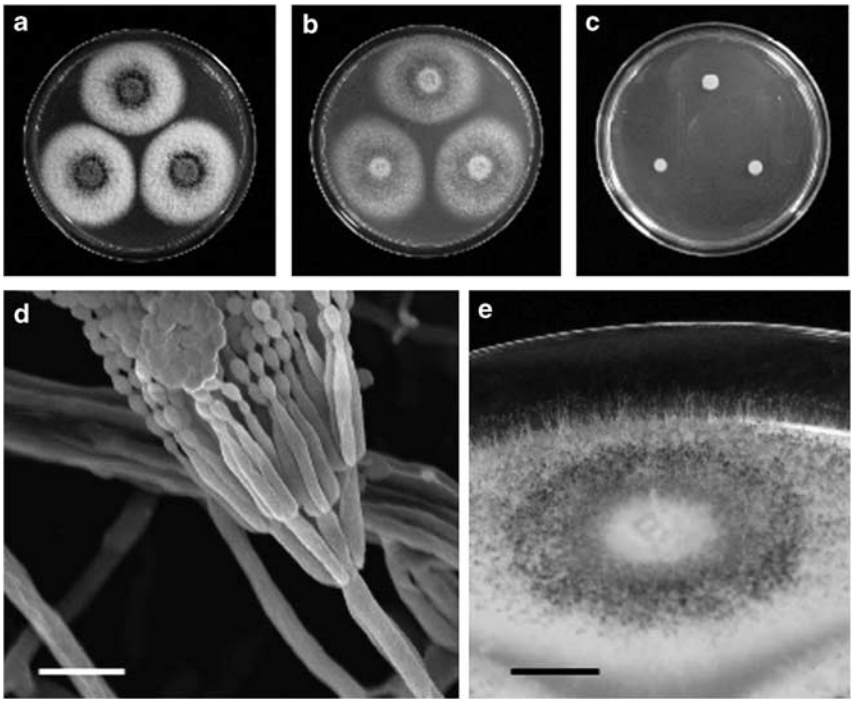

Figure 2 Morphological characteristics of pentacecilide-producing *Penicillium cecidicola* FKI-3765-1. (**a**) Micrography of colonies grown on Czapek yeast agar (CYA) after 7 days. (**b**) Micrograph of colonies grown on malt extract agar (MEA) after 7 days. (**c**) Micrograph colonies grown on G25N after 7 days. (**d**) Scanning electron micrograph of conidiophores grown on MEA. Scale bar, 10 μm. (**e**) Micrograph of synnemata grown on MEA. Scale bar, 10 mm.

incorporated into [^{14}C]CE (approximately 25%) and [^{14}C]TG (approximately 15%), which are the main constituents of lipid droplets in macrophages.[14] As shown in Figure 4, pentacecilides A and B inhibited [^{14}C]CE synthesis in a dose-dependent manner with IC_{50} values of 3.65 and 4.76 μM, respectively, but showed almost no inhibition of [^{14}C]TG synthesis even at the highest dose (20.6 and 21.3 μM), indicating that pentacecilides A and B selectively inhibit CE synthesis in macrophages. In contrast, pentacecilide C did not inhibit [^{14}C]CE, [^{14}C]TG and [^{14}C]PL synthesis. These data are comparable with the results of lipid droplet formation in macrophages, as described above.

Inhibition of post-lysosomal cholesterol metabolism in macrophages. To gain insight into the target molecule of pentacecilides in the inhibition of lipid droplet formation in macrophages, the effects of pentacecilides on the post-lysosomal process of cholesterol metabolism was studied. When macrophages were incubated with [^{14}C]cholesterol-supplemented liposomes in the presence of 10 μM pregnenolone, [^{14}C]CE formation was almost completely suppressed, and unesterified [^{14}C]cholesterol accumulated in the lysosomes of macrophages.[15] After pregnenolone was removed by washing the cells with buffer, the metabolism of lysosomal [^{14}C]cholesterol to [^{14}C]CE was restarted in the presence or absence of pentacecilides. As shown in Figure 5a, pentacecilides A and B inhibited [^{14}C]CE synthesis in a dose-dependent manner with IC_{50} values of 5.17 and 9.12 μM, respectively, which are within similar ranges to those for the synthesis of [^{14}C]CE from [^{14}C]oleic acid (Figure 4). In contrast, pentacecilide C showed almost no effect, even at 24.3 μM. These data indicate that the inhibition site of pentacecilides A and B lies within the post-lysosomal steps in cholesterol metabolism.

Inhibition of ACAT activity in macrophage microsomes. The results using pregnenolone indicated that the inhibition site of pentacecilides is between the point of cholesterol departure from lysosomes and the point of cholesterol esterification in the endoplasmic reticulum. As epicochlioquinone, whose carbon skeleton and configuration are very similar to those of pentacecilides, is known to inhibit acyl-CoA: cholesterol acyltransferase (ACAT) activity,[16] the effect of pentacecilides on ACAT activity was studied. For this purpose, microsomes prepared from mouse macrophages were used as an enzyme source. Pentacecilides A and B inhibited ACAT activity with IC_{50} values of 11.2 and 4.15 μM, respectively (Figure 5b). In contrast, pentacecilide C showed 50% inhibition at 24.3 μM.

Inhibition of CE synthesis in ACAT1- and ACAT2-CHO cells. From the macrophage assays, the potential target of pentacecilides A and B is deduced to be ACAT; therefore, the effect of pentacecilides on ACAT1 and ACAT2 isozymes was evaluated in ACAT1- and ACAT2-CHO cells. As shown in Figure 6, pentacecilides A and B inhibited both ACAT1 and ACAT2 with similar potency. The respective IC_{50} values against ACAT1 and ACAT2 were 1.09 and 0.69 μM for pentacecilide A and 10.8 and 3.97 μM for pentacecilide B. These data indicated that pentacecilides A and B are dual inhibitors of ACAT1 and ACAT2.

DISCUSSION

As described in this study, three pentacecilides (Figure 1) were isolated from the culture broth of *P. cecidicola* FKI-3765-1; however, pentacecilides A and B were found to inhibit lipid droplet formation in mouse macrophages, whereas pentacecilide C showed no activity. These findings suggested that the hydroxy group at C-7 does not favor the inhibitory activity of lipid droplet formation in mouse macrophages.

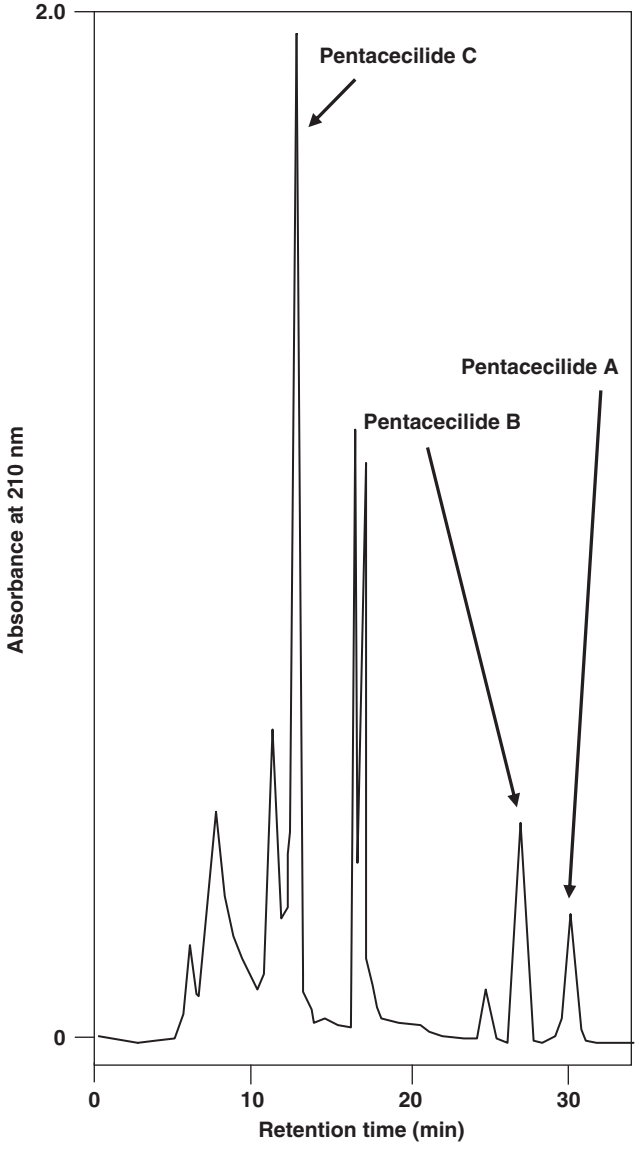

Figure 3 A chromatographic profile of pentacecilide purification by preparative HPLC. Column, PEGASIL ODS (20×250 mm); solvent 70% aqueous acetonitrile; detection, UV at 210 nm; flow rate, 8.0 ml min^{-1}; sample, 35 mg of active materials (obtained through silica gel column chromatography) dissolved in 700 μl methanol.

Thailandolides (Figure 1), structurally related to pentacecilides, were not isolated from the culture broth of strain FKI-3765-1. As they have a hydroxy group at C-7 as well as pentacecilide C, thailandolides might show no activity of lipid droplet formation in macrophages.

From a study of the action mechanism (Figures 4 and 5), we concluded that pentacecilides A and B inhibit ACAT activity in mouse macrophages to selectively block CE synthesis, leading to the inhibition of lipid droplet formation in mouse macrophages. Pentacecilide C showed almost no activity in these assays.

Pentacecilides A and B gave almost the same IC_{50} values in the cell-based assays (Figures 4 and 5a), whereas pentacecilide C showed no effect in the cell-based assays (Figures 4 and 5a). However, pentacecilide C showed weakly inhibitory activity in the microsomal assay (Figure 5b). The discrepancy of IC_{50} values between the assays might be due to the permeability of pentacecilide C to intact cells membrane, as our previously reported in the study of piperine.[17] Furthermore, pentacecilides A and B are dual inhibitors of ACAT1 and ACAT2 isozymes.

METHODS

General experimental procedures

Fungal strain FKI-3765-1 was originally isolated from a soil sample collected in Hilo, Hawaii, USA. This strain was used for the production of pentacecilides A

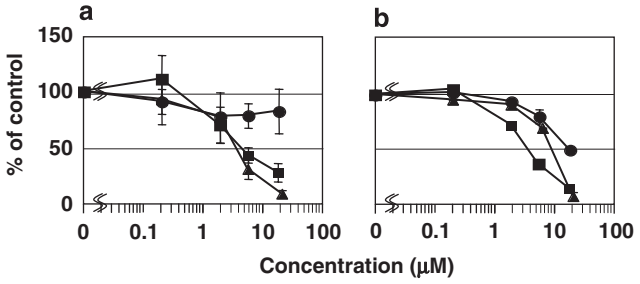

Figure 5 Effect of pentacecilides on [^{14}C]CE synthesis from lysosomal [^{14}C]cholesterol in intact macrophages and on acyl-CoA: cholesterol acyltransferase (ACAT) activity in microsomes of mouse macrophages. (**a**) The amounts of [^{14}C]CE synthesized from lysosomal [^{14}C]cholesterol were determined in the presence of pentacecilides A (▲), B (■) and C (●) as described in Methods. These results are plotted as a percent of control (without a drug). (**b**) ACAT activity in microsomes prepared from mouse macrophages was tested in the presence of pentacecilides A (▲), B (■) and C (●) as described in Methods. These results are plotted as a percent of the control (without a drug).

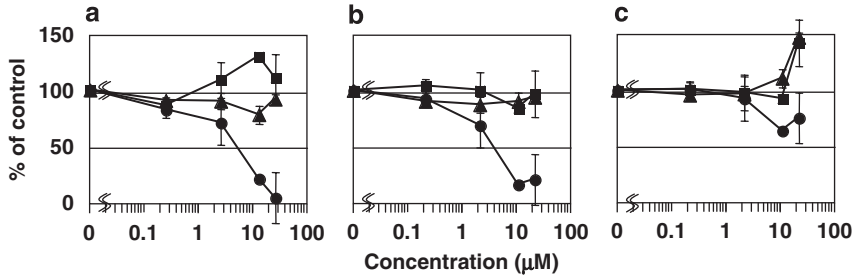

Figure 4 Effect of pentacecilides on the synthesis of [^{14}C]CE, [^{14}C]TG and [^{14}C]PL from [^{14}C]oleic acid by macrophages. Macrophage monolayers obtained from 5×10^5 cells per well in a microplate were incubated in 0.25 ml medium with a phospholipid/cholesterol liposome composed of phosphatidylcholine, phosphatidylserine, dicetylphosphate and cholesterol at a molar ratio 10 : 10 : 2 : 15 and [^{14}C]oleic acid in the absence or presence of the indicated amounts of pentacecilides A (**a**), B (**b**) or C (**c**). After 14-h incubation, cholesteryl [^{14}C]oleate (●), [^{14}C]TG (■) and [^{14}C]PL (▲) were separated on TLC, determined with a radioscanner as described in Methods. The results are plotted as a percent of the control (without a drug).

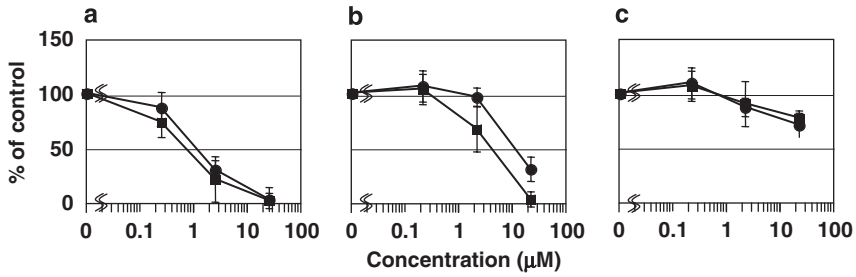

Figure 6 Effect of pentacecilides on [^{14}C]CE synthesis from [^{14}C]oleic acid in ACAT1- or ACAT2-CHO cells. ACAT1- (●) or ACAT2-CHO (■) cell monolayers (1.25×10^5 cells per well) in a microplate were incubated in the absence or presence of the indicated amounts of pentacecilides A (**a**), B (**b**) or C (**c**). After a 6-h incubation, [^{14}C]CE was separated by TLC, and quantified with a bioimage analyzer, as described in Methods. The amounts of [^{14}C]CE signals were plotted as a percent of the control (without drugs).

to C. Kieselgel 60 (Merck KGaA, Darmstadt, Germany) was used for silica gel column chromatography. HPLC was carried out using the L-6200 system (Hitachi Ltd, Tokyo, Japan). To determine the amounts of pentacecilides A to C in culture broths, the samples (ethyl acetate extracts) dissolved in methanol were analyzed by the HP1100 system (Hewlett-Packard Company, Palo Alto, CA, USA) under the following conditions: column, Symmetry (2.1×150 mm; Waters Corporation, Milford, MA, USA); flow rate, 0.2 ml min^{-1}; mobile phase, a 20-min linear gradient from 60% CH_3CN to 100% CH_3CN containing 0.05% H_3PO_4; detection, UV at 210 nm. Under these conditions, pentacecilides A to C were eluted with a retention time of 9.01, 8.71 and 4.67 min, respectively.

Taxonomic studies of the producing strain FKI-3765-1

Morphological studies and identification were conducted according to the procedures described by Pitt.[13] For taxonomic studies, CYA, malt extract agar and 25% glycerol nitrate agar (G25N) were used. Morphological characteristics were observed under a light microscope (Vanox-S AH-2, Olympus Corporation, Tokyo, Japan) and scanning electron microscope (JSM-5600, JEOL Ltd, Tokyo, Japan). Color names and hue numbers were determined according to the Color Harmony Manual.[18] For molecular phylogenetic study, genomic DNA was extracted using the PrepMan Ultra Sample Preparation Reagent (Applied Biosystems Inc., Foster City, CA, USA) according to the manufacturer's protocol. The rDNA internal transcribed spacer (rDNAITS) regions, including the 5.8S rDNA gene, were amplified by PCR using primers ITS1 and ITS4.[19] Amplifications were performed using a PCR Thermal Cycler Dice mini Model TP100 (Takara Bio Inc., Shiga, Japan). The amplified PCR products were purified using a QIAquick PCR DNA Purification Kit (Qiagen Inc., Valencia, CA, USA). Sequencing reactions were directly performed using a BigDye Terminator v3.1 Cycle Sequencing Kit (Applied Biosystems Inc.), and the products were purified with a DyeEX 2.0 Spin Kit (Qiagen Inc.). DNA sequences were read on an ABI PRISM 3130 Genetic Analyzer (Applied Biosystems Inc.) and assembled using the programs SeqMan and SeqBuilder from the Lasergene7 package (DNAStar Inc., Madison, WI, USA). The ITS region rDNA sequence was compared with the database of the National Center for Biotechnology Information, Japan. ITS was deposited in DDBJ with accession number AB457008.

Fermentation

A slant culture of strain FKI-3765-1 grown on LCA (glycerol 0.10%, KH_2PO_4 0.08%, K_2HPO_4 0.02%, $MgSO_4$ $7H_2O$ 0.02%, KCl 0.02%, $NaNO_3$ 0.20%, yeast extract 0.02%, agar 1.5%, pH 6.0) was inoculated into a 50-ml tube containing 10 ml of the seed medium (glucose 2.0%, polypeptone 0.50%, $MgSO_4$ $7H_2O$ 0.05%, yeast extract 0.20%, KH_2PO_4 0.10%, agar 0.10%, pH 6.0). The tube was shaken on a reciprocal shaker for 3 days at 27 °C. A 1 ml portion of the seed culture was then inoculated into a 500-ml Erlenmeyer flask containing the production medium (50 g Italian rice, Japan Europe Trading Co. Ltd, Tokyo, Japan). Fermentation was carried out at 27 °C for 15 days under stable conditions.

Assay for lipid droplet formation in mouse macrophages

The assay for lipid droplet formation in mouse macrophages was carried out according to our established method.[20]

Assay for lipid synthesis by mouse macrophages

An assay for the synthesis of CE, TG and phospholipids by mouse macrophages was carried out according to the method described earlier.[20]

Assay for lysosomal cholesterol metabolism in mouse macrophages

The metabolism of lysosomal [^{14}C]cholesterol in mouse macrophages was measured as described earlier.[14]

Assay for ACAT activity in mouse macrophage microsomes

Acyl-CoA: cholesterol acyltransferase activity was assayed according to our established method.[21]

Culture of ACAT1- and ACAT2-CHO Cells

Two cell lines, CHO cells expressing acyl-CoA: cholesterol acyltransferase 1 (ACAT1) and 2 (ACAT2) isozymes of African green monkey (ACAT1- and ACAT2-CHO cells, respectively)[15] were kind gifts from Dr LL Rudel (Wake Forest School of Medicine, NC). Cells were maintained as described earlier.[22]

Assay for ACAT1 and ACAT2 activities using ACAT1- and ACAT2-CHO cells

An assay for ACAT1 and ACAT2 activities in ACAT1- and ACAT2-CHO cells was carried out by our established method.[22]

ACKNOWLEDGEMENTS

We thank Mr N Ugaki for excellent technical assistance. This study was supported by the Program for the Promotion of Fundamental Studies in Health Sciences (to HT) from the National Institute of Biomedical Innovation (NIBIO).

1 Goldstein, J. L., Ho, Y. K., Basu, S. K. & Brown, M. S. Binding site on macrophages that mediates uptake and degradation of acetylated low density lipoprotein, producing massive cholesterol deposition. *Proc. Natl Acad. Sci. USA* **76,** 333–337 (1979).
2 Brown, M. S., Goldstein, J. L., Krieger, M., Ho, Y. K. & Anderson, R. G. W. Reversible accumulation of cholesteryl esters in macrophages incubated with acetylated lipoproteins. *J. Cell Biol.* **82,** 597–613 (1979).
3 Scaffner, T. *et al.* Arterial foam cells with distinctive immunomorphological and histochemical features of macrophages. *Am. J. Pathol.* **100,** 57–73 (1980).
4 Gerrtiy, R. G. The role of the monocyte in atherogenesis. I. Transition of blood-borne monocytes into foam cells in fatty lesions. *Am. J. Pathol.* **103,** 181–190 (1981).
5 Namatame, I. *et al.* Beauveriolides, specific inhibitors of lipid droplet formation in mouse macrophages, produced by *Beauveria* sp. FO-6979. *J. Antibiot.* **52,** 1–6 (1999).
6 Namatame, I., Tomoda, H., Ishibashi, S. & Ōmura, S. Antiatherogenic activity of fungal beauveriolides, inhibitors of lipid droplet accumulation in macrophages. *Proc. Natl Acad. Sci. USA* **101,** 737–742 (2004).

7 Tomoda, H. *et al*. Phenochalasins, inhibitors of lipid droplet formation in mouse macrophages, produced by *Phomopsis* sp. FT-0211. *J. Antibiot.* **52,** 851–856 (1999).
8 Namatame, I. *et al*. K97-0239A and B, new inhibitors of macrophage foam cell formation, produced by *Streptomyces* sp. K97-0239. *Proc. Japan Acad.* **78B,** 45–50 (2002).
9 Koyama, N. *et al*. Spylidone, a novel inhibitor of lipid droplet accumulation in mouse macrophages by *Phoma* sp. FKI-1840. *J. Antibiot.* **58,** 338–345 (2005).
10 Koyama, N., Ohshiro, T., Tomoda, H. & Ōmura, S. Fungal isobisverthinol, a new inhibitor of lipid droplet accumlation in mouse macrophage. *Org. Lett.* **9,** 425–428 (2007).
11 Dethoup, T. *et al*. Merodrimanes and other constituents from *Talaromyces thailandiasis*. *J. Nat. Pro.* **70,** 1200–1202 (2007).
12 Yamazaki, H., Ōmura, S. & Tomoda, H. Pentacecilides, new inhibitors for lipid droplet formation in mouse macrophages produced by *Penicillium cecidicola* FKI-3765-1. II Physico-chemical properties and structure elucidation. *J. Antibiot.* **62,** 207–211 (2009).
13 Pitt, J. I. *The Genus Penicillium, and its Teleomorphic States Eupenicillium and Talaromyces*. Academic Press, London: 1–634 (Academic Press: London, 1979).
14 Furuchi, T., Aikawa, K., Arai, H. & Inoue, K. Bafilomycin A1, a specific inhibitor of vacuolar-type H(+)-ATPase, blocks lysosomal cholesterol trafficking in macrophages. *J. Biol. Chem.* **268,** 27345–27348 (1993).
15 Lada, A. T. *et al*. Identification of ACAT1- and ACAT2-specific inhibitors using a novel, cell-based fluorescence assay: individual ACAT uniqueness. *J. Lipid. Res.* **45,** 378–386 (2004).
16 Fujioka, T. *et al*. Epi-cochlioquinone A, a novel acyl-CoA:cholesterol acyltransferase inhibitor produced by *Stachybotrys bisbyi*. *J. Antibiot.* **49,** 409–413 (1996).
17 Matsuda, D. *et al*. Molecular target of piperine in the inhibition of lipid droplet accumulation in macrophages. *Biol. Pharm. Bull.* **31,** 1063–1066 (2008).
18 Jacobson, E., Granville, W. C. & Foss, C. E. *Color Harmony Manual*, 4th edn. (Container of America: Chicago, 1958).
19 White, T. J., Bruns, T., Lee, S. & Taylor, J. W. Amplification and direct sequencing of fungal ribosomal RNA genes for phylogenetics. in *PCR protocols: a guide to methods and applications*. (Innis MA, Gelfand RH, Sninsky JJ, White TJ, eds). 315–332 (Academic Press, New York, 1990).
20 Namatame, I., Tomoda, H., Arai, H., Inoue, K. & Ōmura, S. Complete inhibition of mouse macrophage-derived foam cell formation by triacsin C. *J. Biochem.* **125,** 319–327 (1999).
21 Ohshiro, T. *et al*. Absolute stereochemistry of fungal beauveriolide III and ACAT inhibitory activity of four stereoisomers. *J. Org. Chem.* **71,** 7643–7649 (2006).
22 Ohshiro, T., Rudel, L. L., Ōmura, S. & Tomoda, H. Selectivity of microbial acyl-CoA: cholesterol acyltransferase inhibitors toward isozymes. *J. Antibiot.* **60,** 43–51 (2007).

The Journal of Antibiotics (2009) 62, 201–205

www.nature.com/ja

ORIGINAL ARTICLE

NW-G01, a novel cyclic hexadepsipeptide antibiotic, produced by *Streptomyces alboflavus* 313: I. Taxonomy, fermentation, isolation, physicochemical properties and antibacterial activities

Zhengyan Guo, Ling Shen, Zhiqin Ji, Jiwen Zhang, Luzhi Huang and Wenjun Wu

NW-G01, a novel cyclic hexadepsipeptide antibiotic, was isolated by macroporous resin and silica gel column chromatography and HPLC from the fermentation broth of strain no. 313. The producing strain was identified as *Streptomyces alboflavus* on the basis of the morphological characteristics, physiological property and 16S rDNA gene sequence analysis. NW-G01 exhibited strong antibacterial activity against *Bacillus subtilis*, *Bacillus cereus*, *Staphylococcus aureus*, methicillin-resistant *S. aureus*, and their MIC values were 3.90, 3.90, 7.81 and 7.81 μg ml^{-1}, respectively.
The Journal of Antibiotics (2009) **62,** 201–205; doi:10.1038/ja.2009.15; published online 6 March 2009

Keywords: antibacterial activity; cyclic hexadepsipeptide; NW-G01; *Streptomyces alboflavus* 313

INTRODUCTION

In the course of a screening program for new antibiotics from microbial products, an actinomycete strain no. 313, isolated from a soil sample collected from the Shaanxi province of China, was found to produce a novel cyclic hexadepsipeptide antibiotic, designated as NW-G01. The chemical structure of NW-G01 incorporates valine, *N*-methylalanine, a chlorinated pyrroloindoline derivative, and three molecules of piperazic acid (Figure 1). NW-G01 is structurally related to himastatin[1] and chloptosin,[2] two cyclic hexadepsipeptide antitumor antibiotics, but is significantly different in the amino acid content. Another important difference between them is that the two reported antibiotics are the dimers of cyclohexapeptide. Taxonomic studies showed that the producing strain belongs to the species of *Streptomyces alboflavus*. The bioassay results showed that NW-G01 had strong antibacterial activity against gram-positive bacteria, including methicillin-resistant *Staphylococcus aureus* (MRSA), but was ineffective against gram-negative bacteria.

In this paper, we described the taxonomy of the producing organism, fermentation, isolation, physicochemical properties and antibacterial activities. The structural elucidation of NW-G01 will be reported in the following paper.

RESULTS

Taxonomy of the producing strain

Strain no. 313 grew well on most of the media and produced no distinctive soluble pigment. It formed well-developed and branching substrate mycelium, but rare aerial mycelium, and typical a spore chain was observed on the International Streptomyces Project (ISP) media. The mature spore chain was straight or slightly curved and broken easily on modified humic acid–vitamins (HV) agar; the spores were cylindrical to oval shape, in sizes of 0.5–2 μm, with a smooth surface observed through the scanning electron photo microscope (Figure 2).

Good growth could be observed on modified HV agar, Czapek's agar, glucose asparagine agar, ISP2, ISP3, ISP5 and ISP6, but no growth was observed on ISP4. The best medium for the culture of this strain was modified HV agar, on which it grew well. The culture characteristics of the strain are described in detail in Table 1.

Special morphology, such as sclerotia or sporangia, was not observed. Carbon utilization and physiological characteristics of strain no. 313 were summarized in Table 2. The results of diaminopimelic acid (DAP) analysis showed the presence of L-DAP in the peptidoglycan, indicating that strain no. 313 belonged to cell wall type I.[3] Glucose and ribose were detected in the whole-cell hydrolysates. Strain no. 313 utilized D-dextrose, D-maltose, inositol, D-mannitol, L-rhamnose, D-xylose, L-arabinose, D-fructose and D-mannose as sole carbon sources, but not sucrose, D-ribose, lactose and D-galactose. Gelatin liquefaction, coagulation and peptonization of the milk test showed positive results at 7 days. Hydrolysis of starch was not observed before 14 days. The above results support the identification of this strain as a member of the genus *Streptomyces*. Furthermore, 16S rDNA sequence (1471 nucleotides) of strain no. 313 was

Institute of Pesticide Science, Northwest Agricultural & Forestry University, Shaanxi, China
Correspondence: Professor W Wu, Institute of Pesticide Science, Northwest Agricultural & Forestry University, YangLing, Shaanxi 712100, China.
E-mail: wuwenjun@nwsuaf.edu.cn
Received 16 September 2008; accepted 11 February 2009; published online 6 March 2009

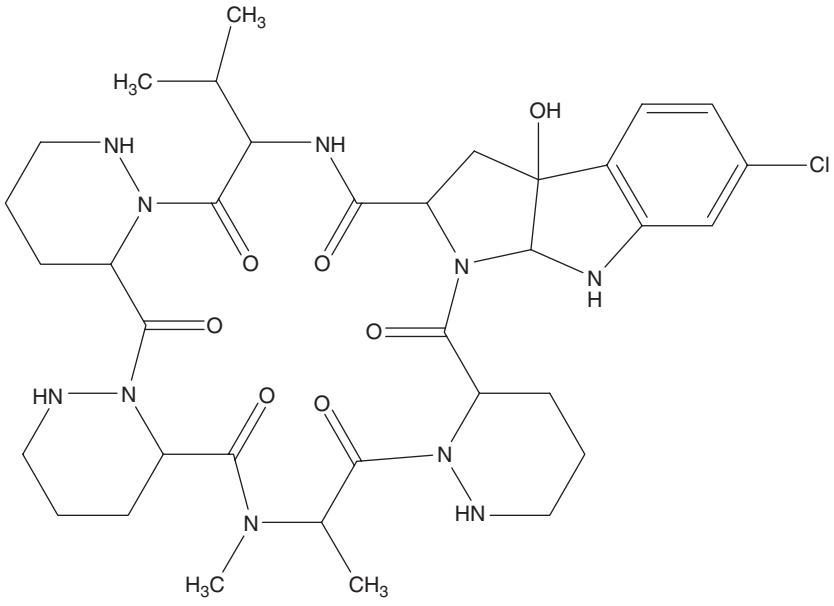

Figure 1 The structure of compound NW-G01.

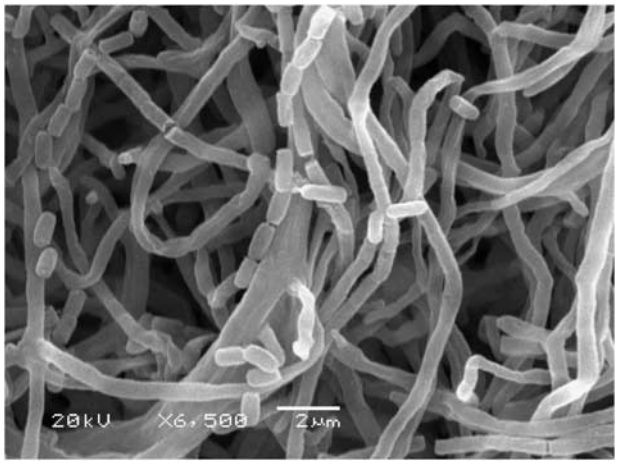

Figure 2 Scanning electron micrograph of *Streptomyces alboflavus* 313 grown on modified HV agar at 27 °C for 5 days. The scale bar represents 2 μm.

determined and registered in the GenBank (FJ032029). The phylogenetic analysis with 16S rDNA database sequences revealed that strain no. 313 branched deeply within a member of the gene *Streptomyces* and was most closely related to *S. alboflavus* NBRC-13196^{T} [4] (Figure 3). As the sequence similarity was high (99.5%) and most morphological and physiological characteristics were highly similar, except for the coagulation of milk, strain no. 313 might be identified as *S. alboflavus* 313.

Cultivation and fermentation

Strain no. 313 was cultivated at 28 °C in the modified HV medium, which contained soluble starch 1%, KCl 0.17%, $FeSO_4$ $7H_2O$ 0.001%, VB_1 0.00005%, VB_3 0.00005%, para-aminobenzoic acid 0.00005%, Na_2HPO_4 0.05%, cycloheximide 0.005%, $MgSO_4$ $7H_2O$ 0.05%, $CaCO_3$ 0.002%, VB_2 0.00005%, VB_6 0.00005%, myoinositol 0.00005%, biotin 0.000025%, KNO_3 0.3% and agar 1.8%, at pH 7.2 adjusted with NaOH. The seed medium consisted of millet extract 1%,

Table 1 Culture characteristics of strain no. 313

Medium	*Growth*	*Aerial medium*	*Sub-medium*	*Pigment*
Modified HV	Very good	Few	Orange yellow	No
Gause's no. 1	Good	No	Orange red	No
Czapek's agar	Good	No	Brownish red	No
Glucose asparagine	Very good	Abundant, gray yellow	Brownish yellow	No
Calcium malate agar	Moderate	Few, light pink	Reddish brown	No
Yeast-mall extract agar (ISP2)	Good	No	Light orange	No
Oatmeal agar(ISP3)	Good	No	Dark orange red	No
Inorganic salts-starch (ISP4)	No	No	No	No
Glycerol asparagine (ISP5)	Good	No	Golden yellow	No
Yeast peptone agar (ISP6)	Good	Moderate, pink	Orange red	No

Abbreviation: HV, humic acid–vitamins.

Table 2 Carbon utilization and physiological characteristics of strain no. 313

Utilization of carbon		*Utilization of carbon*	
D-dextrose	+	D-mannitol	+
Sucrose	–	L-rhamnose	–
D-xylose	–	D-mannose	+
Maltose	+	*Physiological characteristics*	
L-arabinose	+	Coagulation of milk	+
D-fructose	+	Liquefaction of gelatin	+
Inositol	+	Hydrolysis of starch	–
D-ribose	–	Use of cellulose	+
Lactose	–	Peptonization of milk	+
D-galactose	+		

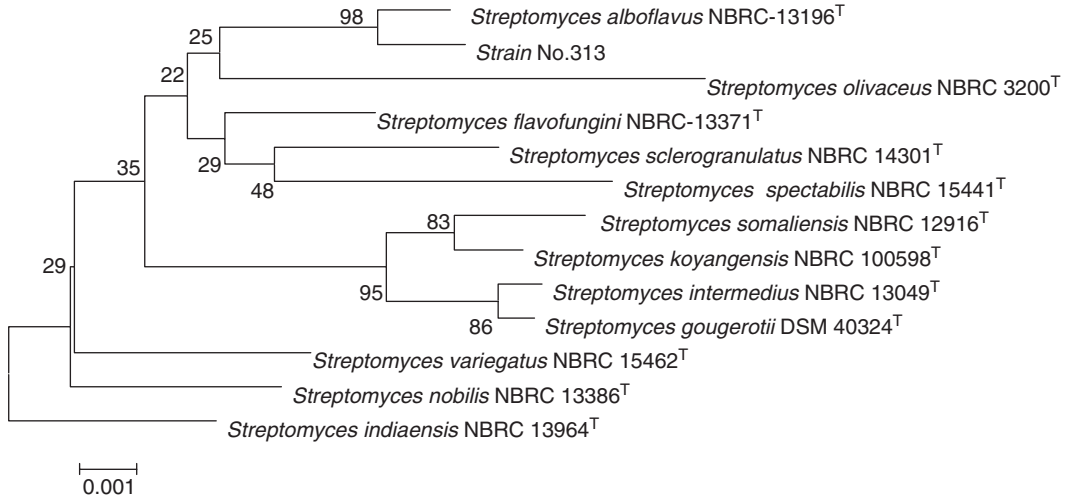

Figure 3 Phylogenetic tree showing the position of strain no. 313 on the basis of 16S rDNA gene sequence analysis. *Streptomyces indiaensis* NBRC-13964T was used as the outgroup.

Table 3 Physicochemical properties of compound NW-G01

Properties	*Compound NW-G01*
Appearance	Pale pink needle crystal
$[\alpha]_D^{25}$	−120°(c 0.2 MeOH)
Melting point	208–211 °C
Molecular formula	$C_{35}H_{49}ClN_{10}O_7$
ESI-MS(*m/z*)	757.21[M+H]+, 779.27[M+Na]+
HR-ESI-MS(*m/z*)	
Found	757.3460[M+H]+
Calcd	756.3474 for $C_{35}H_{49}ClN_{10}O_7$
UV λ_{max}^{MeOH}EQ nm	218
IR ν_{max} (KBr) cm^{-1}	1638, 3425, 1114, 1073, 799, 759
Solubility	
Soluble	DMSO, methanol, EtOAc
Insoluble	H_2O, acetone
Test	
Positive	I_2, $AgNO_3$
Negative	$FeCl_3$, molish

glucose 1%, peptone 0.3%, NaCl 0.25% and $CaCO_3$ 0.1% (pH 7.0). A 500-ml Erlenmeyer flask, containing 150 ml of the seed medium, was incubated with a stock culture of the producing strain maintained on a modified HV agar slant. After incubation for 24 h at 28 °C on a rotary shaker set at 180 r.p.m., 5 ml of the seed culture was transferred to each of the 250 ml Erlenmeyer flasks containing 65 ml of the production medium, which consisted of millet extract 1%, glucose 1%, peptone 0.3%, NaCl 0.25% and $CaCO_3$ 0.2% (pH 7.0). The fermentation was carried out at 28 °C for 5 days on a rotary shaker set at 180 r.p.m.

Extraction and isolation

The culture of 100 l was filtered with a cheesecloth to separate the medium and culture liquid. The culture liquid, which exhibited strong antibacterial activity, was absorbed onto a macroporous resin (HPD400, Cangzhou Baoen, Co. Ltd, Cang Zhou City, China), followed by elution with methanol. The methanol fractions were evaporated at 40 °C in vacuum to yield 60 g of extract. The extract was subjected to a silica gel column (600 g, 200–300 mesh, 6.5×110 cm) and eluted with petroleum ether, EtOAC–MeOH (100:0, 75:25, 50:50, 25:75, 0:100, v/v). The eluents were collected at 2000 ml for each fraction. The antimicrobial fraction was purified by reverse phase-HPLC (Hypersil C_{18}, 20×250 mm, 10 μm) with methanol/water (75:25, v/v) as mobile phase to yield compound NW-G01 (1.60 g).

Physicochemical properties

Physicochemical properties of NW-G01 are summarized in Table 3. The compound was soluble in methanol, ethyl acetate and dimethyl sulfoxide, but was insoluble in water and acetone. The compound displayed a positive reaction to iodine vapor and $AgNO_3$ solution. The spectra of HR-ESI-MS (*m/z* 757.3460[M+H]+) showed that the molecular weight of NW-G01 was 756 (Figure 4).

Antibacterial activities

The compound NW-G01 exhibited significant activity against several gram-positive bacteria (Table 4) with MIC values of less than 10 μg ml^{-1}. No obvious inhibitory effects were observed against gram-negative at the concentration of 250 μg ml^{-1}. The tested gram-positive bacteria were *Bacillus cereus* 1.1846, *Bacillus subtilis* 1.88, *S. aureus* 1.89, MRSA 212 and the gram-negative were *Escherichia coil* 1.1636, *Pseudomonas aeruginosa* 1.2031 and *Erwinia carotovora*.

DISCUSSION

In this paper, we presented a novel antibacterial cyclic hexadepsipeptide, NW-G01, isolated from the fermentation broth of strain no. 313. The results of the studies on morphological and physiological characteristics indicated that strain no. 313 had a high concordance with *S. alboflavus* NBRC-13196T, and the high similarity (99.5%) with 16S rDNA sequence, despite the obvious difference, was that the milk was coagulated for the strain no. 313. Therefore, strain no. 313 was named as *S. alboflavus* 313. The structure of NW-G01 is related to himastatin and chloptosin, which are dimers of cyclic hexadepsipeptide.

In this study, the antibacterial activities of NW-G01 against seven species of representative bacteria were tested. NW-G01 exhibited higher antibacterial activities than did ampicillin against four species of gram-positive bacteria, especially against MRSA, the MIC value of NW-G01 was 7.81 μg ml^{-1} and that of ampicillin was more

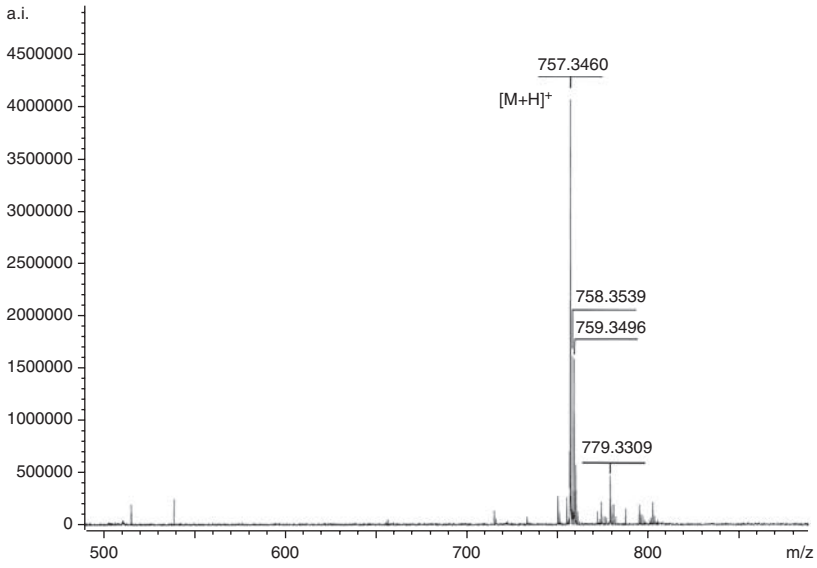

Figure 4 HR-ESI-MS spectrum of compound NW-G01.

Table 4 MICs of NW-G01 against the tested bacteria

Name of the test bacteria	*MIC of NW-G01* ($\mu g\,ml^{-1}$)	*MIC of ampicillin* ($\mu g\,ml^{-1}$)
Bacillus cereus (1.1846)	3.90	25
Bacillus subtilis (1.88)	3.90	12.5
Staphylococcus aureus (1.89)	7.81	25
MRSA 212	7.81	>100
Escherichia coil (1.1636)	>250	>100
Pseudomonas aeruginosa (1.2031)	>250	>100
Erwinia carotovora	>250	>100

than 100 $\mu g\,ml^{-1}$ (Table 4). It was reported that chloptosin[2] and himastatin,[1,5] the two similar cyclopeptides with NW-G01, had antitumor activity. The antitumor activity of NW-G01 will be evaluated subsequently. The above results suggest that NW-G01 may be a potential candidate as a pharmaceutical product.

METHODS

Isolation of the producing strain

The producing strain no. 313 was isolated from a soil sample collected from the Shaanxi province of China. Soil sample 1.0 g, combined with $CaCO_3$ (0.1 g), was incubated for 1 h at 110°C and suspended in 20 ml sterile water. After filtration and dilution with sterile water (10^{-1}, 10^{-2}, 10^{-3} and 10^{-4}) containing 1.5% phenol, 0.1 ml aliquots were spread onto modified HV agar and modified Bennett's agar[6] containing 1 µg potassium dichromate. The plates were incubated for 14 days at 28 °C, and the resulting colonies were transferred and maintained on the modified HV agar. Among the isolated strains, one strain that showed significant antibacterial activity was designated as strain no. 313.

Taxonomy of the producing strain

The studies on cultural and physiological characteristics of the producing strain were carried out following the methods recommended by the ISP[7] and Waksman,[8] and the utilization of carbon sources was tested according to the growth condition on plates containing different sugar sources. The morphological properties were observed with a scanning electron microscope (JSM6360LV JEOL). The isomers of DAP and whole-cell sugar pattern were determined by TLC analysis of the whole-organism hydrolysate.[9] Extraction of genomic DNA and 16S rRNA gene amplification were carried out according to Kim *et al.*[10] The 16S rDNA sequence was aligned using CLUSTAL X software version 1.83. A phylogenetic tree was constructed by the neighbor-joining method[11] using MEGA version 4.0 software, and Bootstrap analyses of 1000 replicates were carried out.

Assay for antibacterial activity

Antibacterial activity was measured by the micro-broth dilution method in 96-well culture plates using the Mueller-Hinton (MH) broth (Hangzhou Microbial Reagent Co. Ltd, Hangzhou City, China), according to the Standard of National Committee for Clinical Laboratory.[12] The standard bacterial strains were obtained from the China General Microbiological Culture Collection center. A clinical isolate of MRSA was obtained from Nanjing Medical University. Ampicillin (Sigma, Shanghai, China) was used as positive control. The tested bacteria were incubated in the MH broth for 12 h at 30 °C at 190 r.p.m., and the spore concentration was diluted to approximately 1×10^5–1×10^6 CFU with MH broth. After incubation for 24 h at 30 °C, the MICs were examined.

General procedure

Melting point was measured on an X-4 apparatus and was uncorrected. Optical rotation was measured on a Perkin-Elmer 341 polarimeter. IR spectra were determined on an IR-450 instrument (KBr plate). HR-ESI-MS was obtained on a Brüker Apex II mass spectrometer. Mass spectra were measured on a Finnigan LCQ Advantage mass spectrometer (ESI, positive mode). The compound was purified by a Shimadzu 6AD HPLC apparatus with preparation column Hypersil C_{18} (20×250 mm, 10 µm). Silica gel (200–300 mesh, Qingdao Haiyang Chemical Co. Ltd, Qingdao City, China) and HPD-400 macroporous resin (Cangzhou Baoen, Co. Ltd) were used for column chromatography.

ACKNOWLEDGEMENTS

This study was supported in part by a grant from The National Key Basic Research Program (973 Program, 2003CB114404) from the Science and Technology Ministry of China.

1 John, E. L. *et al.* Himastatin, a new antitumor antibiotic from *Streptomyces hygroscopicus* III. Structural elucidation. *J. Antibiot.* **49,** 299–311 (1996).

2 Umezawa, K., Ikeda, Y., Uchihata, Y., Naganawa, H. & Kondo, S. Chloptosin, an apoptosis-inducing dimeric cyclohexapeptide produced by *Streptomyces*. *J. Org. Chem.* **65,** 459–463 (2000).
3 Lechevalier, M. P. & Lechevalier, H. A. chemical composition as a criterion in the classification of aerobic actinomycetes. *Int. J. Syst. Bacteriol.* **20,** 435–443 (1970).
4 Shirling, E. B. & Gottlieb, D. Cooperative description of type cultures of *Streptomyces*. III. Additional species descriptions from first and second studies. *Int. J. Syst. Bacteriol.* **18,** 288–289 (1968).
5 Leet, J. E., Schroeder, D. R., Krishnan, B. S. & Matson, J. A. Himastatin, a new antitumor antibiotic from *Streptomyces hygroscopicus*. I. Taxonomy of the producing organism, fermentation and biological activity. *J. Antibiot.* **43,** 956–960 (1990).
6 Atlas, R. M. *Handbook of Microbiological Media*, 3rd edn, 206 (CRC Press, Boca Raton, London, New York, Washington, DC, 2004).
7 Shirling, E. B. & Gottlieb, D. Methods for characterization of *Streptomyces species*. *Int. J. Syst. Bacteriol.* **16,** 313–340 (1966).
8 Waksman, S. A. & Henrici, A. T. The nomenclature and classification of the actinomycetes. *J. Bacteriol.* **46,** 337–341 (1943).
9 Becker, B., Lechvalier, M. P. & Lechvalier, H. A. Chemical composition of cell-wall preparation from strains of various form-genera of aerobic actinomycetes. *Appl. Microbiol.* **13,** 236–243 (1965).
10 Kim, S. B. & Goodfellow, M. *Streptomyces thermospinisporus* sp. *nov.*, a moderately thermophilic carboxydotrophic streptomycete isolated from soil. *Int J. Syst. Evol. Microbiol.* **52,** 1225–1228 (2002).
11 Saitou, N. & Nei, M. The neighbor-joining method: a new method for reconstructing phylogenetic trees. *Mol. Biol. Evol.* **4,** 406–425 (1987).
12 Clinical and Laboratory Standards Institute. Methods for dilution antimicrobial susceptibility tests for bacteria that grow aerobically. Approved standard M7-A7 (2006).

The Journal of Antibiotics (2009) 62, 207–211

www.nature.com/ja

ORIGINAL ARTICLE

Pentacecilides, new inhibitors of lipid droplet formation in mouse macrophages produced by *Penicillium cecidicola* FKI-3765-1: II. Structure elucidation

Hiroyuki Yamazaki[1], Satoshi Ōmura[2] and Hiroshi Tomoda[1]

The structures of pentacecilides, new inhibitors of lipid droplet formation in mouse macrophages produced by *Penicillium cecidicola* FKI-3765-1, were elucidated by spectroscopic studies, including various NMR experiments. Pentacecilides have a common pentacyclic meroterpene core, which contains an aromatic ring and a δ-lactone ring.
The Journal of Antibiotics (2009) **62,** 207–211; doi:10.1038/ja.2009.19; published online 20 March 2009

Keywords: pentacecilides; structure elucidation; fungal metabolites; lipid droplet formation

INTRODUCTION

Three new compounds, designated pentacecilides A to C (Figure 1) were isolated as inhibitors of lipid droplet formation in mouse macrophages from the culture broth of *P. cecidicola* FKI-3765-1.[1] The taxonomy of the producing strain, fermentation, isolation and biological properties of pentacecilides were described in an earlier paper.[1] In this study, the physicochemical properties and structure elucidation of pentacecilides are described.

RESULTS

Physicochemical properties

The physicochemical properties of pentacecilides A to C are summarized in Table 1. They have a similar pattern with absorption maxima at 214–219 nm, 273–274 nm and 309–310 nm in UV spectra. IR absorption at 1619–1745 cm^{-1} and 3401–3434 cm^{-1} suggested the presence of carbonyl and hydroxy groups in their structures. These data indicated that they share a similar skeleton.

Structure elucidation of pentacecilide C

The molecular formula of pentacecilide C was determined to be $C_{27}H_{34}O_8$ on the basis of HRESI-TOF-MS measurement (Table 1). The ^{13}C NMR spectrum (in $CDCl_3$) showed 27 resolved signals, which were classified into six methyl carbons, four methylene carbons, two sp^3 methine carbons, one sp^2 methine carbon, three oxygenated sp^3 methine carbons, two sp^3 quaternary carbons, one oxygenated sp^3 quaternary carbon, three sp^2 quaternary carbons, two oxygenated sp^2 quaternary carbons and three carbonyl carbons by analysis of the DEPT and heteronuclear single quantum coherence (HSQC) spectra. The ^1H NMR spectrum (in $CDCl_3$) displayed 33 proton signals, one of which was suggested to be a hydroxyl proton (δ 11.08), as reported in thailandolides.[2] Taking the molecular formula into consideration, the presence of another hydroxy proton was suggested. The connectivity of proton and carbon atoms was established by the ^{13}C–^1H HSQC spectrum (Table 2). Analyses of ^1H–^1H COSY revealed the presence of partial structures I to IV, as shown in Figure 2. Furthermore, ^{13}C–^1H long-range couplings of ^2J and ^3J observed in the ^{13}C–^1H HMBC spectrum gave the following linkages (Figure 3a): (1) Cross-peaks from H_2-7′ (δ 2.70, 2.85) to C-1′ (δ 110.7), C-2′ (δ 139.3) and C-3′ (δ 102.2), from OH-4′ (δ 11.08) to C-3′, C-4′ (δ 162.3) and C-5′ (δ 103.5) and from H-5′ (δ 6.30) to C-1′, C-3′, C-4′ and C-6′ (δ 159.1) indicated that a phenol skeleton connects the partial structure I at C-2′. Furthermore, the findings that the chemical shift of C-8′ (δ 74.7) corresponds to an oxygenated carbon and the OH-4′ proton (δ 11.08) shifted to a lower field because of a hydrogen bonding indicated that C-3′ and C-8′ are connected through an ester bond, which form δ-lactone. This was also supported by the IR absorption (1619–1666 cm^{-1}). Although observation of a cross-peak from H-8′ to C-10′ (δ 169.9) was important and simple to show the presence of δ-lactone, the cross-peak was not observed because the dihedral angle between H-8′ and C-10′ is 90°. Therefore, the coupling constant in HMBC experiment was changed from J_{C-H}=8.0 Hz to J_{C-H}=3.0 Hz. As a result, the long-range coupling of ^4J from H-5′ to C-10′ was observed, supporting the presence of δ-lactone. (2) Cross-peaks from H_2-11 (δ 2.52) to C-8 (δ 79.0), from H_3-12 (δ 1.23) to C-7 (δ 71.8), C-8 and C-9 (δ 43.0), from H-7 (δ 4.11) to C-8 and C-9, from H-9 (δ 2.23) to C-8, C-10 (δ 36.2) and C-15 (δ 24.6), from H_2-6

[1]Graduate School of Pharmaceutical Sciences, Kitasato University, Shirokane, Minato-ku, Tokyo, Japan and [2]Kitasato Institute for Life Sciences, Kitasato University, Shirokane, Minato-ku, Tokyo, Japan
Correspondence: Professor H Tomoda, Graduate School of Pharmaceutical Sciences, Kitasato University, 5-9-1 Shirokane, Minato-ku, Tokyo 108-8641, Japan.
E-mail: tomodah@pharm.kitasato-u.ac.jp
Received 15 January 2009; revised 6 February 2009; accepted 19 February 2009; published online 20 March 2009

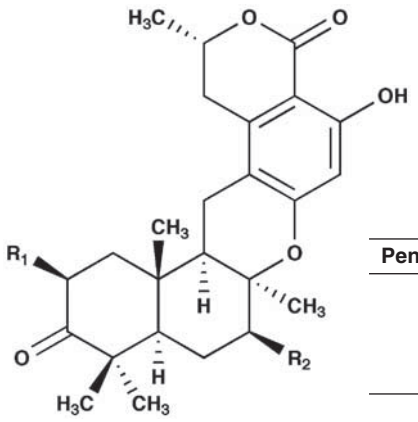

Pentacecilide	R_1	R_2
A	-H	-H
B	-OAc	-H
C	-OAc	-OH

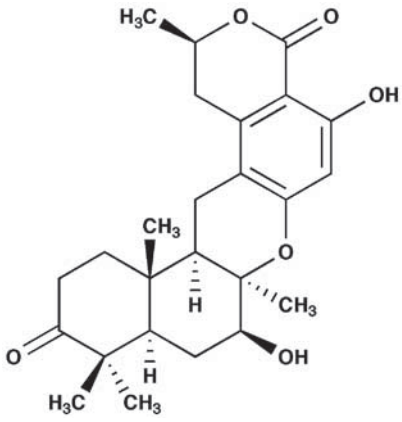

Thailandolide A

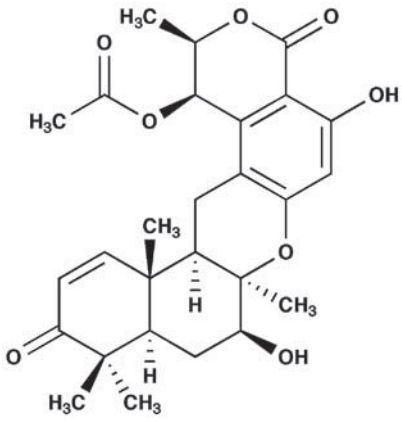

Thailandolide B

Figure 1 Structures of pentacecilides A to C and thailandolides A and B.

Table 1 Physicochemical properties of pentacecilides A, B and C

	Pentacecilide A	*Pentacecilide B*	*Pentacecilide C*
Appearance	White crystalline solid	White crystalline solid	White crystalline solid
Molecular weight	412	470	486
Molecular formula	$C_{25}H_{32}O_5$	$C_{27}H_{34}O_7$	$C_{27}H_{34}O_8$
HRESI-TOF-MS (*m/z*)			
Calcd:	435.2147 $(M+Na)^+$	493.2225 $(M+Na)^+$	509.2151 $(M+Na)^+$
Found:	435.2141 $(M+Na)^+$	493.2202 $(M+Na)^+$	501.2162 $(M+Na)^+$
UV (MeOH) λ_{max} nm (ε)	219 (18647), 274 (11846), 309 (4194)	219 (33055), 274 (18226), 309 (4784)	214 (54432), 273 (32736), 310 (4947)
$[\alpha]_D^{26}$	-4.38^o (*c*=0.38, $CHCl_3$)	-32.6^o (*c*=0.68, $CHCl_3$)	-32.3^o (*c*=0.48, $CHCl_3$)
IR (KBr) ν_{max} (cm^{-1})	3401, 1697. 1662, 1465, 1380	3440, 1747, 1727, 1666, 1475	3434, 1745, 1666, 1619, 1473

(δ 1.86, 2.18) to C-10, from H_3-15 (δ 1.54) to C-9, C-10 and C-1 (δ 41.1), from H-5 (δ 1.82) to C-4 (δ 48.3), C-10 and C-15, from H_2-1 (δ 1.88, 2.20) to C-3 (δ 207.8), C-5, C-10 and C-15, from H_3-13 (δ 1.14) to C-3, C-4, C-5 and C-14 (δ 25.7), from H_3-14 (δ 1.20) to C-3, C-4, C-5 and C-13 (δ 20.8) and from H-2 (δ 5.63) to C-3 showed the presence of a 3-oxo-decalin skeleton containing the partial structures II to IV. (3) Cross-peaks from H-2 and H_3-17 (δ 2.17) to C-16 (δ 170.3) showed that an acetoxy group is connected to C-2. The chemical shift of C-7 (δ 71.8) and the molecular formula showed the presence of a hydroxy group. (4) The finding that cross-peaks were observed from H-11 to C-1′, C-2′ and C-6′ and that the chemical shifts of C-8 (δ 79.0) and C-6′ (δ 159.1) correspond to an oxygenated carbon indicated that a phenol and a decalin ring are connected by a pyran ring. The pentacyclic structure was found to consist of a six-membered lactone, a phenol, a pyran and a decalin ring. Thus, the structure of pentacecilide C was elucidated as shown in Figure 1. The structure satisfied the degree of unsaturation and the molecular formula. Furthermore, all chemical shifts, except for C-2 in pentacecilide C, were comparable with those reported for thailandolide A.[2]

Table 2 ^{1}H and ^{13}C NMR chemical shift of pentacecilides A, B and C

	Pentacecilide A		*Pentacecilide B*		*Pentacecilide C*	
No.	δ_C	δ_H (J *in Hz*)	δ_C	δ_H (J *in Hz*)	δ_C	δ_H (J *in Hz*)
1	31.7	1.67 m	40.7	1.85 m	41.1	1.88 m
		2.06 m		2.18 m		2.20 m
2	33.7	2.44 m	72.6	5.59 (12.0, 7.0)	72.2	5.63 (12.0, 7.0)
		2.68 m				
3	219.6	—	208.6	—	207.8	—
4	47.2	—	48.6	—	48.3	—
5	48.1	1.88 m	48.0	1.77 m	45.6	1.82 m
6	18.5	1.58 m	17.7	1.68 m	26.7	1.86 m
				1.75 m		2.18 m
7	33.7	2.08 m	36.6	2.10 m	71.8	4.11 dd (10.0, 3.0)
		2.24 m				
8	78.3	—	78.1	—	79.0	—
9	44.8	1.86 m	48.5	1.88 m	43.0	2.23 m
10	35.4	—	36.6	—	36.2	—
11	20.3	2.44 m	21.2	2.44 dd (10.0, 2.5)	20.7	2.52 m
12	25.5	1.35 s	24.0	1.26 s	21.2	1.23 s
13	20.0	1.09 s	21.3	1.18 s	20.8	1.20 s
14	29.3	1.12 s	26.3	1.16 s	25.7	1.14 s
15	23.0	0.96 s	24.9	1.39 s	24.6	1.54 s
16			170.3	—	170.3	—
17			21.0	2.17 s	21.0	2.17 s
1′	110.5	—	110.9	—	110.7	—
2′	139.2	—	139.3	—	139.3	—
3′	101.7	—	101.9	—	102.2	—
4′	162.5	—	162.6	—	162.3	—
5′	103.3	6.27 s	103.5	6.27 s	103.5	6.30 s
6′	160.4	—	160.2	—	159.1	—
7′	32.0	2.72 dd (17.0, 11.0)	32.1	2.70 dd (17.0, 11.0)	31.8	2.70 dd (17.0, 11.0)
		2.84 dd (17.0, 3.5)		2.85 dd (17.0, 3.5)		2.85 dd (17.0, 3.5)
8′	75.0	4.64 m	74.9	4.62 m	74.7	4.62 m
9′	21.2	1.54 d (7.0)	21.2	1.55 d (7.0)	20.9	1.55 d (7.0)
10′	170.5	—	170.3	—	169.9	—
4′-OH		11.08 s		11.07 s		11.08 s

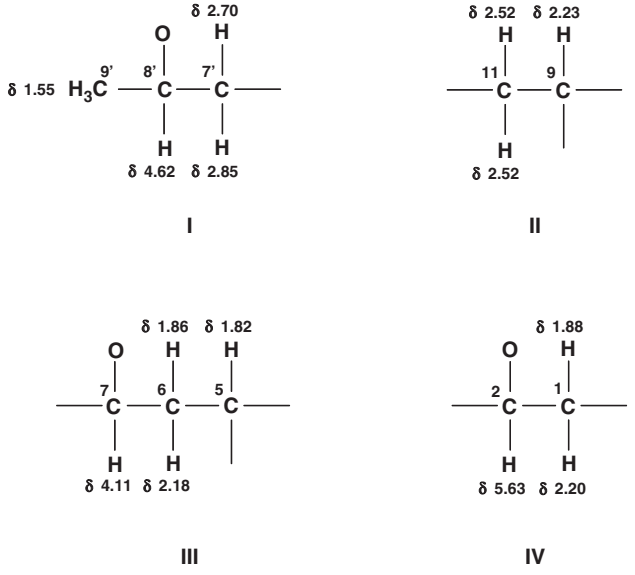

Figure 2 Partial structures of pentacecilide C.

Structure elucidation of pentacecilide B

The molecular formula $C_{27}H_{34}O_7$ of pentacecilide B is smaller by one oxygen atom than that of pentacecilide C. Comparison of the ^{1}H NMR spectra between pentacecilides B and C indicated that the oxygenated sp^3 methine proton (H-7) in pentacecilide C is replaced by methylene protons (δ 2.10) in pentacecilide B. In fact, analyses of the ^{1}H–^{1}H COSY revealed the presence of the partial structure V containing the replaced part (Figure 3b). The partial structure V was also confirmed by observing cross-peaks from H_3-12 (δ 1.26) to C-7 (δ 36.6), C-8 (δ 78.1) and C-9 (δ 48.5), from H_2-7 (δ 2.10) to C-8, from H-9 (δ 1.88) to C-8, C-10 (δ 36.6) and C-15 (δ 24.9), from H_2-6 (δ 1.68, 1.75) to C-10, from H_3-15 (δ 1.39) to C-9 and C-10 and from H-5 (δ 1.77) to C-10 in ^{13}C–^{1}H HMBC experiments (Figure 3b). Taken together, the structure of pentacecilide B was elucidated as 7-dehydroxy pentacecilide C (Figure 1).

Structure elucidation of pentacecilide A

The molecular formula $C_{25}H_{32}O_5$ of pentacecilide A is smaller by $C_2H_2O_3$ than that of pentacecilide C. Comparison of the ^{1}H NMR spectra of pentacecilides A and B showed that the methyl protons (H_3-17) disappear and the oxygenated sp^3 methine proton (H-2) is

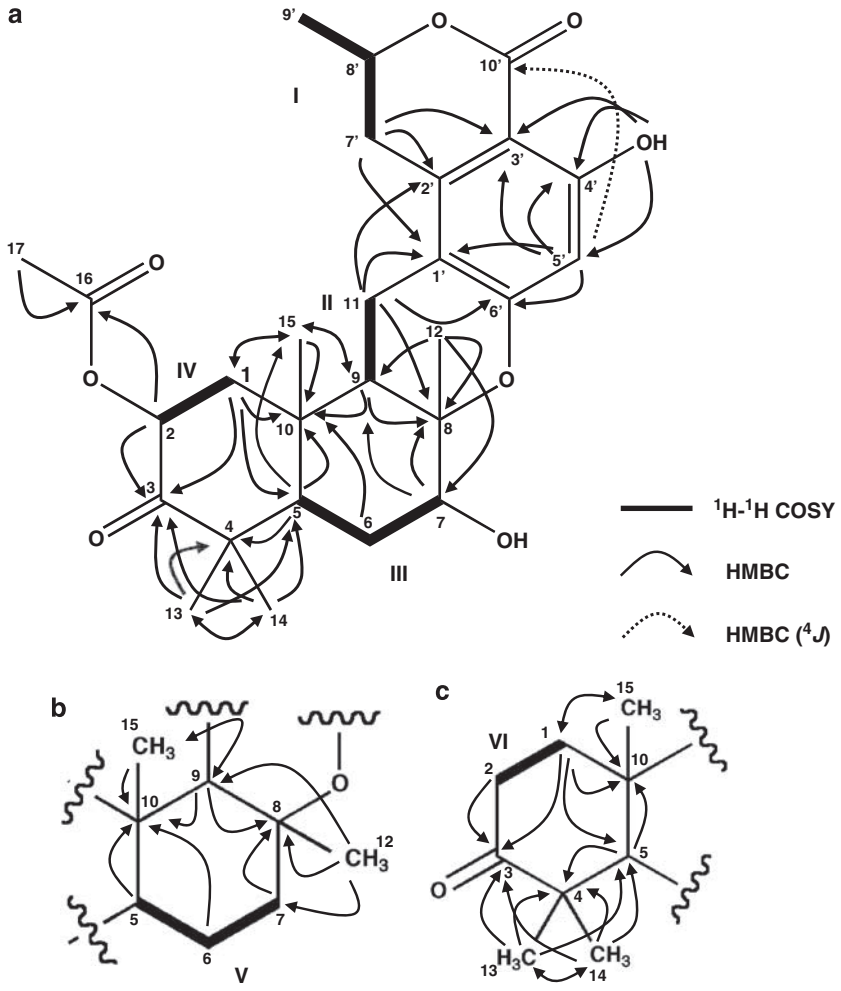

Figure 3 ^{1}H–^{1}H COSY and ^{13}C–^{1}H HMBC experiments of pentacecilides A (**a**), B (**b**) and C (**c**).

replaced by methylene protons (δ 2.44, 2.68). Analyses of the ^{1}H–^{1}H COSY revealed that the partial structure VI contains the replaced part (Figure 3c). The partial structure VI was also confirmed by observing cross-peaks from H_3-15 (δ 0.96) to C-1 (δ 31.7) and C-10 (δ 35.4), from H-5 (δ 1.88) to C-4 (δ 47.2) and C-10, from H_2-1 (δ 1.67, 2.06) to C-3 (δ 219.6), C-5 (δ 48.1), C-10 and C-15 (δ 23.0), from H_3-13 (δ 1.09) to C-3, C-4, C-5 and C-14 (δ 29.3), from H_3-14 (δ 1.12) to C-3, C-4, C-5 and C-13 (20.0) and from H_2-2 to C-3 in ^{13}C–^{1}H HMBC experiments (Figure 3c). Taken together, the structure of pentacecilide A was elucidated as 2-deacetoxy pentacecilide B (Figure 1).

Stereochemistry of pentacecilides

Pentacecilide C has seven chiral carbons in its structure. The relative stereochemistry at C-2, C-5, C-7, C-8, C-9 and C-10 of the tricyclic skeleton (A–B–C) was investigated by NOESY experiments. As shown in Figure 4, cross-peaks were observed between H-2 (δ 5.63) and H_3-13 (δ 1.20)/H_3-15 (δ 1.54), between H_3-15 and H_{ax}-6 (δ 2.18)/H_3-13, between H-5 (δ 1.82) and H-7 (δ 4.11)/H-9 (δ 2.23) and H-7 and H-9, indicating that they are oriented in a 1,3-diaxial conformation. Accordingly, rings A and B are oriented in a chair-chair form. Secondly, cross-peaks were observed between H_3-12 (δ 1.23) and H-7/H_2-11 (δ 2.52) and between H_3-15 and H_2-11, suggesting that rings B and C are oriented in a chair-boat form. Thirdly, cross-peaks were observed between H_{eq}-7′ (δ 2.85) and H-11/H-8′ (δ 4.62) and

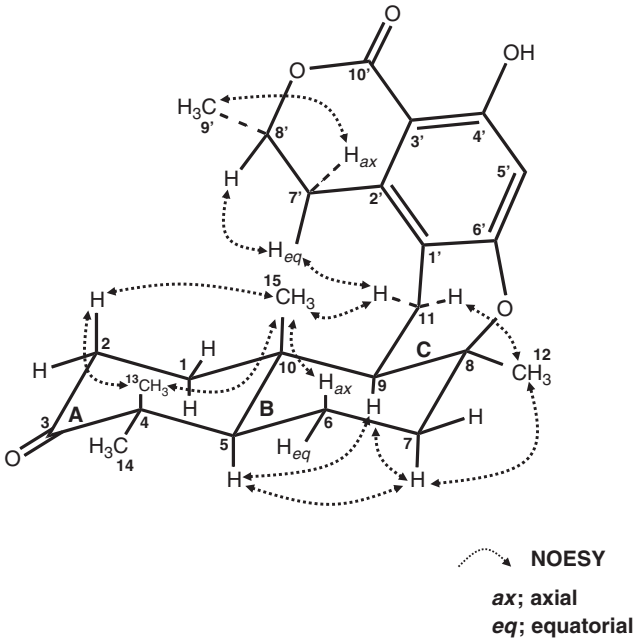

Figure 4 NOESY experiments of pentacecilide C.

between H_{ax}-7′ and H_3-9 (δ 1.55), indicating that the conformation of H_3-9′ is equatorial, which was also supported by a large coupling constant (J=11 Hz) between H_{ax}-7′ and H-8′. Taken together, the relative stereochemistry of pentacecilide C was determined as shown in Figure 1. These results were consistent with those of thailandolide A except for the stereochemistry at C-8′, although chemical shifts at C-8′ of pentacecilide C and thailandolide A were almost the same.[2]

The relative stereochemistry of pentacecilides A and B was deduced to be the same as that of pentacecilide C by the similarity of NOESY experiments and the coupling constants in ^{1}H NMR.

DISCUSSION

Pentacecilides A to C, structurally related to thailandolides, were isolated from the culture broth of *P. cecidicola* FKI-3765-1, and were found to have a common pentacyclic core containing an aromatic ring and a δ-lactone ring. The core seemed to be a meroterpene, consisting of a sesquiterpene and a pentaketide. Thailandolides were reported to be produced by *Talaromyces thailandiasis*,[2] whereas pentacecilides were produced by a different genus *Penicillium*. Thailandolides A and B were not detected in the culture broth of *P. cecidicola* FKI-3765-1.

From the structure elucidation, the planar structures of pentacecilides were seen to be similar to those of thailandolides. The relative stereochemistry of the compounds is almost the same, but the C-8′ stereochemistry is different; the C-8′ methyl group of thailandolides is oriented in the axial conformation,[2] whereas that of pentacecilides is in the equatorial conformation.

METHODS

General experimental procedures

UV spectra were recorded on a spectrophotometer (8453 UV-Visible spectrophotometer, Agilent Technologies Inc., Santa Clara, CA, USA). IR spectra were recorded on a Fourier transform infrared spectrometer (FT-710, Horiba Ltd, Kyoto, Japan). Optical rotations were measured with a digital polarimeter (DIP-1000, JASCO Corporation, Tokyo, Japan). ESI-TOF-MS and HRESI-TOF-MS spectra were recorded on a mass spectrometer (JMS-T100LP, JEOL Ltd, Tokyo, Japan). Various NMR spectra were measured with a spectrometer (XL-400, Varian Inc., Palo Alto, CA, USA).

ACKNOWLEDGEMENTS

This study was supported by the Program for the Promotion of Fundamental Studies in Health Sciences (to HT) from the National Institute of Biomedical Innovation (NIBIO). We express our thanks to Ms N Sato for measuring NMR experiments, and Mr K Nagai and Ms A Nakagawa for measuring mass spectra. We also thank Mr N Ugaki for excellent technical assistance.

1 Yamazaki, H *et al.* Pentacecilides, new inhibitors for lipid droplet formation in mouse macrophages produced by *Penicillium cecidicola* FKI-3765-1. I. Taxonomy, fermentation, isolation and biological properties. *J. Antibiot.* **62,** 195–200 (2009).
2 Dethoup, T *et al.* Merodrimanes and other constituents from *Talaromyces thailandiasis*. *J. Nat. Prod.* **70,** 1200–1202 (2007).

The Journal of Antibiotics (2009) 62, 213–216

www.nature.com/ja

NOTE

Effect of cobalt and vitamin B_{12} on the production of salinosporamides by *Salinispora tropica*

Ginger Tsueng and Kin Sing Lam

The Journal of Antibiotics (2009) **62,** 213–216; doi:10.1038/ja.2009.7; published online 6 February 2009

Keywords: cobalt; NPI-0047; NPI-0052; NPI-2065; *Salinispora tropica*; salinosporamide A; vitamin B_{12}

NPI-0052 (Figure 1) is a novel, potent proteasome inhibitor[1,2] isolated from a marine actinomycete *Salinispora tropica*.[3] It possesses a broad spectrum of activities against various tumors in animal models,[1,2,4,5] and is currently being evaluated in clinical trials for the treatment of patients with hematologic and solid tumor malignancies.[2] A saline fermentation process for the large scale production of NPI-0052 has been developed to supply NPI-0052 for clinical study. Owing to the structure similarity of NPI-0052 and cometabolites, NPI-0047 (Figure 1) and NPI-2065 (Figure 1), and their close chromatographic elution profiles, the recovery yield of NPI-0052 is highly dependent on the amount of NPI-0047 and NPI-2065 present in the fermentation.

During the development of the defined salt formulations to replace the nondefined synthetic sea salt formulation in supporting the cGMP production of NPI-0052 by *S. tropica* NPS21184, we observed that the production of NPI-0047 in a medium containing the defined salt formulation I was significantly lower than that in a medium containing the synthetic sea salt formulation.[6] Inductively coupled plasma dynamic reaction cell mass spectrometry (ICP-DRC-MS) analysis of seven major ion concentrations in the two salt formulations revealed that the defined salt formulation contained a fivefold higher cobalt concentration than the synthetic sea salt formulation.[6] This observation suggested that cobalt may play a role in the production of NPI-0047. In this study, we provide data on the effect of cobalt on the production of NPI-0047 and the two closely related salinosporamides, NPI-0052 and NPI-2065. As cobalt is an essential component of vitamin B_{12}, a coenzyme involved in methylation and carbon skeletal rearrangement reactions,[7] we also examined the effect of vitamin B_{12} on the production of salinosporamides.

MATERIALS AND METHODS

Microorganism

Three *S. tropica* strains, CNB440,[8] CNB476[8] and NPS21184,[9] were used in this study. The CNB440, CNB476 and NPS21184 were deposited with ATCC (the American type culture collection) and assigned the accession numbers ATCC BAA-916 T, PTA-5275 and PTA-6685, respectively.

Growth media and salt formulations

The composition of seed medium SD2, production medium SHY and defined salt formulation I was described by Tsueng *et al.*[6] Synthetic sea salt formulation, Instant Ocean, from Aquarium Systems (Mentor, OH, USA) was used in this study. Defined salt formulation I and Instant Ocean were supplemented with cobalt chloride hexahydrate (Mallinckrodt, Paris, KY, USA) and vitamin B_{12} (cyanocobalamin; Tokyo Kasei Kogyo, Tokyo, Japan), as described in the Results.

Culturing conditions, extraction and HPLC analysis

The culturing conditions, the preparation of fermentation extracts and the analysis of salinosporamides in the extracts by HPLC were described by Tsueng *et al.*[6] For the butyric acid-feeding study, sodium butyrate (Sigma, St Louis, MO, USA) was added to the production culture at a final concentration of 0.9 μM at 47 h followed by the addition of 2 g of Amberlite XAD-7 resin (Sigma, St Louis, MO, USA) after 1 h.

In the synthetic sea salt formulation medium without cobalt or vitamin B_{12} supplement, the production of NPI-0047 was 15 mg l^{-1}, 6.6% of NPI-0052 production (control, Table 1). When the synthetic sea salt formulation was supplemented with cobalt chloride as low as 0.055 μM, the production of NPI-0047 was reduced by 41% to 8.9 mg l^{-1} (Table 1). Maximal inhibition of NPI-0047 production (65%, 5.3 mg l^{-1}) was observed at an added cobalt concentration of 0.22 μM (Table 1). The amount of NPI-0047 produced was 2% of the titer of NPI-0052. Increasing the cobalt concentration to 2.2 μM in the synthetic sea salt formulation did not exert an additional inhibitory effect on the production of NPI-0047 (5.4 mg l^{-1}, Table 1). The addition of cobalt to the synthetic sea salt formulation also decreased the production of NPI-2065 by 30%, and increased the production of NPI-0052 by 16% (Table 1).

The effect of supplementing vitamin B_{12} to the synthetic sea salt formulation on the production of salinosporamides was also

Nereus Pharmaceuticals Inc., San Diego, CA, USA
Correspondence: Dr KS Lam, Nereus Pharmaceuticals Inc., 10480 Wateridge Circle, San Diego, CA 92121, USA.
E-mail: rlam@nereuspharm.com
Received 25 September 2008; accepted 13 January 2009; published online 6 February 2009

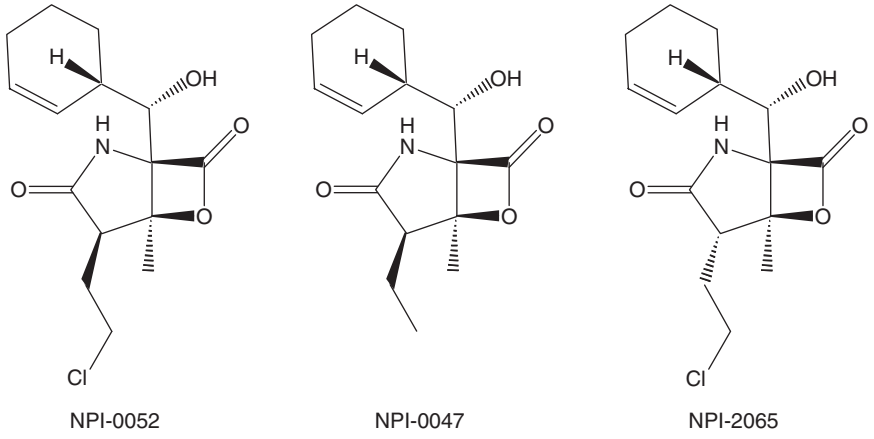

Figure 1 Structure of NPI-0052, NPI-0047 and NPI-2065.

Table 1 The effect of cobalt and vitamin B_{12} on the production of salinosporamides by *Salinispora tropica* NPS21184 in media containing synthetic sea salt or defined salt formulations

Salt formulation	*Additive*	*NPI-0047 (mg l^{-1})*	*NPI-0052 (mg l^{-1})*	*NPI-2065 (mg l^{-1})*
Synthetic sea salt formulation	Control, no addition	15 ± 0.8	228 ± 8	7.8 ± 0.5
	0.055 μM cobalt chloride	8.9 ± 0.9	261 ± 10	5.8 ± 0.2
	0.22 μM cobalt chloride	5.3 ± 0.4	265 ± 8	5.5 ± 0.1
	0.88 μM cobalt chloride	5.4 ± 0.4	274 ± 11	5.3 ± 0.1
	2.2 μM cobalt chloride	5.8 ± 0.3	271 ± 7	5.5 ± 0.2
	0.055 μM vitamin B12	3.7 ± 0.4	269 ± 9	5.6 ± 0.3
	0.22 μM vitamin B_{12}	2.8 ± 0.2	266 ± 9	4.9 ± 0.2
	0.88 μM vitamin B_{12}	2.8 ± 0.3	266 ± 11	5.4 ± 0.2
	2.2 μM vitamin B_{12}	2.5 ± 0.2	247 ± 10	4.9 ± 0.2
Defined salt formulation	Control, no addition	11 ± 0.8	248 ± 6	7.8 ± 0.3
	0.22 μM cobalt chloride	1.2 ± 0.1	292 ± 9	5.4 ± 0.3
	0.88 μM cobalt chloride	1.4 ± 0.1	293 ± 10	6.5 ± 0.3
	0.22 μM vitamin B_{12}	0.96 ± 0.05	275 ± 12	5.8 ± 0.2
	0.88 μM vitamin B_{12}	0.90 ± 0.08	270 ± 9	5.9 ± 0.3

examined and the results are shown in Table 1. Although the effect of vitamin B_{12} on the production of salinosporamides was similar to that of cobalt, vitamin B_{12} exerted a stronger inhibitory effect than cobalt on the production of NPI-0047, maximally inhibiting the production of NPI-0047 by 83%. The production of NPI-0047 was 2.8 mg l^{-1}, 1.1% of the production of NPI-0052, in the vitamin B_{12} salt formulation medium.

We examined the effect of cobalt and vitamin B_{12} at two different concentrations (0.22 and 0.88 μM) on the production of salinosporamides by *S. tropica* strain, NPS21184, in medium containing defined salt formulation. The results are summarized in Table 1. In the defined salt formulation medium without cobalt or vitamin B_{12} supplement, the production of NPI-0047 was 11 mg l^{-1}, 4.5% of the NPI-0052 production. Vitamin B_{12} (92%) exerted a stronger inhibitory effect on the production of NPI-0047 than did cobalt (88%) in the medium containing defined salt formulation. The production of NPI-0047 was 0.9 mg l^{-1}, 0.3% of the production of NPI-0052, in the vitamin B_{12} salt formulation medium. In the cobalt salt formulation medium, the production of NPI-0047 was 1.4 mg l^{-1}, 0.5% of the production of NPI-0052. The production of NPI-0047 in the defined salt formulation medium was lower than that in the synthetic sea salt formulation medium. Cobalt and vitamin B_{12} inhibited the production of NPI-2065 by 17 and 26%, respectively, and increased the production of NPI-0052 by 18 and 11%, respectively.

The effect of cobalt on the production of salinosporamides in the medium containing the defined salt formulation by three *S. tropica* strains, CNB440, CNB476 and NPS21184, was compared, and the results are summarized in Table 2. Although cobalt exerted an inhibitory effect on the production of NPI-0047 in all three *S. tropica* strains, the extent of inhibition was different in each strain. Cobalt inhibited the production of NPI-0047 in CNB440, CNB476 and NPS21184 by 48 (6.8 mg l^{-1}), 52 (8.1 mg l^{-1}) and 89% (1.2 mg l^{-1}), respectively. Cobalt increased the production of NPI-0052 in NPS21184 by 18%, but had no effect on the production of NPI-0052 in CNB440 and CNB476. In CNB476 and NPS21184, cobalt inhibited the production of NPI-2065 by 31% each, but had no effect on the production of NPI-2065 in CNB440. The maximal production of NPI-0052 by NPS21184 in a defined salt formulation medium supplemented with cobalt was 292 mg l^{-1}, approximately threefold higher than the production of NPI-0052 by CNB440 (84 mg l^{-1}) and CNB476 (111 mg l^{-1}).

In our earlier biosynthetic study, we showed that sodium butyrate incorporated into NPI-0047, but not into NPI-0052.[9] Feeding sodium butyrate to cultures of NPS21184 (grown in synthetic sea salt

Table 2 The effect of cobalt and vitamin B_{12} on the production of salinosporamides in defined salt formulation medium by *Salinispora tropica* strains CNB440, CNB476 and NPS21184

	NPI-0047 (mg l^{-1})	*NPI-0052 (mg l^{-1})*	*NPI-2065 (mg l^{-1})*
CNB440, control	13 ± 0.9	100 ± 3	0.8 ± 0.06
CNB440, 0.22 μM cobalt chloride	6.8 ± 0.5	84 ± 2	0.7 ± 0.07
CNB476, control	17 ± 0.7	111 ± 3	1.3 ± 0.10
CNB476, 0.22 μM cobalt chloride	8.1 ± 0.4	111 ± 2	0.9 ± 0.04
NPS21184, control	11 ± 0.8	248 ± 6	7.8 ± 0.30
NPS21184, 0.22 μM cobalt chloride	1.2 ± 0.1	292 ± 9	5.4 ± 0.30

Table 3 Inhibition of butyric acid incorporation into NPI-0047 by cobalt and vitamin B_{12} in *Salinispora tropica* NPS21184

	NPI-0047 (mg l^{-1})	*NPI-0052 (mg l^{-1})*	*NPI-2065 (mg l^{-1})*
Control, no addition	11 ± 0.7	252 ± 9	6.3 ± 0.4
Control+9 μM sodium butyrate	34 ± 3	200 ± 6	4.6 ± 0.2
Control+9 μM sodium butyrate+0.22 μM cobalt chloride	15 ± 0.8	181 ± 5	4.0 ± 0.5
Control+9 μM sodium butyrate+0.22 μM vitamin B_{12}	5.6 ± 0.3	159 ± 6	3.2 ± 0.3

formulation medium) enhanced the production of NPI-0047 by as much as 319% while inhibiting the production of NPI-0052 by 26%.[9] The effect of cobalt and vitamin B_{12} on the incorporation of sodium butyrate into NPI-0047 by NPS21184 grown in a medium containing defined salt formulation was examined. Supplementing the growth medium with sodium butyrate (9 μM) without added cobalt or vitamin B_{12} increased the production of NPI-0047 from 11 mg l^{-1} (control, no sodium butyrate) to 34 mg l^{-1}, an increase of 209% (Table 3). Adding 0.22 μM cobalt and vitamin B_{12} to the butyrate-supplemented cultures decreased the production of NPI-0047 to 15 and 5.6 mg l^{-1}, respectively (Table 3). Vitamin B_{12} exerted a stronger inhibitory effect on the incorporation of sodium butyrate into NPI-0047 than cobalt.

In this study, we show that cobalt and vitamin B_{12} inhibit the production of NPI-0047 through *S. tropica* by examining their effects on the production of NPI-0047 in media containing two different salt formulations. This is an important finding with practical applications to the manufacturing of NPI-0052. The cometabolites, NPI-0047 and NPI-2065, have elution profiles similar to NPI-0052 in both normal and reverse phase chromatography. The effectiveness in separating NPI-0047 from NPI-0052 in the crude extract by flash column chromatography without lowering the recovery yield of NPI-0052 is dependent on the relative ratio of NPI-0047 to NPI-0052. Inclusion of cobalt and vitamin B_{12} at a concentration of 0.88 μM in the defined salt formulation medium significantly reduced the production of NPI-0047 by 87–92% and slightly increased the production of NPI-0052 by 8.9–18% by NPS21184, thereby lowering the ratio of NPI-0047 to NPI-0052 from 4.4 to 0.3–0.5%. Furthermore, cobalt and vitamin B_{12} also slightly reduced the production of the other interfering analog, NPI-2065, by 17–26% in NPS21184. This might improve the recovery yield of NPI-0052 by removing NPI-2065 from NPI-0052 in the subsequent purification step. A simple addition of a metal ion or a cofactor to the salt formulation has significant effect in improving the metabolite production profile without using laborious genetic engineering techniques.

As vitamin B_{12} exerted a stronger inhibitory effect on the production of NPI-0047 than did cobalt, the inhibitory effect of cobalt may be the result of increased production of vitamin B_{12} in the microorganism. Vitamin B_{12} is a coenzyme for the methyltransferase, mediating the terminal step in the biosynthesis of methionine, a common donor of methyl groups through S-adenosylmethionine.[7] Numerous reports on the increase in production of methylated antibiotics and the decrease in production of demethylated antibiotics by the addition of cobalt or vitamin B_{12} to fermentation have been reported.[10–13] All the above methylated antibiotics require methionine as methyl donor. Using [13C-methyl]-methionine in a feeding study experiment, we found that the methyl group of methionine did not incorporate into NPI-0047 and NPI-0052 (data not shown). Although we have not determined the molecular mechanism in inhibiting the production of NPI-0047 by cobalt and vitamin B_{12}, we showed that cobalt and vitamin B_{12} exerted their effects on the inhibition of incorporation of precursor butyric acid into NPI-0047. The slight increase in the production of NPI-0052 might be because of shunting the precursors from the NPI-0047 pathway toward the NPI-0052 pathway.

In this study, we observed that different strains of *S. tropica* respond differently to the effect of cobalt on the production of salinosporamides. *S. tropica* CNB440 is the type strain isolated from a sediment sample by Jensen *et al.*,[8] and its taxonomical characterization has been described by Maldonado *et al.*[14] *S. tropica* CNB476 was isolated from another sediment sample by Jensen *et al.*[8] *S. tropica* NPS21184 is a single colony isolate derived from CNB476 by Tsueng *et al.*[9] Cobalt exerted a significantly stronger inhibitory effect on the production of NPI-0047 in NPS21184 (89%) than that in CNB440 (48%) and CNB476 (52%). We have recently shown that these three *S. tropica* strains are true marine actinomycetes even though they do not require seawater for growth; they have a certain osmotic pressure growth requirement.[15] However, these three strains have different sensitivities to the medium ionic strength for the maintenance of viability and growth;[15] therefore, it is not surprising to observe different responses of the cobalt effect exhibited by these three strains. As there is very limited knowledge of the physiology of marine actinomycetes, further work is required to identify the mechanisms that lead to the different responses to cobalt and medium ionic strength in these *S. tropica* strains.

1 Chauhan, D. *et al.* A novel orally active proteasome inhibitor induces apoptosis in multiple myeloma cells with mechanisms distinct from bortezomib. *Cancer Cell* **8**, 407–419 (2005).

2 Chauhan, D., Hideshima, T. & Anderson, K. C. A novel proteasome inhibitor NPI-0052 as an anticancer therapy. *Brit. J. Cancer* **95,** 961–965 (2006).
3 Feling, R. H. *et al.* Salinosporamide A: a highly cytotoxic proteasome inhibitor from a novel microbial source, a marine bacterium of the new genus *Salinispora*. *Chem. Int. Ed.* **42,** 355–357 (2003).
4 Cusack, J. C. *et al.* NPI-0052 enhances tumoricidal response to conventional cancer therapy in a colon cancer model. *Clin. Cancer. Res.* **12,** 6758–6764 (2006).
5 Sloss, C. M. *et al.* Proteasome inhibition activates epidermal growth factor receptor (EGFR) and EGFR-independent mitogenic kinase signaling pathways in pancreatic cancer cells. *Clin. Cancer Res.* **14,** 5116–5123 (2008).
6 Tsueng, G., Teisan, S. & Lam, K. S. Defined salt formulations for the growth of *Salinispora tropcia* strain NPS21184 and the production of salinosporamide A (NPI-0052) and related analogs. *Appl. Microbiol. Biotechnol.* **78,** 827–832 (2008).
7 Matthews, R. G. Cobalamin-dependent methyltransferases. *Acc. Chem. Res.* **34,** 681–689 (2001).
8 Jensen, P. R., Dwight, R. & Fenical, W. Distribution of actinomycetes in near-shore tropical marine sediments. *Appl. Environ. Microbiol.* **57,** 1102–1108 (1991).
9 Tsueng, G., McArthur, K. A., Potts, B. C. M. & Lam, K. S. Unique butyric acid incorporation patterns for salinosporamides A and B reveal distinct biosynthetic origins. *Appl. Microbiol. Biotechnol.* **75,** 999–1005 (2007).
10 Favret, M. E. & Boeck, L. D. Effect of cobalt and cyanocobalamin on biosynthesis of A10255, a thiopeptide antibiotic complex. *J. Antibiot.* **45,** 1809–1811 (1992).
11 Gastaldo, L. & Marinelli, F. Changes in GE2270 antibiotic production in *Planobispora rosea* through modulation of methylation metabolism. *Microbiology* **149,** 1523–1532 (2003).
12 Nishikohri, K. & Fukui, S. Biosynthesis of mitomycin in *Streptomyces caepitosus*. Relationship of intracellular vitamin B_{12} level to mitomycin synthesis and enzymatic methylation of a demethylated derivative of mitomycin. *Eur. J. Appl. Microbiol.* **2,** 129–145 (1975).
13 Schulman, M. D. *et al.* Demethylavermectins. Biosynthesis, isolation and characterization. *J. Antibiot.* **38,** 1494–1498 (1985).
14 Maldonado, L. A. *et al. Salinispora arenicola* gen. nov., sp. nov. and *Salinispora tropica* sp. nov., obligate marine actinomycetes belonging to the family *Micromonosporaceae*. *Int. J. Syst. Evol. Microbiol.* **55,** 1759–1766 (2005).
15 Tsueng, G. & Lam, K. S. Growth of *Salinispora tropica* strains CNB440, CNB476, and NPS21184 in nonsaline, low-sodium media. *Appl. Microbiol. Biotechnol.* **80,** 873–880 (2008).

The Journal of Antibiotics (2009) 62, 217–219

www.nature.com/ja

NOTE

The cytotoxic and antifungal activities of two new sesquiterpenes, malfilanol A and B, derived from *Malbranchea filamentosa*

Daigo Wakana[1], Tomoo Hosoe[1], Hiroshi Wachi[1], Takeshi Itabashi[1], Kazutaka Fukushima[2], Takeshi Yaguchi[2] and Ken-ichi Kawai[1]

The Journal of Antibiotics (2009) **62,** 217–219; doi:10.1038/ja.2009.9; published online 13 February 2009

Keywords: antifungal activity; cytotoxic activity; *Malbranchea filamentosa*; malfilanol; sesquiterpene

Fungi of the genus *Malbranchea* belong to the family *Onygenaceae* and are taxonomically close to human and animal pathogenic fungi.[1] These facts prompted us to investigate the chemical constituents of *Malbranchea* fungi. We recently reported the isolation and structural characterization of 4-benzyl-3-phenyl-5*H*-furan-2-one as a vasodilator, malfilamentosides A and B as furanone glycosides and malbrancheosides A–D as triterpene glycosides, from the fungus *Malbranchea filamentosa* IFM41300.[2–4] Further purification of extracts of rice cultivated by the above fungus allowed us to isolate two new sesquiterpenes, designated malfilanol A (**1**) and B (**2**). Characterization of their structures, cytotoxic activities and antifungal activities are described in this paper.

The molecular formula of malfilanol A (**1**) (Figure 1) was determined as $C_{15}H_{24}O_3$ (four degrees of unsaturation) by high-resolution chemical-ionization mass spectrometry (HRCI-MS). Detailed analyses of the ^{1}H- and ^{13}C-NMR spectra and HMQC correlations of **1** revealed the presence of one exchangeable proton, three methyl units, five methylene units, two methine units, two quaternary carbons (one of which is oxygenated) and one olefine unit with an attached carboxylic acid (δ 172.6). These data accounted for the ^{1}H- and ^{13}C-NMR resonances and required the compound to be bicyclic. Interpretation of the ^{1}H–^{1}H COSY data led to the identification of two isolated proton spin systems corresponding to C-2–C-3 and C-5–C-7, including the branched C-9–C-11 chain subunits of structure **1**. The heteronuclear multiple bond coherence (HMBC) correlations (Figure 2) from H_3-12 to C-1, C-2, C-11; from H_3-13 to C-4, C-5, C-14; from H_3-14 to C-3, C-13; from H_2-2 to C-4, C-11; from H_2-3 to C-5; from H_2-5 to C-13, C-7; from H-7 to C-6, C-9, C-11, C-15; and from H_2-9 to C-7, C-8, C-10, C-11 enabled the determination of structure **1**.

Analysis of NOESY data (Figure 3) and ^{1}H NMR *J*-values enabled assignment of the relative configuration of malfilanol A (**1**). The coupling constant observed between H-6 and H-11 (2.8 Hz) indicated these two protons to be in a *cis* configuration. NOESY correlations of H-6 both with H_3-14 and with one proton of H_2-10 (δ_H 1.41) revealed that all these protons have a *syn* orientation. Further, the NOESY correlation between another proton of H_2-10 (δ_H 1.77) and H_3-12 was used to place these protons on opposite faces of the molecule against H-6, thereby establishing the relative configuration of malfilanol A (**1**).

The elemental composition of malfilanol B (**2**) was determined as $C_{16}H_{26}O_3$ (four degrees of unsaturation) on the basis of HRCI-MS and NMR data, which weighs 14 mass units higher than **1**. Analysis of ^{1}H- and ^{13}C-NMR data revealed the presence of a methoxy group (δ_C 51.4, δ_H 3.69) in **2**, instead of a hydroxyl group attached to C-15. On the basis of this consideration, the structure of **2** was presumed to be the methyl ester of **2**. Further, methylation of **1** with CH_2N_2 provided **2**, which was identical to the naturally occurring one, including the optical rotation (CD spectra). Therefore, malfilanol B (**2**) was identified as the methyl ester of **1**, and was established to have the same stereochemistry at C-1, C-6 and C-11 as **1**.

Antifungal activity was determined using the paper disk method, as described in a previous study.[5] Malfilanol A (**1**) and malfilanol B (**2**) showed specific antifungal activities against *Cryptococcus neoformans* (the diameters of the inhibition circles for **1** and **2** were 15 and 13 mm, respectively), but there was no antifungal activity against *Aspergillus fumigatus*, *A. niger* or *Candida albicans*, at 50 μg per disk. Malfilanol A (**1**) and B (**2**) were tested for cytotoxic activities against human umbilical vein endothelial cells (HUVEC) and A549 human lung cancer cells. Malfilanol A (**1**) and B (**2**) inhibited the cell proliferation of HUVEC with IC_{50} values of 14.6 and 19.8 μM respectively, while

[1]Faculty of Pharmaceutical Sciences, Hoshi University, Tokyo, Japan and [2]Research Center for Pathogenic Fungi and Microbial Toxicoses, Chiba University, Chiba, Japan
Correspondence: Dr T Hosoe, Faculty of Pharmaceutical Sciences, Hoshi University, Ebara 2-4-41, Shinagawa-ku, Tokyo 142-8501, Japan.
E-mail: hosoe@hoshi.ac.jp
Received 22 September 2008; accepted 21 January 2009; published online 13 February 2009

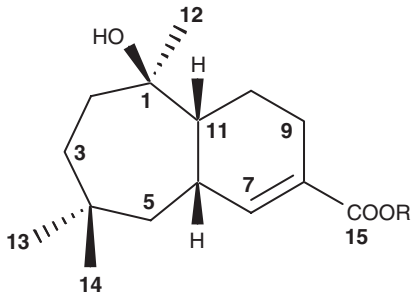

Malfilanol A (**1**) R = H

Malfilanol B (**2**) R = CH_3

Figure 1 Structures of malfilanol A (**1**) and B (**2**).

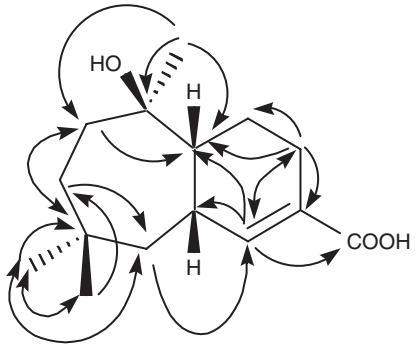

Figure 2 Important HMBC correlations of malfilanol A (**1**).

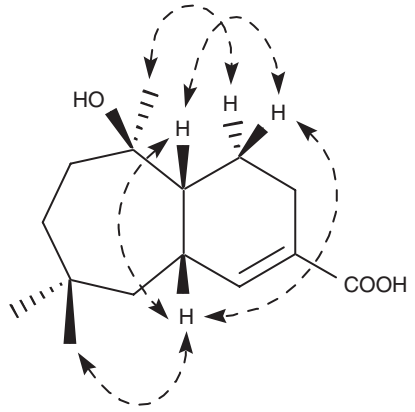

Figure 3 Important NOESY correlations of malfilanol A (**1**).

malfilanol B (**2**) inhibited proliferation of A549 cells with an IC_{50} value of 7.8 μM. Malfilanol A (**1**) showed no inhibition of A549 cell proliferation at 79.4 μM.

EXPERIMENTAL SECTION

General

Melting points were determined on a micro-melting point apparatus (Yanagimoto Ltd, Kyoto, Japan) and are uncorrected. CI-MS data were measured using a JMS-MS600W spectrometer (JEOL Co. Ltd, Tokyo, Japan). UV and IR spectra were recorded on an Ultrospec 2100 pro UV–visible spectrophotometer (Amersham Biosciences Ltd, Tokyo, Japan) and a JASCO FT/IR-4100 instrument (JASCO Co. Ltd, Tokyo, Japan), respectively. ^{1}H- and ^{13}C-NMR spectra were recorded using a JEOL Lambda-500 (500.00 MHz for ^{1}H, 125.25 MHz for ^{13}C, JEOL Co. Ltd) and/or a Bruker AV-400 spectrometer (400.13 MHz for ^{1}H, 100.61 MHz for ^{13}C, Bruker Biospin K. K., Kanagawa, Japan). Chemical shifts (δ) were measured in ppm using tetramethylsilane as an internal standard. CD curves were determined using a J-820 spectropolarimeter (JASCO Co. Ltd). Column chromatography was performed using Kieselgel 60 (Art. 7734, Merck Ltd, Tokyo, Japan) and Wakogel C-200 (Art. 237-00071, Wako Pure Chemical Industries, Ltd, Osaka, Japan). LPLC was performed using a Chemco Low-Prep 81-M-2 pump (Chemco Scientific Co. Ltd, Osaka, Japan) and a glass column (200×10 mm) packed with Silica gel CQ-3 (30–50 μm, Wako Pure Chemical Industries, Ltd). HPLC was performed using a Senshu SSC-3160 pump (flow rate, 7 ml min^{-1}, Senshu Scientific Co. Ltd, Tokyo, Japan) and a YMC-Pack PEGASIL Silica 60-5 column (300×10 mm, YMC Co. Ltd, Kyoto, Japan), equipped with a Shimamura YRD-883 RI detector (Shimamuratech Ltd, Tokyo, Japan). TLC was detected by UV light at 254 nm and/or by spraying with phosphomolybdic acid (5%)-ceric acid (trace) in 5% H_2SO_4 and then heating.

Fermentation, extraction and isolation

Rice (Akitakomachi, 560 g) was moisturized with water for 30 min and then dispensed to four Roux flasks, and sterilized by steaming under pressure. *M. filamentosa* IFM 41300 was inoculated in these Roux flasks and cultivated at 25 °C for 21 days, after which the rice was extracted with acetone and the organic layer was evaporated *in vacuo*. The residue (42 g) was suspended in water and extracted with AcOEt. The evaporated residue was extracted sequentially with hexane (100 ml), benzene (100 ml), CH_2Cl_2 (100 ml) and MeOH (100 ml). The benzene extract (2 g) was chromatographed using a silica gel column (solvent system: CH_2Cl_2/acetone (30:1), (10:1), (5:1), (3:1), (1:1) and acetone) to yield 13 fractions. Fraction 11 (the acetone eluate) was re-chromatographed using HPLC with a silica gel (CH_2Cl_2/ethanol (8:1)) to give malfilanol A (**1**: 4.0 mg). The hexane extract (1 g) was chromatographed using a Sephadex LH-20 column (solvent system: hexane/$CHCl_3$ (1:4) 400 ml, $CHCl_3$/acetone (4:1) 200 ml, (3:2) 200 ml, and acetone 300 ml) to yield nine fractions. Fraction 3 ($CHCl_3$: acetone (4:1), 219 mg) was chromatographed using HPLC with a silica gel (hexane/acetone (4:1)) to give malfilanol B (**2**: 5.0 mg).

Malfilanol A (1)

Colorless amorphous solid. CI-MS *m/z* (%): 253.1833 ((M+H)$^+$, 253.1804 for $C_{15}H_{25}O_3$). UV λ_{max} (MeOH) nm (ε): 218 (4.00). IR ν_{max} (KBr) cm^{-1}: 3420, 2945, 1690 and 1650. CD (MeOH) $\Delta\varepsilon$ (nm): +0.76(249) and −7.72(215). $[\alpha]_D^{25}$: −96° (c 0.525, MeOH). ^{1}H-NMR ($CDCl_3$): δ 0.86 (3H, s, 13-H_3), 0.96 (3H, s, 14-H_3), 1.05 (1H, d, *J*=15.0 Hz, 5-H), 1.20 (1H, m, 2-H), 1.21 (3H, s, 12-H_3), 1.22 (1H, m, 3-H), 1.41 (1H, m, 10-H), 1.46 (1H, m, 5-H), 1.54 (1H, td, *J*=14.0, 9.0 Hz, 2-H), 1.69 (1H, btd, *J*=13.1, 2.8 Hz, 11-H), 1.73 (1H, m, 3-H), 1.77 (1H, dd, *J*=13.1, 6.7 Hz, 10-H), 2.16 (1H, m, 9-H), 2.40 (1H, dd, *J*=18.0, 5.8 Hz, 9-H), 2.69 (1H, m, 6-H) and 6.97 (1H, dd, *J*=5.8, 1.2 Hz, 7-H). ^{13}C-NMR ($CDCl_3$): δ 19.6 (C-10), 25.1 (C-9), 29.3 (C-14), 30.1 (C-12), 31.4 (C-6), 32.0 (C-13), 32.7 (C-4), 34.2 (C-3), 34.5 (C-2), 41.3 (C-5), 48.3 (C-11), 74.2 (C-1), 126.9 (C-8), 147.8 (C-7) and 172.6 (C-15).

Malfilanol B (2)

Colorless crystalline powder (m.p. 109 °C). CI-MS *m/z* (%): 267.1950 ((M+H)$^+$, 267.1960 for $C_{16}H_{27}O_3$). UV λ_{max} (MeOH) nm (ε): 220 (3.92). IR ν_{max} (KBr) cm^{-1}: 3465, 2950, 1715 and 1650. CD (MeOH) $\Delta\varepsilon$ (nm): +0.80(247) and −4.84(218). $[\alpha]_D^{25}$: −68° (c 0.365, MeOH). ^{1}H-NMR ($CDCl_3$): δ 0.86 (3H, s, 13-H_3), 0.96 (3H, s, 14-H_3), 1.05 (1H, d, *J*=15.0 Hz, 5-H), 1.19 (1H, m, 2-H), 1.21 (3H, s, 12-H_3), 1.23 (1H, m, 3-H), 1.42 (1H, m, 10-H), 1.45 (1H, m, 5-H), 1.53 (1H, m, 2-H), 1.67 (1H, btd, *J*=12.3, 3.3 Hz, 11-H), 1.73 (1H, m, 3-H), 1.77 (1H, bdd, *J*=12.3, 6.9 Hz, 10-H), 2.16 (1H, m, 9-H), 2.41 (1H, dd, *J*=18.4, 6.0 Hz, 9-H), 2.68 (1H, bs, 6-H), 3.69 (3H, s, $COOCH_3$) and 6.85 (1H, bd, *J*=5.9 Hz, 7-H). ^{13}C-NMR ($CDCl_3$): δ 19.6 (C-10), 25.4 (C-9), 29.2 (C-14), 30.0 (C-12), 31.2 (C-6), 32.0 (C-13), 32.7 (C-4), 34.2 (C-3), 34.5 (C-2), 41.5 (C-5), 48.4 (C-11), 51.4 ($COOCH_3$), 74.0 (C-1), 127.5 (C-8), 145.5 (C-7) and 168.1 (C-15).

Methylation of malfilanol A (1) with CH_2N_2

An excess ethereal solution (2 ml) of diazomethane was added to an ether solution (0.5 ml) of malfilanol A (**1**) (1.0 mg), and the solution was stirred for 1 min followed by evaporation to give malfilanol B (**2**) (0.8 mg).

Cytotoxicity assay

Cells were seeded into 96-well microplates at 3000 cells per well, allowed to attach for 4–6 h and then incubated in Dulbecco's modified Eagle's medium (Invitrogen Co. Ltd, Carlsbad, CA, USA) for A549 human lung cancer cells, or in endothelial cell growth medium-2 Single Quots medium (Lonza Co., Ltd, Valais, Switzerland) supplemented with 10% fetal bovine serum, penicillin G (100 U ml^{-1}), streptomycin (100 μg ml^{-1}) and amphotericin B (0.25 μg ml^{-1}) for HUVEC until they were 80% confluent. The media were supplemented with the indicated concentrations of isolated compounds for 48–72 h. Cell proliferation was measured using the Cell Counting Kit8 (Dojindo, Kumamoto, Japan) to count living cells by combining WST-8 (2-(2-methoxy-4-nitrophenyl)-3-(4-nitrophenyl)-5-(2,4-disulfophenyl)-2H-tetrazolium) and 1-methoxy PMS (1-methoxy-phenazine methosulfate).[6] Briefly, after the medium was removed, 10 μl of Cell Counting Kit8 solution was added to each well, and the plates were incubated for 4 h, then cell numbers were obtained by scanning with a Bio-Rad Model 550 microplate reader (Bio-Rad Laboratories, Inc., Hercules, CA, USA) at 450 nm.

Antifungal assay using the paper disk method

The antifungal assay was performed using a method reported earlier.[5] The antifungal assay was performed using the paper disk method against *A. niger* IFM 41398, *A. fumigatus* IFM 41362, *C. albicans* IFM 40009 and *C. neoformans* ATCC 90112 as test organisms. Malfilanol A (**1**) and malfilanol B (**2**) were applied to the paper disk (diameter: 8 mm) at 50 μg per disk and the disks were placed on the assay plates. The test organisms were cultivated in potato dextrose agar (Nissui Pharmaceutical Co., Ltd, Tokyo, Japan) at 25 °C. After 48–72 h of incubation, zones of inhibition (the diameter measured in millimeters) were recorded.

ACKNOWLEDGEMENTS

We thank Dr H Kasai and Dr M Ikegami of Hoshi University for their technical assistance. This work was supported by an 'Open Research Center' Project from the Ministry of Education, Culture, Sports, Science and Technology, Japan.

1 Udagawa, S. Taxonomical outline of dermatophytes in the Ascomycetes. *Jpn. J. Med. Mycol.* **38,** 1–4 (1997).
2 Hosoe, T. *et al.* 4-Benzyl-3-phenyl-5H-furan-2-one, a vasodilator isolated from *Malbranchea filamentosa* IFM 41300. *Phytochemistry* **65,** 2776–2779 (2005).
3 Wakana, D. *et al.* Structures of new triterpene glycosides, malbrancheoside A-D, from *Malbranchea filamentosa. Heterocycles* **75,** 1109–1122 (2008).
4 Wakana, D. *et al.* Structures of two new glycosides of furanone derivatives, malfilamentosides A and B, isolated from *Malbranchea filamentosa. Mycotoxins* **58,** 1–7 (2008).
5 Wakana, D. *et al.* New citrinin derivatives isolated from *Penicillium citrinum. J. Nat. Med.* **60,** 279–284 (2006).
6 Weisskopf, M. *et al.* A Vitex agnus-castus extract inhibits cell growth and induces apoptosis in prostate epithelial cell lines. *Planta Med.* **71,** 910–916 (2005).

The Journal of Antibiotics (2009) 62, 221–224

www.nature.com/ja

NOTE

Kerriamycin B inhibits protein SUMOylation

Isao Fukuda[1,2], Akihiro Ito[1,3,4], Masakazu Uramoto[5,6], Hisato Saitoh[7], Hisashi Kawasaki[8], Hiroyuki Osada[2,5,6] and Minoru Yoshida[1,2,3,4]

The Journal of Antibiotics (2009) **62,** 221–224; doi:10.1038/ja.2009.10; published online 6 March 2009

Keywords: kerriamycin B; SUMO-1; SUMO-activating enzyme (E1)

Post-translational conjugation of small ubiquitin-related modifier protein (SUMO) to protein substrates (SUMOylation) has been revealed as one of the major post-translational regulatory systems in animals and other eukaryotes. SUMO conjugation is catalyzed by a multi-step enzymatic reaction cascade similar to ubiquitinylation.[1] In the first step, the SUMO precursor is cleaved near the C-terminus by SUMO-specific proteases to expose a C-terminal diglycine. The C-terminal glycine of mature SUMO then forms a thioester linkage to the cysteine residue of SUMO-activating enzyme (E1), the Aos1/Uba2 heterodimer, to generate the E1-SUMO intermediate in an ATP-dependent manner. Next, SUMO is transferred to the active site of the cysteine residue of the SUMO-conjugating enzyme (E2), Ubc9, through another thioester bond. In the last step, E2 and the SUMO ligase (E3) catalyze SUMOylation of substrate proteins at the ε-amino group of internal lysine residues. Although enzymatic reactions by E1 and E2 are sufficient for catalyzing *in vitro* SUMOylation in most cases, E3s facilitate both *in vivo* and *in vitro* conjugation and are important for substrate specificity.[1]

The structure of SUMO is similar to that of ubiquitin, but its functions are different. SUMOylation regulates protein subcellular localization, enzymatic activity and protein stability, which are associated with the cell cycle, transcription, DNA repair and innate immunity.[2,3] In addition, SUMOylation has been recently linked causally to diseases, such as Alzheimer's and Huntington's diseases,[4] viral infection[5] and cancer.[6,7] Notwithstanding the importance of SUMOylation in regulating diverse life phenomena and diseases, small molecule inhibitors of SUMOylation have been unexplored. Here, we report novel activity of kerriamycin B that inhibits protein SUMOylation, which will provide useful information about the role of SUMOylation in cells and drug development.

MATERIALS AND METHODS

Materials

Kerriamycin B was purified from a culture broth of an unidentified strain of actinomycetes. A goat polyclonal anti-SUMO-1 (N-19) antibody was purchased from Santa Cruz Biotechnologies (Santa Cruz, CA, USA). A mouse monoclonal anti-T7 antibody was from Novagen (Darmstadt, Germany). Mouse monoclonal anti-α-tubulin (B-5-1-2) and anti-FLAG (M2) antibodies were purchased from Sigma (St Louis, MO, USA). Recombinant His and T7-tagged RanGAP1-C2, GST-Aos1-Uba2 fusion protein (E1), His-tagged Ubc9 (E2) and His-tagged SUMO-1 proteins were purified as previously described.[8]

Isolation of kerriamycin B

After extraction of kerriamycin B from the 4-day cultured broth filtrate with 50 ml of *n*-BuOH, the crude material was partitioned between water and EtOAc. After removal of EtOAc from the organic layer, the extract was dissolved in MeOH and subjected to ODS open column chromatography. Active substance (2 mg) was given by concentration of the fraction eluted by 80% aq. MeOH. Further purification was carried out by using preparative HPLC (Waters 600, column (Waters, Milford, MA, USA); PEGASIL ODS 20×250 mm, monitor (Senshu Scientific, Tokyo, Japan); 220 nm, mobile phase; 30% aq. CH_3CN). The active eluate at 28 min was collected to give a yellow powder (1.6 mg). HR-ESI-MS $m\,z^{-1}$ 843.34507 $[M\text{-}H]^-$ (843.34392 calculated for $C_{43}H_{55}O_{17}$); UV λ_{max} (MeOH) nm (ε) 296.0 (sh, 5595), 320.0 (4895), 422.0 (5038); $[\alpha]_{589}^{22}$+11.4° (c 0.084, MeOH); ^{1}H-NMR (600 MHz, CD_3OD) δ_H (p.p.m., *J* value≒Hz):7.8 (d, *J*=7.9, 10-H), 7.5 (d, *J*=7.2, 11-H), 6.89 (d, *J*=9.7, 6-H), 6.39 (d, *J*=9.3, 5-H), 5.27 (brs, *J*=2.0, 1‴-H), 4.96 (brs, *J*=2>, 1″-H), 4.56 (dd, *J*=9.6, 1.4, 1⁗-H), 4.24 (q, *J*=6.5, 5″-H), 3.78 (ddd, *J*=11.2, 8.8, 4.8, 3′-H), 3.64 (q, *J*=6.7, 5‴-H), 3.54 (brs, *J*=2>, 4″-H), 3.48 (m, 1′-H), 3.48 (m, 3⁗-H), 3.48 (m, 5′-H), 3.35 (brs, 4‴-H), 3.21 (dq, *J*=6.2, 3.1, 5⁗-H), 3.14 (d, *J*=9.0, 4′-H), 2.89 (q, *J*=9.0, 4⁗-H), 2.72 (d, *J*=13.1, 2-Ha), 2.56 (d, *J*=13.1, 2-Hb), 2.54 (m, 2′-Ha), 2.18 (ddd, *J*=12.6, 5.0, 1.4, 2⁗-Ha), 2.07 (4-Ha), 2.06 (m, 3‴-Ha), 2.04 (m, 3″-Ha), 2.04 (m, 2″-Ha), 1.98 (4-Hb), 1.94 (m, 3″-Hb), 1.88 (d, *J*=13.4, 2‴-Ha), 1.81 (d, *J*=13.4, 2‴-Hb), 1.58 (m, 3‴-Hb), 1.54 (ddd, *J*=12.6, 5.0, 1.4, 2⁗-Hb), 1.41 (m, 2″-Hb), 1.38

[1]Chemical Genetics Laboratory, RIKEN Advanced Science Institute, Wako, Saitama, Japan; [2]Graduate School of Science and Engineering, Saitama University, Saitama, Saitama, Japan; [3]Chemical Genomics Research Group, RIKEN Advanced Science Institute, Wako, Saitama, Japan; [4]Japan Science and Technology Corporation, CREST Research Project, Kawaguchi, Saitama, Japan; [5]Antibiotics Laboratory, RIKEN Advanced Science Institute, Wako, Saitama, Japan; [6]Chemical Library and Bioprobe Research Group, RIKEN Advanced Science Institute, Wako, Saitama, Japan; [7]Department of Biological Sciences, Graduate School of Science and Technology, Kumamoto University, Kumamoto, Japan and [8]Department of Green and Sustainable Chemistry, Tokyo Denki University, Kanda, Chiyoda-ku, Tokyo, Japan
Correspondence: Dr A Ito, Chemical Genetics Laboratory, RIKEN Advanced Science Institute, Wako, Saitama, 351-0198, Japan.
E-mail: akihiro-i@riken.jp
Received 15 December 2008; revised 19 January 2009; accepted 21 January 2009; published online 6 March 2009

(d, J=5.8, 6′-H), 1.28 (m, 2′-Hb), 1.24 (d, J=6.2, 6′′′′-H), 1.20 (s, 3-CH_3), 1.15 (d, J=6.5, 6′′-H) and 0.51 (d, J=6.5, 6′′′-H); ^{13}C-NMR (150 MHz, CD_3OD) δ_C (p.p.m.): 204.9 (C_1), 189.6 (C_7), 184.1 (C_{12}), 159.0 (C_8), 146.3 (C_5), 141.5 (C_{12a}), 139.2 (C_9), 138.6 (C_{6a}), 134.3 (C_{10}), 132.4 (C_{11a}), 120.2 (C_{11}), 117.9 (C_6), 115.5 (C_{7a}), 102.8 ($C_{1''''}$), 95.5 ($C_{1'''}$), 95.2 ($C_{1''}$), 82.7 (C_{4a}), 82.6 (C_{12b}), 78.4 ($C_{4''''}$), 77.78 ($C_{5'}$), 77.75 ($C_{3'}$), 77.72 ($C_{4''}$), 77.1 (C_3), 76.8 ($C_{4'}$), 73.2 ($C_{5''''}$), 72.35 ($C_{3''''}$), 72.32 ($C_{1'}$), 68.1 ($C_{5'''}$), 67.8 ($C_{4'''}$), 67.7 ($C_{5''}$), 54.7 (C_2), 44.4 (C_4), 40.6 ($C_{2''''}$), 37.7 ($C_{2'}$), 29.9 (C_{3-CH3}), 26.3 ($C_{3'''}$), 25.5 ($C_{2''}$), 25.4 ($C_{3''}$), 24.1 ($C_{2'''}$), 18.8 ($C_{6'}$), 18.3 ($C_{6''''}$), 17.3 ($C_{6''}$) and 16.8 ($C_{6'''}$).

In vitro SUMOylation assay

The *in vitro* SUMOylation reaction was performed for 2 h at 30 °C in 20 µl buffer (50 mM Tris (pH 7.4), 6 mM $MgCl_2$, 2 mM ATP and 1 mM DTT) containing 0.1 µg of His and T7-tagged RanGAP1-C2, 0.3 µg of GST-Aos1/Uba2 (E1), 0.01 µg of His-tagged Ubc9 (E2) and 0.1 µg of His-tagged SUMO-1. Samples were separated by 10% SDS-PAGE followed by immunoblotting using an anti-T7 antibody to detect RanGAP1-C2 or an anti-SUMO-1 antibody.

Assay for SUMO-1 thioester bond formation

The reaction for the thioester bond formation was performed for 20 min at 37 °C in 20 µl buffer (50 mM Tris (pH 7.4), 6 mM $MgCl_2$, 2 mM ATP) containing 1 µg of purified GST-Aos1/Uba2 (E1) and 0.1 µg of biotinylated SUMO-1 in the absence of DTT. The reaction was stopped by adding loading buffer without the reducing agent. Reaction products were separated by 11% SDS-PAGE and the E1-biotinylated SUMO-1 intermediate was detected by using avidin-conjugated horseradish peroxidase (Sigma).

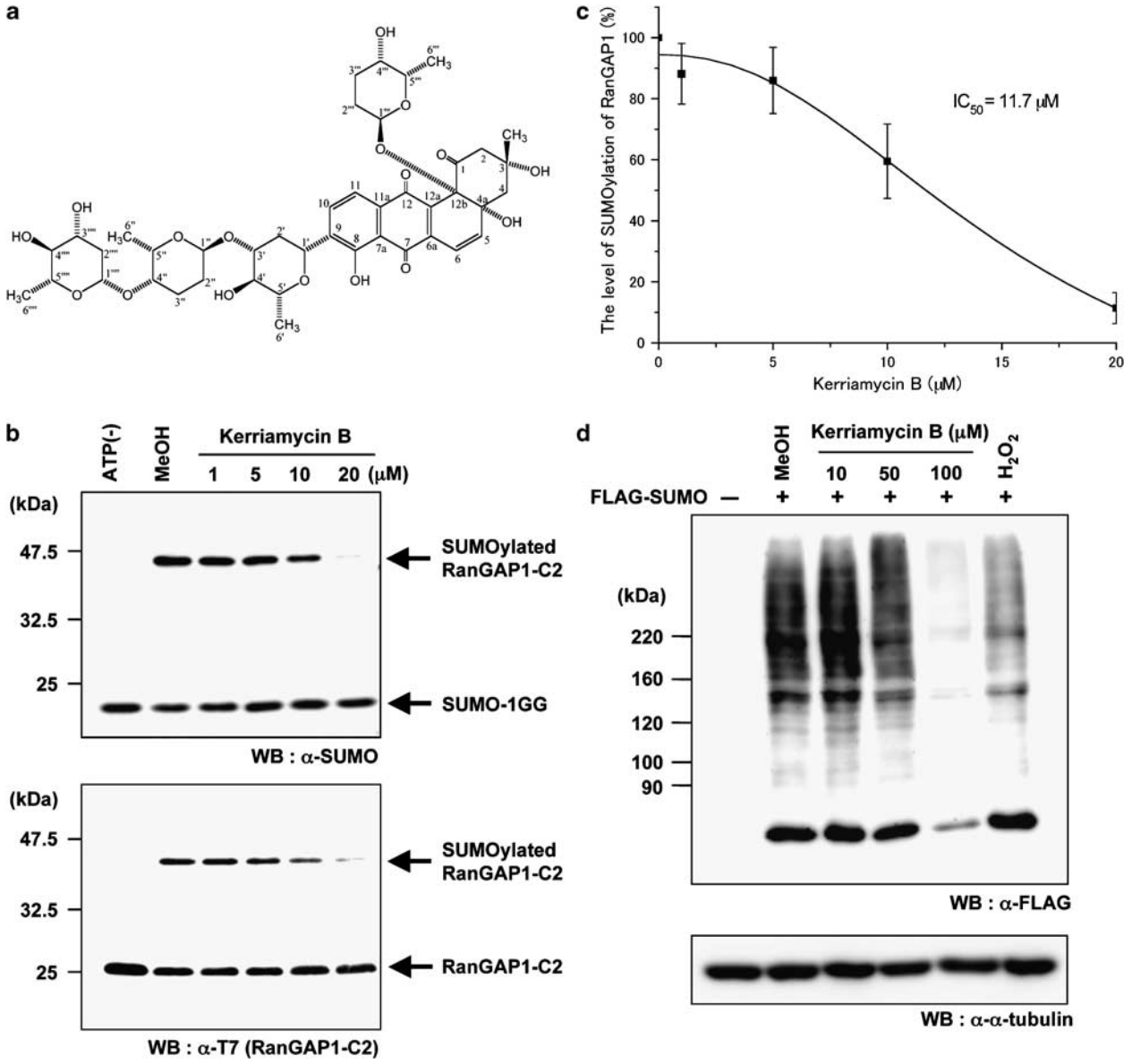

Figure 1 Kerriamycin B inhibition of protein SUMOylation. (**a**) Structure of kerriamycin B. (**b**) Dose response of kerriamycin B for SUMOylation inhibition. Indicated concentrations of kerriamycin B (1–20 µM) were added to the SUMOylation reaction mixture containing His-tagged SUMO-1, His and T7-tagged RanGAP1-C2, the GST-Aos1-Uba2 fusion protein (E1), His-tagged-Ubc9 (E2) in the presence of 2 mM ATP. SUMOlylated RanGAP1-C2 was detected by immunoblotting using an anti-T7 or an anti-SUMO-1 antibody. (**c**) IC_{50} value of kerriamycin B. The level of *in vitro* SUMOylation of RanGAP1-C2 was determined by measuring the intensity of SUMOylated RanGAP1-C2 using Image Gauge Version 4.22 (FUJIFILM). The error bars show the s.d. from three independent assays and the IC_{50} value was calculated. (**d**) Inhibition of *in vivo* protein SUMOylation by kerriamycin B. 293T cells were transfected with Flag-tagged SUMO and then treated with various concentrations of kerriamycin B (10–100 µM) for 12 h or treated with 1 mM H_2O_2 for 1 h. Cells were lysed in RIPA buffer containing 50 mM *N*-ethylmaleimide, and the lysates were separated by 6% SDS-PAGE followed by immunoblotting using an anti-FLAG antibody.

Using an *in situ* cell-based SUMOylation assay method,[9] we screened 1,839 samples of microbial cultured broth, and found extracts from three actinomycete strains showing activity to inhibit protein SUMOylation. We extracted the active substance with EtOAc from one of the extracts, and the active component was separated by using various adsorption column chromatographies. Finally, the pure compound was obtained by reverse phase HPLC. Physico-chemical properties and analysis of NMR and mass spectra showed that this compound was identical with a known antibiotic kerriamycin B (Figure 1a).[10]

To quantitatively analyze the SUMOylation inhibitory activity of kerriamycin B, we first characterized the effect of kerriamycin B on the *in vitro* protein SUMOylation using RanGAP1-C2 as a substrate. Kerrriamycin B completely inhibited SUMOylation of RanGAP1-C2 *in vitro* at 20 μM (Figure 1b) but not *in vitro* ubiquitinylation (data not shown). The IC_{50} value of kerriamycin B against SUMOylation of RanGAP1-C2 was determined to be 11.7 μM (Figure 1c). We then asked whether kerriamycin B also inhibits *in vivo* protein SUMOylation by analyzing the effect of the level of protein SUMOylation in 293T cells expressing Flag-tagged SUMO (Figure 1d). Immunoblotting using an anti-Flag antibody showed that kerriamycin B reduced the amount of high-molecular weight SUMO conjugates at 100 μM. Treatment with hydrogen peroxide also reduced the level of high-molecular weight SUMO conjugates (Figure 1d) as recently reported.[11]

Finally, we sought to determine the target of kerriamycin B. The complex of E1 with biotinylated SUMO-1 through the thioester bond can be detected in the presence of ATP under non-reducing conditions using a biotin–avidin detection system.[8] The band corresponding to the E1-biotinylated SUMO-1 intermediate was detected after incubating E1 with biotinylated SUMO-1 in the presence of ATP, but this band disappeared after addition of the reducing agent DTT (Figure 2). The formation of the E1-biotinylated SUMO-1 intermediate was blocked by kerriamycin B at 20 μM (Figure 2). These results suggest that kerriamycin B inhibits protein SUMOylation by blocking the formation of the E1-SUMO-1 intermediate.

Most recently, we identified ginkgolic acid and its related compound anacardic acid present in the plant extract as the first small molecule inhibitors of protein SUMOylation.[12] Binding assays using a fluorescently labeled ginkgolic acid revealed that ginkgolic acid inhibited protein SUMOylation by directly binding to E1 to block the formation of the E1-SUMO intermediate. In this study, we rediscovered kerriamycin B as a novel inhibitor of protein SUMOylation from microbial metabolites, which also inhibited the formation of the E1-SUMO intermediate. These observations suggested that E1 is the common target for these structurally unrelated compounds.

In addition to its antibacterial activity, kerriamycin B has been shown to possess antitumor activity against Ehrlich ascites carcinoma.[10] However, the mechanism underlying the antitumor activity is totally unknown. Involvement of the aberrant SUMO system in tumorigenesis has recently been suggested. The increased expression of *ubc9* encoding SUMO E2 was reported in several human ovarian cancer cell lines, such as PA-1 and OVCAR-8 as well as in ovarian tumor tissues,[13,14] human lung adenocarcinomas,[15] and LNCaP metastatic prostate cancer cell line.[16] These observations might reflect a possible role of Ubc9 in tumorigenesis by regulating SUMOylation of various cellular targets. Therefore, it seems possible that kerriamycin B activity to inhibit SUMOylation is responsible, at least in part, for its antitumor activity. Further analyses on the mechanisms of SUMOylation inhibition and structure–activity relationship of kerriamycin B are necessary for developing a novel anticancer agent targeting aberrant protein SUMOylation.

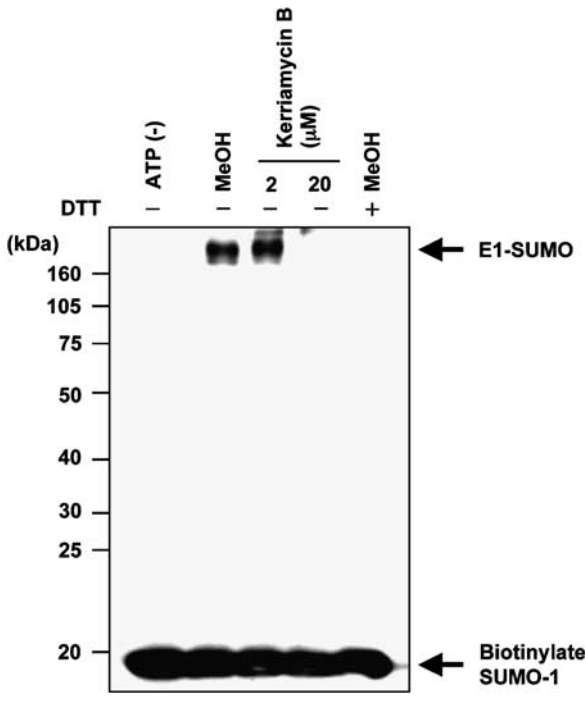

Figure 2 Impairment of the thioester bond formation between E1 and biotinylated SUMO-1 by kerriamycin B. Indicated concentration of kerriamycin B was added to a reaction mixture containing 5 ng μl^{-1} of biotinylated SUMO-1 and 50 ng μl^{-1} of GST-Aos1/Uba2 in the presence or absence of 2 mM ATP. After the mixtures had been incubated at 37 °C for 20 min, they were separated by SDS-PAGE, followed by analysis using avidin-conjugated horseradish peroxidase. Addition of 1 mM DTT to the reaction completely abolished the complex formation of biotinylated SUMO-1 and GST-Aos1/Uba2.

ACKNOWLEDGEMENTS

We thank Dr Y Uchimura (Kumamoto University) for technical advice. Microbial cultured broth was supplied from the Broth Screening Network (BSN). This work was supported in part by the Chemical Genomics Research Project, RIKEN ASI, the CREST Research Project, the Japan Science and Technology Corporation, and a Grant-in-Aid for Scientific Research on Priority Area 'Cancer' from the Ministry of Education, Culture, Sports, Science and Technology of Japan.

1 Johnson, E. S. Protein modification by SUMO. *Annu. Rev. Biochem.* **73,** 355–382 (2004).
2 Hay, R. T. SUMO: a history of modification. *Mol. Cell* **18,** 1–12 (2005).
3 Verger, A., Perdomo, J. & Crossley, M. Modification with SUMO. A role in transcriptional regulation. *EMBO Rep.* **4,** 137–142 (2003).
4 Dorval, V. & Fraser, P. E SUMO on the road to neurodegeneration. *Biochim. Biophys. Acta* **1773,** 694–706 (2007).
5 Boggio, R. & Chiocca, S. Viruses and sumoylation: recent highlights. *Curr. Opin. Microbiol.* **9,** 430–436 (2006).
6 Alarcon-Vargas, D. & Ronai, Z. SUMO in cancer—wrestlers wanted. *Cancer Biol. Ther* **1,** 237–242 (2002).
7 Moschos, S. J. & Mo, Y. Y. Role of SUMO/Ubc9 in DNA damage repair and tumorigenesis. *J. Mol. Histol.* **37,** 309–319 (2006).
8 Uchimura, Y., Nakao, M. & Saitoh, H. Generation of SUMO-1 modified proteins in E. coli: towards understanding the biochemistry/structural biology of the SUMO-1 pathway. *FEBS Lett.* **564,** 85–90 (2004).
9 Saitoh, N. *et al In situ* SUMOylation analysis reveals a modulatory role of RanBP2 in the nuclear rim and PML bodies. *Exp. Cell Res.* **312,** 1418–1430 (2006).
10 Hayakawa, Y. *et al* Kerriamycins A B and C, New Isotetracenone Antibiotics. *Agric. Biol. Chem.* **51,** 1397–1405 (1987).

11 Bossis, G. & Melchior, F. Regulation of SUMOylation by reversible oxidation of SUMO conjugating enzymes. *Mol. Cell* **21,** 349–357 (2006).
12 Fukuda, I. *et al* Ginkgolic acid inhibits protein SUMOylation by blocking formation of the E1-SUMO intermediate. *Chem. Biol.* (in press).
13 Mo, Y. Y. & Moschos, S. J. Targeting Ubc9 for cancer therapy. *Expert. Opin. Ther. Targets* **9,** 1203–1216 (2005).
14 Mo, Y. Y. *et al* A role for Ubc9 in tumorigenesis. *Oncogene* **24,** 2677–2683 (2005).
15 Doniels-Silvers, A. L., Nimri, C. F., Stoner, G. D., Lubet, R. A. & You, M. Differential gene expression in human lung adenocarcinomas and squamous cell carcinomas. *Clin. Cancer Res.* **8,** 1127–1138 (2002).
16 Kim, J. H. *et al* Roles of sumoylation of a reptin chromatin-remodelling complex in cancer metastasis. *Nat. Cell Biol.* **8,** 631–639 (2006).

The Journal of Antibiotics (2009) 62, 225–227

www.nature.com/ja

NOTE

Pennicitrinone D, a new citrinin dimer from the halotolerant fungus *Penicillium notatum* B-52

Zhi-Hong Xin[1,2], Wen-Liang Wang[1], Ya-Peng Zhang[1], Hua Xie[3], Qian-Qun Gu[1] and Wei-Ming Zhu[1]

The Journal of Antibiotics (2009) **62,** 225–227; doi:10.1038/ja.2009.12; published online 13 March 2009

Keywords: citrinin dimers; cytotoxic metabolite; halotolerant fungus; *Penicillium notatum*

Halotolerant microorganisms are considered to be extreme microbes because they thrive in high-salt environments, such as marine, salt lake, soda lake, the Dead Sea, salt field, etc.[1,2] It has been postulated that extreme environments, such as high-salt could awaken some silent genes and activate some unique biosynthesis pathways and, thus, make it possible to produce structurally unique and biologically active secondary metabolites.[3,4] In the course of our search for new bioactive compounds from halotolerant fungi,[5–8] a fungal strain, B-52, identified as *Penicillium notatum*, was observed to produce cytotoxic metabolites against the mouse temperature-sensitive *cdc2* mutant cell line, tsFT210. This strain was isolated from salt sediments collected in Qinghai Lake, Qinghai, China. Bioassay-guided fractionation led to the identification of a new citrinin dimer, pennicitrinone D (**1**), along with three known compounds, pennicitrinone A (**2**),[9] citrinin (**3**)[10–12] and mycophenolic acid (**4**) (Figure 1).[13,14]

MATERIALS AND METHODS

General experimental procedures

Optical rotations were obtained on a JASCO P-1020 digital polarimeter (JASCO, Tokyo, Japan). UV spectra were recorded on a Beckmen DU 640 spectrophotometer (Beckman Coulter, Beijing, China). IR spectra were taken on a Nicolet Nexus 470 spectrophotometer (Thermo Scientific, Beijing, China) in KBr disks. 1D- and 2D-NMR spectra were recorded on a JEOL JNM-ECP 600 spectrometer (JEOL Ltd, Beijing, China) using tetramethylsilane as the internal standard, and chemical shifts were recorded as δ-values. Electrospray ionization mass spectrometry was measured on a Q-Tof Ultima Global GAA076 LC mass spectrometer (Waters Asia, Ltd, Singapore). Semi-preparative HPLC was performed on a SHIMAD-ZU LC-6AD liquid chromatograph with an SPD-M10A vp diode array detector (both from Shimadzu International Trading Co. Ltd, Beijing, China).

Strain

The fungus, *P. notatum* B-52, was isolated from salt sediments collected from the Qinghai Lake, Qinghai Province of China. It was identified according to its morphological characteristics and preserved in the China Center for Type Culture Collection (No. CCTCC M205047). The working strain was prepared on potato dextrose agar slants containing 10% NaCl and stored at 4 °C.

Fermentation

The producing strain, *P. notatum* B-52, was inoculated into a 500-ml conical flask containing 100 ml of the liquid medium composed of mannitol (20 g l^{-1}), maltose (20 g l^{-1}), glutamine (10 g l^{-1}), glucose (10 g l^{-1}), yeast extract (3 g l^{-1}), NaCl (80 g l^{-1}), KCl (10 g l^{-1}), $MgSO_4$ (10 g l^{-1}) and seawater (adjusted to pH 6.5 before sterilization) and cultured at 28 °C for 48 h on a rotary shaker at 120 r.p.m. The seed culture was transferred into two-hundred 500-ml conical flasks (150 ml per flask), and fermentation was carried out at 28 °C for 10 days with an agitation rate of 120 r.p.m.

Extraction and isolation

The fermented whole broth (30 l) of *P. notatum* B-52 was filtered through a cheesecloth to separate into filtrate and mycelia. The filtrate was concentrated under reduced pressure to approximately a quarter of the original volume and then extracted thrice with ethyl acetate. The mycelia were extracted thrice with acetone. The acetone solution was concentrated under reduced pressure to afford an aqueous solution. The aqueous solution was extracted thrice with ethyl acetate. The combined ethyl acetate extract was concentrated under reduced pressure to give a crude extract (30 g). The crude extract was separated into five fractions on a flash silica gel column using a step gradient elution of *n*-hexane-EtOAc and then of EtOAc-MeOH. Fractions 2 (1.5 g) and 3 (1.3 g) showed cytotoxicity against tsFT210 cells. Fraction 2 was further separated into four sub-fractions over a silica gel column eluted with *n*-hexane-EtOAc (20:80). Sub-fractions 2-3 (45 mg) and 2-4 (50 mg) were separated by semi-preparative HPLC on a Shin-pak octadecylsilyl column using MeOH-H_2O (50:50 and 70:30, respectively) as an eluting solvent to give **3** (22 mg) and **4** (36 mg), respectively. Fraction 4 (2 g) was further purified into three sub-fractions by vacuum silica gel column chromatography using a step gradient elution of $CHCl_3$-MeOH. Sub-fractions 4-2 (350 mg) were subjected to chromatography over Sephadex LH-20 eluted with $CHCl_3$-MeOH (1:1), and the obtained fraction was further purified by

[1]Key Laboratory of Marine Drugs, Chinese Ministry of Education; School of Medicine and Pharmacy, Ocean University of China, Qingdao, PR China; [2]Department of Food Quality and Safety, College of Food and Technology, Nanjing Agriculture University, Nanjing, PR China and [3]State Key Laboratory of Drug Research, Shanghai Institute of Materia Medica, Chinese Academy of Sciences, Shanghai, PR China
Correspondence: Professor W-M Zhu, Key Laboratory of Marine Drugs, Chinese Ministry of Education, School of Medicine and Pharmacy, Ocean University of China, Qingdao, Shandong 266003, China.
E-mail: weimingzhu@ouc.edu.cn
Received 28 August 2008; accepted 28 January 2009; published online 13 March 2009

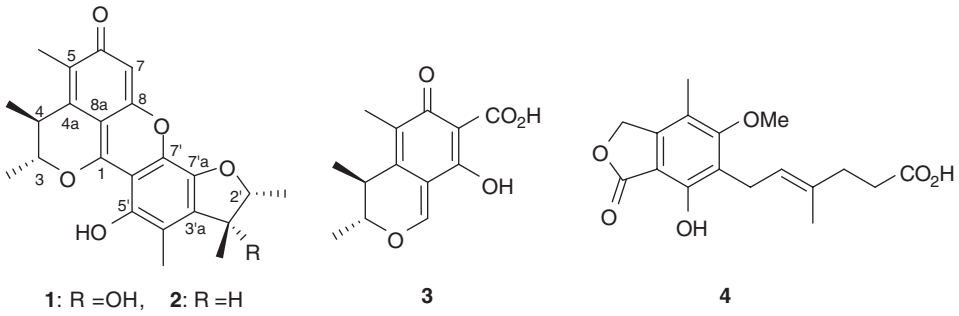

Figure 1 Structures of compounds **1**–**4.**

Table 1 ^{1}H and ^{13}C NMR (600 and 150 MHz) data for 1 and 2[a]

	1		*2*	
Position	*^{1}H (J in Hz)*	*^{13}C*	*^{1}H (J in Hz)*	*^{13}C*
1	—	156.0 s	—	155.4 s
3	4.89 q (6.0)	82.9 d	4.98 q (6.8)	82.3 d
4	2.97 q (7.3)	34.8 d	3.13 q (7.3)	35.0 d
4a	—	130.0 s	—	130.8 s
5	—	131.8 s	—	131.9 s
6	—	183.8 s	—	184.4 s
7	6.24 s	103.5 d	6.37 s	103.3 d
8	—	157.4 s	—	158.0 s
8a	—	99.6 s	—	100.1 s
3-Me	1.28 d (6.0)	18.7 q	1.45 d (6.8)	18.9 q
4-Me	1.29 d (7.3)	19.1 q	1.32 d (7.3)	19.1 q
5-Me	1.91 s	10.4 q	2.12 s	10.7 q
2	5.07 q (6.0)	89.6 d	4.62 dq (4.1, 6.4)	88.0 d
3	—	80.7 s	3.17 dq (4.1, 6.9)	44.6 d
3a	—	140.5 s	—	139.2 s
4	—	117.0 s	—	116.4 s
5	—	146.8 s	—	147.4 s
6	—	101.7 s	—	102.2 s
7	—	135.8 s	—	135.8 s
7a	—	138.1 s	—	137.8 s
2-Me	1.55 d (6.0)	14.5 q	1.42 d (6.4)	20.9 q
3-Me	1.43 s	21.1 q	1.34 d (6.9)	18.8 q
4-Me	2.32 s	9.4 q	2.21 s	11.5 q
3-OH	4.98	—	—	—
5-OH	7.99	—	8.36	—

Abbreviations: COSY, correlated spectroscopy; ^{13}C NMR, carbon-13 nuclear magnetic resonance; DEPT, distortionless enhancement by polarization transfer; HMQC, heteronuclear multiple quantum coherence; HMBC, heteronuclear multiple bond coherence.
[a]The assignments were based on DEPT, ^{1}H-^{1}H COSY, HMQC and HMBC experiments, and recorded in $CDCl_3$.

preparative HPLC (60% MeOH as the eluant) to yield compound **1** (9 mg). By the same procedure, compound **2** (16 mg) was obtained from the sub-fraction 4-3 (750 mg).

Biological assay

Active fractions were assayed using the methylthiazoletetrazolium (MTT) method[15] with the mouse temperature-sensitive *cdc2* mutant cell line, tsFT210. Compounds **1**–**4** were evaluated for cytotoxic effects on P388 and HL-60 cell lines using the MTT method and on A-549 and BEL-7402 cell lines using the sulforhodamine B (SRB) method.[16]

In the MTT assay, cell lines were grown in RPMI-1640 supplemented with 10% fetal bovine serum under a humidified atmosphere of 5% CO_2 and 95% air at 37 °C (tsFT210 cell line at 32 °C). Cell suspensions of 200 µl, at a density of 5×10^4 cell ml^{-1}, were plated in 96-well microtiter plates and incubated for 24 h at the above conditions. Next, 2 µl of the test compounds in DMSO at different concentrations was added to each well and further incubated for 72 h under the same conditions. MTT solution (20 µl, 5 mg ml^{-1} in IPMI-1640 medium) was added to each well and incubated for 4 h. Old medium (150 µl) containing MTT was then gently replaced by DMSO and pipetted to dissolve any formazan crystals that had formed. Absorbance was then determined on a Spectra Max Plus plate reader at 540 nm.

In the SRB assay, 200-µl portions of cell suspension were plated in 96-well plates at a density of 2×10^5 cell ml^{-1}. Then, 2 µl of the test solutions (in MeOH) was added to each well and the culture was further incubated for 24 h. The cells were fixed with 12% TCA and the cell layer was stained with 0.4% SRB. The absorbance of the SRB solution was measured at 515 nm. Dose-response curves were generated, and the IC_{50} values, the concentration of compound required to inhibit cell proliferation by 50%, were calculated from the linear portion of log dose-response curves.

Compound **1**: yellow amorphous powder; $[\alpha]_D^{17}$+111. 1 (*c* 0.16, $CHCl_3$); high-resolution electrospray ionization mass spectrometry (HRESI-MS) *m/z* 397.1624 (calcd for $C_{23}H_{25}O_6$, 397.1651); UV ($CHCl_3$) λ_{max} (logε) nm 204 (4.85), 227 (4.93), 272 (4.43), 436 (4.38); UV (MeOH) λ_{max} (logε) nm 202 (4.54), 225 (4.58), 270 (4.23), 274 (4.31), 430 (4.19); IR ν_{max} cm^{-1} (KBr) 3450, 2972, 2930, 1616, 1508, 1447, 1360, 1189, 1136, 1023, 890, 838; ^{1}H ($CDCl_3$, 600 MHz) and ^{13}C ($CDCl_3$, 150 MHz), see Table 1.

Compound **2**: yellow amorphous powder; $[\alpha]_D^{17}$+106.9 (*c* 0.36, $CHCl_3$); HRESI-MS *m/z* 381.1673 (calcd for $C_{23}H_{25}O_5$, 381.1702); UV ($CHCl_3$) λ_{max} (logε) nm 202 (3.46), 226 (3.57), 278 (4.35), 426 (4.24); UV (MeOH) λ_{max} (logε) nm 201 (4.60), 225 (4.50), 267 (4.46), 277 (4.47), 421 (4.40); IR ν_{max} cm^{-1} (KBr) 3440, 2966, 2909, 1617, 1509, 1431, 1324, 1281, 1138, 1042, 984, 884; ^{1}H ($CDCl_3$, 600 MHz) and ^{13}C ($CDCl_3$, 150 MHz), see Table 1.

Pennicitrinone D (**1**) was obtained as a yellow amorphous powder. Its molecular formula was determined as $C_{23}H_{24}O_6$ based on HRESI-MS at *m/z* 397.1624 $[M+H]^+$ (calcd 397.1651). The diagnostic IR peaks were observed for hydroxyl, conjugated carbonyl and benzene ring at 3450, 1616 and 1508 cm^{-1}, respectively. 1D-NMR spectra of **1** displayed six methyls, three sp^3 methines (two oxygenated), one sp^2 methine, one carbonyl, 11 sp^2 quaternary carbons and one sp^3-oxygenated quaternary carbon (Table 1). Except for an oxygenated quaternary carbon signal (δ_{OH} 4.98 and δ_C 80.7) instead of a methine signal (δ_H 3.17 and δ_C 44.6), the ^{1}H- and ^{13}C-NMR spectra of **1** were similar to those of **2**[9], suggesting that they shared the same molecular skeleton. Further comparison of the ^{13}C-NMR spectra of **1** with that of **2** revealed +1.6, +36.1, +1.3, +2.3, –6.4 and –2.1 p.p.m. of chemical shift effects for C-2′, C-3′, C-3′a, C-3′-Me, C-2′-Me and C-4′-Me, respectively, showing that **1** is a 3′-hydroxy derivative of **2**. This conclusion was further confirmed by ^{1}H-^{1}H COSY, heteronuclear

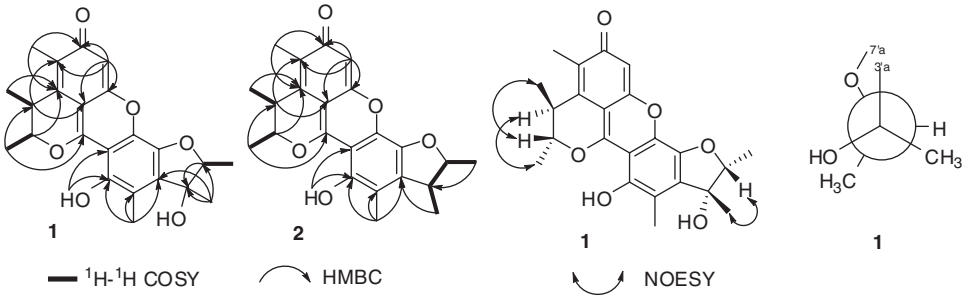

Figure 2 The key HMBC, ^{1}H-^{1}H COSY and NOESY correlations of **1** and **2** and *Gauche* conformation along the $C_{3'}$~$C_{2'}$ of **1.** COSY, correlated spectroscopy; NOESY, nuclear overhauser enhanced and exchange spectroscopy; HMBC, heteronuclear multiple bond coherence.

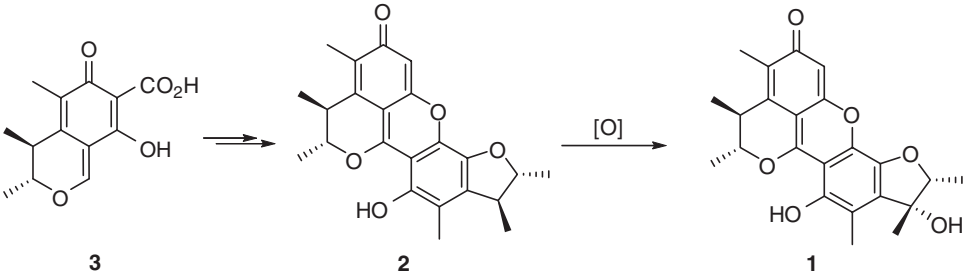

Scheme 1 The postulated biosynthesis of **1**.

multiple quantum coherence (HMQC), NOESY and heteronuclear multiple bond coherence (HMBC) experiments (Figure 2). The upfield shifts of C-2′-Me and C-4′-Me were caused by the γ-*gauche* effect and by the stereospecific blockade of 3′α-OH, respectively. The absolute configuration of **1** was determined as shown by the NOE correlations and further by comparing the $[\alpha]_D$ value, +111.1, with that of **2**, +106.9 and a possible biogenic pathway (Scheme 1). Compound **1** is most likely produced from the oxidation of **2** that is produced by a Diels–Alder reaction of **3**.[5,17] Thus, the structure of **1** was elucidated as (3′*R*)-3′-hydroxypennicitrinone A.

According to ^{1}H-^{1}H COSY, HMQC and HMBC experiments, ^{13}C NMR data of 3-Me, 2′-Me and 3′-Me of **2** in the literature[9] should be interchanged as 19.1, 21.0 and 18.8 p.p.m., respectively.

The cytotoxicity of compounds **1**–**4** was evaluated against P388 and HL-60 cell lines by the MTT method,[15] and against BEL-7402 and A-549 cell lines by the SRB method.[16] Compound **2** showed weak cytotoxicity against P388 and BEL-7402 cells with IC_{50} values of 25 and 16 μM, respectively. Compound **4** exhibited moderate cytotoxicity against A-549 cells with an IC_{50} value of 0.95 μM, whereas compounds **1** and **3** were inactive.

ACKNOWLEDGEMENTS

This work was supported by the National Natural Science Foundation of China (No. 30470196, 30670219 and 30572246). The fungus strain, *P. notatum* B-52, was identified by Professor Li Tian, First Institute of Oceanography, State Oceanic Administration of China.

1 Kamekura, M. Diversity of extremely halophilic bacteria. *Extremophiles* **2,** 289–295 (1998).
2 Aguilar, A., Ingemansson, T. & Magnien, E. Extremophile microorganisms as cell factories: support from the European Union. *Extremophiles* **2,** 367–373 (1998).
3 Koch, A. L. Genetic response of microbes to extreme challenges. *J. Theor. Biol.* **160,** 1–21 (1993).
4 Méjanelle, L., Lòpez, J. F., Gunde-Cimerman, N. & Grimalt, J. O. Ergosterol biosynthesis in novel melanized fungi from hypersaline environments. *J. Lipid. Res.* **42,** 352–358 (2001).
5 Lu, Z. Y. *et al.* Citrinin dimers from the halotolerant fungus *Penicillium citrinum* B-57. *J. Nat. Prod.* **71,** 543–546 (2008).
6 Wang, W. L. *et al.* Two new cytotoxic quinone type compounds from the halotolerant fungus *Aspergillus variecolor. J. Antibiot.* **60,** 603–607 (2007).
7 Wang, W. L. *et al.* Isoechinulin-type alkaloids, variecolorin A-L, from halotolerant *Aspergillus variecolor. J. Nat. Prod.* **70,** 1558–1564 (2007).
8 Wang, W. L. *et al.* Three novel, structurally unique spirocyclic alkaloids from the halotolerant B-17 fungus strain of *Aspergillus variecolor. Chem. Biodivers.* **4,** 2913–2919 (2007).
9 Wakana, D. *et al.* New citrinin derivatives isolated from *Penicillium citrinum. J. Nat. Med.* **60,** 279–284 (2006).
10 Rödel, T. & Gerlach, H. Enantioselective synthesis of the polyketide antibiotic (3*R*,4*S*)-(−)-citrinin. *Liebigs Ann.* **1995,** 885–888 (1995).
11 Rodig, O. R., Shiro, M. & Fernando, Q. The crystal and molecular structure of citrinin. *J. Chem. Soc. Chem. Commun* 1553–1554 (1971).
12 Chien, M. M., Schiff, P. L. Jr, Slatkin, D. J. & Knapp, J. E. Metabolites of Aspergilli. III. The isolation of citrinin, dihydrocitrinone and sclerin from *Aspergillus carneus. Lloydia* **40,** 301–302 (1977).
13 Nelson, P. H., Eugui, E., Wang, C. C. & Allison, A. C. Synthesis and immunosuppressive activity of some side-chain variants of mycophenolic acid. *J. Med. Chem.* **33,** 833–888 (1990).
14 Anderson, W. K., Boehm, T. L., Makara, G. M. & Swann, R. T. Synthesis and modeling studies with monocyclic analogues of mycophenolic acid. *J. Med. Chem.* **39,** 46–55 (1996).
15 Mosmann, T. Rapid colorimetric assay for cellular growth and survival: application to proliferation and cytotoxicity assays. *J. Immunol. Methods* **65,** 55–63 (1983).
16 Skehan, P. *et al.* New colorimetric cytotoxicity assay for anticancer drug screening. *J. Natl Cancer Inst.* **82,** 1107–1112 (1990).
17 Clark, B. R., Capon, R. J., Lacey, E., Tennant, S. & Gill, J. H. Citrinin revisited: from monomers to dimers and beyond. *Org. Biomol. Chem.* **4,** 1520–1528 (2006).

The Journal of Antibiotics (2009) 62, 229–231

www.nature.com/ja

NOTE

A novel macrolide compound from *Streptomyces bingchenggensis*: fermentation, isolation, structure elucidation and biological properties

Wen-Sheng Xiang[1], Ji-Dong Wang[2], Xiang-Jing Wang[1] and Ji Zhang[1]

The Journal of Antibiotics (2009) **62,** 229–231; doi:10.1038/ja.2009.14; published online 13 March 2009

Keywords: cytotoxic activity; novel macrolide compound; ST906 (***1***); *Streptomyces bingchenggensis*

Natural products play an important role in drug discovery and have been used for the treatment of diseases for decades. They constitute a leading source of novel molecules for the development of new drug candidates.[1–3] To search for more bioactive compounds, we have reported earlier the isolation and structure elucidation of milbemycins, β_{13}, β_{14}, α_{28}, α_{29}, and α_{30}, and secomilbemycins A and B from *Streptomyces bingchenggensis*.[4–6] In this paper, we obtained a novel macrolide compound, ST906 (**1**), from *S. bingchenggensis*, and described the fermentation, isolation, structural elucidation and cytotoxic activity.

MATERIALS AND METHODS

Microorganism

The producing organism, *S. bingchenggensis*, was isolated from a soil sample collected in Harbin, China. *S. bingchenggensis* has been deposited at the China General Microbiology Culture Collection Center (accession no. CGMCC1734; Institute of Microbiology, Chinese Academy of Sciences), and we have determined the 16S rDNA sequence (accession no. DQ449953 in GenBank, National Center for Biological Information).

Fermentation

The seed for preculture was spores. The medium for sporulation contained sucrose (Bei Jing Ao Bo Xing, Beijing, China) 4 g, yeast extract (Bei Jing Ao Bo Xing) 2 g, malt extract (Bei Jing Ao Bo Xing) 5 g and skimmed milk (Nmyili, Huhehaote, China) 1 g in 1 l water. The pH was adjusted to 7.0 with 1 M NaOH to which 20 g of agar was added, and this mixture was sterilized at 121 °C for 30 min. The spore suspension was prepared from the agar plates (20 ml) incubated at 28 °C for 7–8 days.

A spore suspension of the culture of strain *S. bingchenggensis*, 1 ml, was transferred to a 250-ml Erlenmeyer flask that contained 25 ml of the seed medium containing sucrose 0.25 g, polypepton (Bei Jing Ao Bo Xing) 0.1 g and K_2HPO_4 1.25 mg. The inoculated flasks were incubated at 28 °C for 42 h on a rotary shaker at 250 r.p.m. Then, 8.0 ml of the culture was transferred into a 1-l Erlenmeyer flask containing 100 ml of the producing medium consisting of sucrose (Bei Jing Ao Bo Xing) 8.0%, soybean powder (Comwin, Beijing, China) 1.0%, yeast extract (Bei Jing Ao Bo Xing) 0.2%, meat extract (Bei Jing Ao Bo Xing) 0.1%, $CaCO_3$ (Bei Jing Hong Xin) 0.3%, K_2HPO_4 0.03%, $MgSO_4{\cdot}7H_2O$ 0.1% and $FeSO_4{\cdot}7H_2O$ 0.005%; pH 7.2 before sterilization. Fermentation was carried out at 28°C for 8 days on a rotary shaker at 250 r.p.m.

Isolation and purification

The fermentation broth (15 l) was filtered. The resulting cake was washed with water, and both filtrate and wash were discarded. MeOH (3 l) was used to extract the washed cake. The MeOH extract was concentrated to ~1 l under reduced pressure and the resulting concentrate was extracted three times with an equal volume of EtOAc. The combined EtOAc phase was concentrated under reduced pressure to yield 25 g of an oily substance. The residual oily substance was chromatographed on silica gel (Qing Dao Hai Yang Chemical Group Co., Qingdao, China, 100–200 mesh) and eluted with petroleum ether–Me_2CO (95:5–50:50) to give five fractions that were separated by TLC with petroleum ether–acetone (3:1, v/v). Spots were detected on TLC under UV or by heating after spraying with sulfuric acid–ethanol (5:95, v/v). To obtain pure compound ST906 (**1**), the fourth fraction (petroleum ether–acetone 70:30, v/v) of the silica gel chromatography was separated by semipreparative HPLC (Agilent 1100, Santa Clara, CA, USA, Zorbax SB-C18, 5 μm, 250×9.4 mm i.d.) using a solvent of 96% CH_3OH/H_2O. The eluates were monitored with a photodiode array detector at 220 nm, and the flow rate was 1.5 ml min^{-1} at a room temperature (ST906 (**1**), 17.3 min).

General

UV spectra were obtained on a CARY 300 BIO spectrophotometer (Varian, Palo Alto, CA, USA); IR spectra were recorded on a Nicolet Magna FT-IR 750 spectrometer (Thermo Scientific, Waltham, MA, USA); ^1H and ^{13}C NMR spectra were measured with a DRX-400 (400 MHz for ^1H and 100 MHz for ^{13}C) spectrometer (Bruker, Bremen, Germany). Chemical shifts are reported on parts per million (δ), using the residual $CHCl_3$ (δ_H 7.26; δ_C 77.0) as an internal standard, and coupling constant (J) in Hertz. ^1H and ^{13}C NMR assignments were supported by ^1H-^1H COSY, heteronuclear multiple quantum coherence and heteronuclear multiple bond coherence (HMBC) experiments. The electrospray ionization-MS (ESI-MS) and high-resolution electrospray ionization-MS (HRESI-MS) spectra were taken on a Q-TOF Micro LC–MS–MS mass

[1]School of Life Science, Northeast Agricultural University, Harbin, China and [2]Zhejiang Hisun Pharmaceutical Co. Ltd, Taizhou, Zhejiang, China
Correspondence: Professor X-J Wang, School of Life Science, Northeast Agricultural University, Harbin 150030, China.
E-mail: wangxiangjing2008@yahoo.com.cn
Received 8 January 2009; revised 3 February 2009; accepted 4 February 2009; published online 13 March 2009

spectrometer. Optical rotation was measured on a 341 Polarimeter (PerkinElmer, Shanghai, China).

Biological assays

The cytotoxicity of compound on tumor cells was assayed according to published procedures.[7] Human colon carcinoma cell line, HCT-116, was routinely cultured in Dulbecco's modified Eagle's medium containing 10% calf serum at 37 °C for 4 h in a humidified atmosphere of 5% CO_2 incubator. The adherent cells at their logarithmic growth stage were digested, and were inoculated onto a 96-well culture plate at a density of 1.0×10^4/well for the determination of proliferation. Test samples were added to the medium, and incubation was continued for 72 h. Coloration substrate, cell counting kit-8 (CCK-8, Dojindo, Kumamoto, Japan), was added to the medium followed by further incubation for 3 h. Absorbance at 450 nm with a 600 nm reference was measured thereafter. Media and DMSO control wells, in which compound was absent, were included in all the experiments to eliminate the influence of DMSO. The inhibitory rate of cell proliferation was calculated by the following formula:

$$\text{Growth inhibition}\,(\%) = [OD_{control} - OD_{treated}]/OD_{control}\times 100$$

The cytotoxicity of the compound on tumor cells was expressed as IC_{50} values (the drug concentration reducing the absorbance in treated cells by 50%, with respect to untreated cells) and was calculated by the LOGIT method.

Physicochemical properties of compound ST906 (1)

ST906 (**1**, Figure 1) $C_{32}H_{42}O_7$, colorless oil; $[\alpha]_D^{20}$ +25.7° (*c* 0.07, EtOH); UV (EtOH) λ_{max} nm (log ε): 206 (4.18), 228 (4.34) and 290 (3.84); IR (KBr), ν_{max} cm^{-1}: 3360, 2924, 1704, 1619, 1510, 1457, 1376, 1263, 1207, 1101, 1027 and 985; ^1H NMR ($CDCl_3$, 400 MHz) and ^{13}C NMR ($CDCl_3$, 100 MHz) see Table 1; ESI-MS *m/z* 537 $[M-H]^+$; HRESI-MS *m/z* 537.2843 $[(M-H)^+$, calcd for $C_{32}H_{41}O_7$, 537.2846].

Structural elucidation

Compound ST906 (**1**) was obtained as a colorless oil with the UV absorptions at λ_{max} nm: 206, 228, 257 and 290. In its IR spectrum, the hydroxyl and carbonyl absorptions were presented at 3360 cm^{-1} and 1704 cm^{-1}, respectively. The molecular formula of **1** was established as $C_{32}H_{42}O_7$ on the basis of HRESI-MS and NMR analyses, which indicated the presence of 12° of unsaturation. The ^1H NMR spectrum (see Table 1) of ST906 (**1**) showed two downfield singlet signals at δ 7.83 (s) and 7.59 (s), two doublet methyls at δ 1.03 (d) and δ 0.83 (d), a methyl triplet at δ 1.01 (t) and two singlet olefinic methyls at δ 2.35 (s) and δ 1.74 (br s). A *trans*-double bond was also presented by the signals at δ 6.94 (d, *J*=15.8 Hz) and δ 6.15 (dd, *J*=15.8, 9.4 Hz) in the ^1H NMR spectrum. The ^{13}C NMR and DEPT spectra of ST906 (**1**) indicated 32 carbons, including one ester carbonyl carbon, 12 sp^2 carbons, one ketal carbon, 5 methyls, 7 aliphatic methylenes and 6 sp^3 methines (including four oxygenated ones). These data suggested that ST906 (**1**) was the analog of milbemycin β_{14}.[4] Besides the six olefins, the presence of five rings was required to satisfy the degrees of unsaturation, so a five-membered ether ring was formed between C-6 and C-27 similar to other milbemycin α-series. The observed HMBC correlations (Figure 2) from δ_H 1.03 to δ_C 40.1, 43.3 and 86.6, and a ^1H-^1H COSY correlation between δ_H 4.56 and δ_H 6.15 suggested that a hydroxyl was presented at C-11 and the *trans*-double bond was in C-9 and C-10. The long-range ^1H-^{13}C correlation between δ_H 7.83 and δ_C 120.0, 123.6 and 142.4, and between δ_H 6.94 and δ_C 144.4 showed that a double bond was present in C-8 and C-27. Thus, the gross planar structure of ST906 (**1**) was established.

The relative stereochemistry of ST906 (**1**) was established on the basis of that of other milbemycins, except that of the new chiral center of C-11. In the NOESY experiment, the absent correlated signal

Table 1 ^1H and ^{13}C NMR data of ST906 (1) (coupling constants in parenthesis)

Number	*Proton*	*Carbon*	*Number*	*Proton*	*Carbon*
1		167.2 s[a]	19	5.63 m	70.0 d
2		117.1 s	20	2.16 m	41.3 t
3	7.59 s	129.7 d		1.33 m	
4		119.6 s	21		97.5 s
5		142.4 s	22	1.65 m	35.6 t
6		142.4 s		1.53 m	
7		123.6 s	23	1.50 m	27.9 t
8		120.0 s	24	1.33 m	34.3 d
9	6.94 d (15.8)	126.7 d	25	3.11 m	76.0 d
10	6.15 dd (15.8, 9.4)	126.4 d	26	2.35 s	14.8 q
11	4.56 br d (9.4)	86.6 d	27	7.83 br s	144.4 d
12	1.86 m	40.1 d	28	1.03 d (7.1)	14.0 q
13	2.14 m	43.3 t	29	1.74 br s	18.3 q
14		137.2 s	30	0.83 d (6.5)	17.8 q
15	5.35 br t (7.3)	122.2 d	31	1.67 m	25.7 t
16	2.46 m	33.3 t		1.35 m	
	2.32 m		32	1.01 t (6.2)	10.1 q
17	3.93 m	67.0 d			
18	2.14 m	35.6 t			
	1.42 m				

[a]By DEPT sequence.

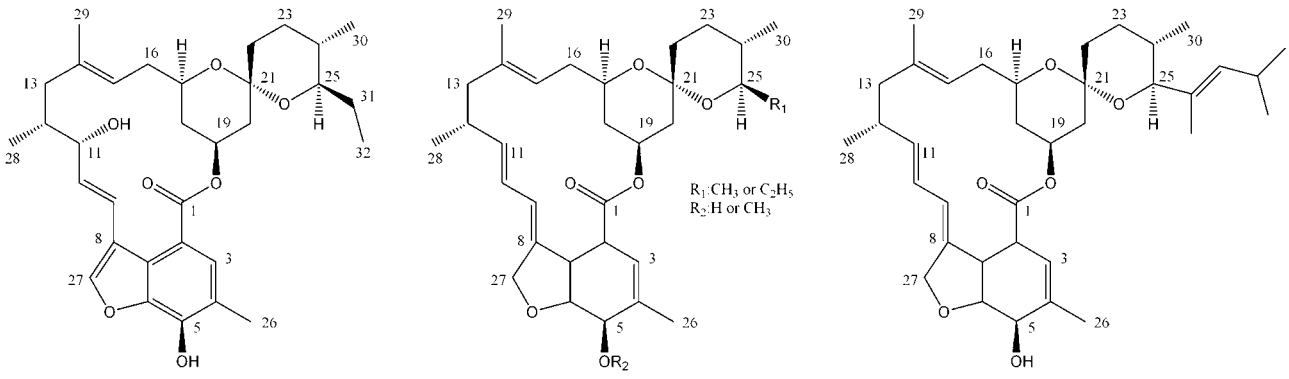

Figure 1 The structures of ST906 (**1**), milbemycin α-class and LL-F 28249v.

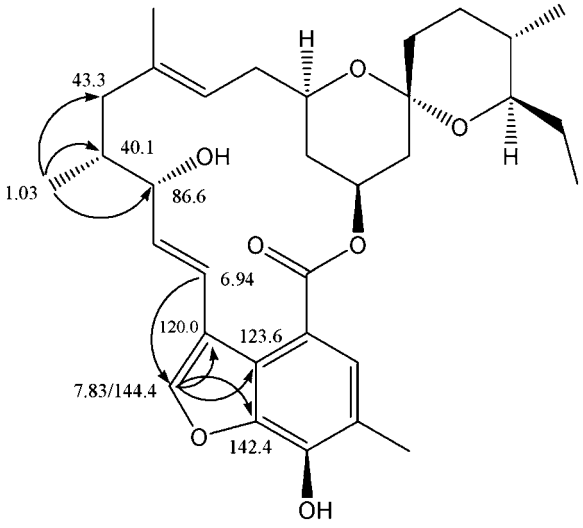

Figure 2 The important HMBC correlations of ST906 (**1**).

between H-11 and H_3-28 attempted to assign the hydroxyl of C-11 in the same orientation as the methyl of C-28.

The structure of ST906 (**1**) is similar to milbemycin α-class; however, there are significant differences between them. Milbemycins have a double bond between C-3 and C-4, whereas ST906 (**1**) possesses a benzene structure. Although a benzene structure was found in the milbemycin β-class,[4] only compound LL-F 28249ν presents a benzene structure in milbemycin α-class (Figure 1).[8,9] ST906 (**1**) possesses both double bond between C-8 and C-27, and between C-9 and C-10. For milbemycin α- and β-classes, the position of two double bonds is presented at C-8 and C-9, and at C-10 and C-11, respectively. Moreover, ST906 (**1**) got a hydroxyl at C-11, whereas for milbemycins there is no such evidence. It is concluded that ST906 (**1**) is a novel macrolide compound.

Biological activity

We examined the inhibitory activity of compound ST906 (**1**) against the growth of human colon carcinoma cell line, HCT-116, using the CCK-8 colorimetric method as described in the Materials and methods section. Compound ST906 (**1**) dose-dependently inhibited the growth of HCT-116 cells with an IC_{50} value of 4.8 μg ml^{-1}. However, the IC_{50} value for control doxorubicin was 4.2 μg ml^{-1}. Bioassay results showed that ST906 (**1**) had strong cytotoxic activity.

ACKNOWLEDGEMENTS

This study was supported by the National Natural Science Foundation of China (Grant nos. 30571234 and 30771427), the National Key Technology R&D Program (Grant no. 2006BAD31B02) and the Outstanding Youth Foundation of Heilongjiang Province (Grant no. JC200706).

1 Lam, K. S. New aspects of natural products in drug discovery. *Trends Microbiol.* **15,** 279–289 (2007).
2 Harvey, A. L. Natural products as a screening resource. *Curr. Opin. Chem. Biol.* **11,** 480–484 (2007).
3 Gullo, V. P., McAlpine, J., Lam, K. S., Baker, D. & Petersen, F. Drug discovery from natural products. *J. Ind. Microbiol. Biotechnol.* **33,** 523–531 (2006).
4 Xiang, W. S., Wang, J. D, Wang, X. J. & Zhang, J. Two new-class milbemycins from *Streptomyces bingchenggensis* fermentation, isolation, structure elucidation and biological properties. *J. Antibiot.* **60,** 351–356 (2007).
5 Xiang, W. S., Wang, J. D., Wang, X. J., Zhang, J. & Wang, Z. Further new milbemycin antibiotics from *Streptomyces bingchenggensis*. *J. Antibiot*. **60,** 608–613 (2007).
6 Xiang, W. S., Wang, J. D., Fan, H. M., Wang, X. J. & Zhang, J. New seco-milbemycins from *Streptomyces bingchenggensis*: fermentation, isolation and structure elucidation. *J. Antibiot.* **60,** 27–32 (2008).
7 Wang, J. D. *et al*. HS071, a new furan-type cytotoxic metabolite from *Streptomyces* sp. HS-HY-071. *J. Antibiot.* **61,** 623–626 (2008).
8 Nonaka, K. *et al*. New milbemycins from *Streptomyces hygroscopicus* subsp. *aureolacrimosus*: fermentation, isolation and structure elucidation. *J. Antibiot.* **53,** 694–704 (2000).
9 Bovden, W. I., Anthony, P. J., Thomas, C. G., Jennings, T. M. & Michael, G. Method and compositions for helmintic, arthropod ectoparasitic and acaridal infections with novel agents. European Patent. 170006, 2 May (1986).